Regulation of RNA Editing by Intracellular Acidification

By

Turnee N. Malik

Dissertation

Submitted to the Faculty of the

Graduate School of Vanderbilt University

in partial fulfillment of the requirements

for the degree of

DOCTOR OF PHILOSOPHY

in

Neuroscience

December 12, 2020

Nashville, Tennessee

Approved:

Ronald B. Emeson, Ph.D.

Edward Levine, Ph.D.

Douglas G. McMahon, Ph.D.

James G. Patton, Ph.D.

Richard B. Simerly, Ph.D.

This work is dedicated to my beloved parents:

My mother, Afroza Begum, and my father, Abdul Malik, for all of their love and sacrifices,

And

To my brother, Upom Malik, for being my role model.

ACKNOWLEDGMENTS

I am deeply grateful to so many people who have helped and inspired me throughout my doctoral studies.

I would first like to thank my graduate advisor, Ron Emeson, for allowing me to join his lab, for his mentorship, and for his kindness and encouragement. I would also like to thank members of my committee—Edward Levine, Doug McMahon, Jim Patton, and Rich Simerly—for their help in critically discussing my research.

I would like to thank both of my undergraduate research advisors, Graeme Conn and Francisco Alvarez, for giving me my first opportunities to participate in research.

I would like to thank all previous and current members of the Emeson Lab, especially Kayla Shumate, Katie Patterson, and Teddy Hill, for helping me in ways big and small. I feel so lucky to have been in the company of such intelligent, hard-working, and kind people.

I would like to thank my collaborators, Peter Beal, Erin Doherty, and Vandana Gaded, whose scientific contributions were essential to my doctoral research.

I am very grateful for my many friends in Nashville and abroad. My friendships have simultaneously kept me grounded and lifted me up.

Finally, I would like to express my deepest gratitude to my wonderful family for their endless love and support. All that I have done is a product of the great sacrifices made by my selfless parents. I am also tremendously grateful to my brother, who has been the greatest friend and role model in my life.

TABLE OF CONTENTS

Page

LIST OF TABLES

LIST OF FIGURES

Chapter I

Introduction

RNA processing expands genetic diversity

All cells store hereditary information in nucleic acids formed by the polymerization of nucleotides containing derivatives of different nitrogenous bases: adenine (A), cytosine (C), guanine (G), thymine (T) and uracil (U) (1). The precise sequence and base-pairing properties of these nucleotides dictate how hereditary units, known as genes, are decoded by cellular machinery. In general, gene expression relies on transcription of deoxyribonucleic acid (DNA) into ribonucleic acid (RNA), which in turn directs the synthesis of proteins during translation (1,2). However, this simplistic view of gene expression was challenged by the publication of eukaryotic genome sequences that revealed a surprisingly small number of protein-coding genes (3-5). These findings suggested that genomically-encoded information cannot fully account for biological complexity and underscored the importance of understanding how post-transcriptional processing of RNAs generates functional diversity.

Discoveries over the past six decades have revealed various RNA species, virtually all of which undergo biochemical modifications upon their genesis (6,7). In particular, nascent protein-coding transcripts (called precursor messenger RNAs or pre-mRNAs) undergo a maturation process that includes the addition of a 5’ 7-methylguanylate cap and a 3’-polyadenlyated tail, as well as the removal of intervening non-coding sequences (introns) from expressed sequences (exons) through an RNA-mediated mechanism known as splicing (1). Following the discovery of splicing, it soon became apparent that greater than 90% of human genes generate many unique RNA isoforms through the joining of different exon combinations from a single pre-mRNA (termed, “alternative splicing”) (8).

Beyond capping, polyadenylation, and splicing, hundreds of other RNA processing events also contribute to transcriptomic diversification (9). Canonical ribonucleotides/ribonucleosides (denoted as A, C, G, and U according to the corresponding constituent nucleobase) can be chemically modified to modulate intra- or intermolecular RNA interactions. The first modified ribonucleoside to be identified was pseudouridine, an isomer of uridine resulting from internal transglycosylation (6,10,11). Present in transfer RNAs (tRNAs) and ribosomal RNAs (rRNAs), the fundamental components of translational machinery, pseudouridines stabilize RNA structure during protein synthesis. Methylation of ribose at the 2' position (2'-*O*-methylation) is another common modification that also plays an important structural role within rRNAs, tRNAs, and other small RNAs (1,12). The most abundant internal modification to mRNAs is the methylation of the adenosine to form N^6-methyladenosine (m6A). m6A is enriched in 5' and 3' untranslated regions (UTRs) and affects various aspects of RNA metabolism (13). There are many other types of RNA modifications including acylation, aminoacylation, hydroxylation, and thiolation (14).

Although many different types of RNA modifications exist, only a few of these constitute "RNA editing" events—broadly defined as any alteration in the primary nucleotide sequence of transcripts by means other than splicing (15). RNA editing encompasses several different types of modifications including nucleotide insertion, deletion, or substitution. This type of RNA processing was originally discovered in mitochondrial mRNAs of trypanosomes (16,17). In these organisms, extensive insertion and deletion of uridines via RNA editing can generate more than 50% of coding sequences in mature mitochondrial transcripts. Insertion/deletion editing requires cleavage of phosphodiester bonds in the RNA backbone and has only been described in kinetoplastids (6). By contrast, base substitutions converting cytidine-to-uridine (C-to-U) or adenosine-to-inosine (A-to-I) within intact RNAs are common editing mechanisms in all metazoans (18). Substitutional base editing was first demonstrated as a C-to-U modification in transcripts encoding apolipoprotein B (ApoB) (19-21). Editing at position 6666 within the ApoB mRNA converts a glutamine codon (CAA) to a stop codon (UAA) and produces a truncated form

of the ApoB protein that is functionally distinct from the full-length isoform. While both C-to-U and A-to-I editing represent mechanisms for generating diversity, the latter is more prevalent in higher eukaryotes and therefore is the focus of the current work. Except where otherwise noted, the term "RNA editing" (or simply "editing") will be used to refer only to A-to-I editing throughout the following sections and chapters.

Discovery of Adenosine-to-Inosine RNA editing

Foundational studies in the late 1980s characterized the developmentally-regulated unwinding of RNA:RNA hybrids formed by injection of antisense RNA into *Xenopus* oocytes (22,23). This unwinding activity was found to be specific for double-stranded RNAs (dsRNAs) as it was inhibited by molar excess of RNA duplexes, but unaffected by single-stranded RNA, single-stranded DNA, or double-stranded DNA (23). Upon further investigation, this unwinding resulted from destabilization, but not full denaturation, of RNA duplexes in which many of the adenosine residues were converted to non-canonical inosine (I) residues, thereby forming unstable I:U mismatches (24). Shortly thereafter, A-to-I conversions of *in vitro* transcribed RNA substrates were also detected in mammalian cell extracts (25,26).

Initial discoveries of endogenous RNA editing substrates relied upon the serendipitous identification of A-to-G discrepancies between genomic and complementary DNA (cDNA) sequences (27,28). Although experiments using thin-layer chromatography later confirmed the presence of inosine at the putative editing sites, such A-to-G disparities were initially presumed to represent A-to-I events based on the preferential base-pairing of both inosine and guanosine to cytidine during reverse transcription (28). Among the editing targets identified in this way were the GluA2 subunit of the α-amino-3-hydroxy-5-methyl-4-isoxazolepropionic acid (AMPA)-subtype of ionotropic glutamate receptor and the 2C-subtype of serotonin receptor ($5HT_{2C}$). These transcripts were shown to contain imperfect inverted repeats that give rise to hairpin-like

structures via intramolecular base-pairing. Moreover, specific adenosines within these targets were shown to undergo editing to change the amino acid coding potential and ultimately alter the function of the encoded proteins. Since these early studies, advances in DNA sequencing technology and the development of powerful computational pipelines have facilitated the identification of RNA editing sites across the transcriptome of many species (29).

Soon after the initial characterization of A-to-I editing in pre-mRNAs, three unique but related mammalian RNA editing enzymes were cloned and purified (30-33). Many subsequent studies have investigated their structures and functions, which are discussed in the following sections.

Adenosine Deaminases Acting on RNAs: Diversity of A-to-I editing enzymes within and across species

Adenosine is converted to inosine through a hydrolytic deamination catalyzed by adenosine deaminases acting on dsRNAs (ADARs) (31,32,34). Three members of the ADAR family—ADAR1, ADAR2, and ADAR3—are highly conserved within vertebrates (35,36). ADAR1 and ADAR2 are expressed in many tissues and deaminate a variety of dsRNAs with distinct but overlapping editing site preferences (37). ADAR3 expression is restricted to the brain but does not exhibit catalytic activity on any known substrate (33). Though ADAR3 appears only within the vertebrate lineage, orthologs of ADAR1 and/or ADAR2 are found in the genomes of all metazoans including primitive chordates (38). For example, *Caenorhabditis elegans* and *Doryteuthis pealeii* each possess two ADAR genes, CeADR1-2 and SqADAR1-2, respectively; and *Drosophila melanogaster* possesses a single ADAR2-like gene, dADAR (39-42).

The transcripts encoding ADARs undergo a number of RNA processing events that can in turn modulate the activity of these enzymes. Transcription of ADAR1 initiating from an interferon-inducible promoter generates an alternatively spliced 150 kilodalton (kD) ADAR1

protein isoform (p150) that exhibits some properties different from those of the ADAR1 p110 isoform arising from a constitutively active promoter (43,44). Like ADAR1 p110 and ADAR2, ADAR p150 is catalytically active. While ADAR1 p110 and ADAR2 primarily localize to the nucleus, ADAR1 p150 accumulates in the cytoplasm (45). Interestingly, ADAR2 transcripts are also subject to alternative splicing as a direct consequence of ADAR2 editing its own intronic sequence, creating a site that is recognized as an alternative 3' splice acceptor (46). This event ultimately decreases the level of ADAR2 protein expression and thus serves as an autoregulatory mechanism (46,47).

ADAR structure

All ADAR proteins have a common modular structure with one to three dsRNA binding domains (dsRBDs) as well as a nuclear localization signal in the amino terminus, and a deaminase domain in the carboxyl terminus (Figure 1.1) (32,48,49). In addition to these shared features, both ADAR1 isoforms (p110 and p150) harbor amino-terminal Z-DNA binding domains, but only ADAR1 p150 contains a nuclear export signal (50). ADAR3 is the only ADAR family member that has an arginine-rich domain for binding single-stranded RNA (51).

ADARs share a common ancestry with other nucleoside deaminases including adenosine deaminases acting on free nucleosides (ADAs), adenosine deaminases acting on tRNAs (ADATs), and cytidine deaminase (CDAs) (49). As members of the adenosine and cytidine deaminase superfamily, these enzymes are defined by the presence of a Zinc Dependent Deaminase (ZDD) (49). The ZDD contains a conserved amino acid motif: (H/C)xEx$_{25\text{-}30}$PCxxC, where H represents histidine, C represents cysteine, x represents any amino acid, E represents glutamate, and P represents proline (52). Proteins harboring a ZDD motif have a helix-strand-helix structure that coordinates a zinc ion to activate a water molecule for nucleophilic attack

during hydrolytic deamination. Mutations that displace water at this site abolish catalytic activity (53). Interestingly, structural and phylogenetic data suggest that ADARs and ADATs are more

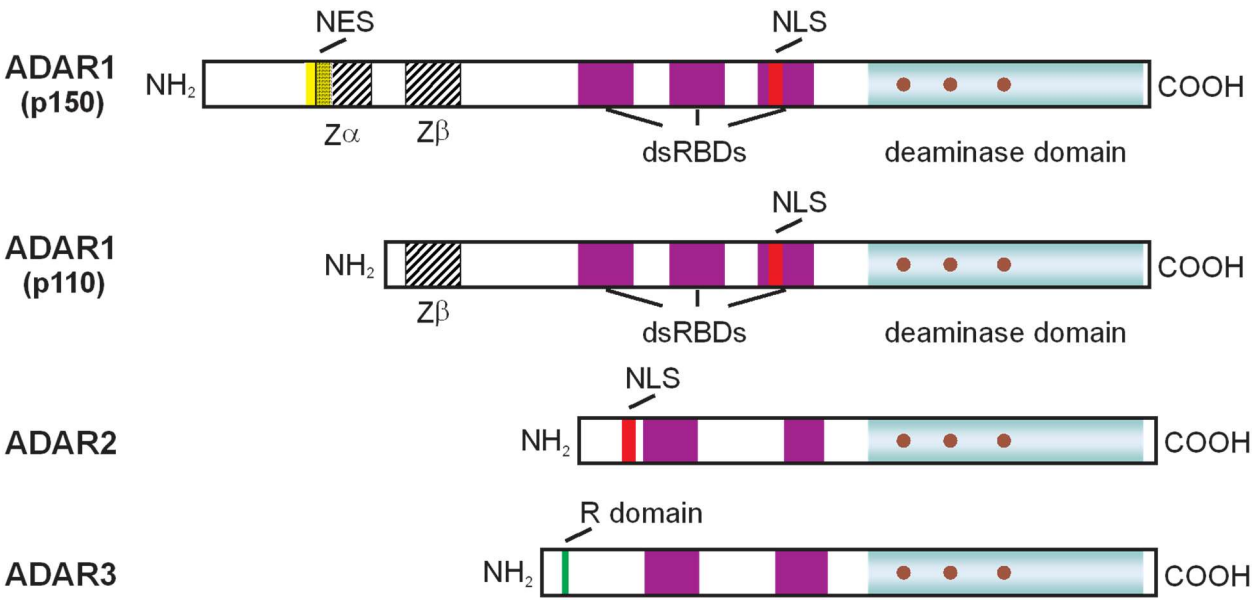

Figure 1.1. Domain organization of ADAR family members. Protein domain organization for each ADAR family member is shown. Purple rectangles represent double-stranded RNA binding domains (dsRBDs), blue rectangles represent deaminase domains, hatched rectangles represent Z-DNA binding domains, and the green rectangle represents an arginine rich (R) domain. Nuclear localization signals (NLS) and nuclear export signals (NES) are represented by red and yellow rectangles, respectively.

closely related to CDAs than ADAs (48,54). Whereas the core deaminase domains of ADAs contain an 8-stranded α/β barrel, those of ADARs and CDAs include a conserved motif comprising a 5-stranded β-sheet flanked by a single α-helix on one side (α1) and two α-helices on the opposite side (α2 and α3) (55-60). Within the ADAR family, the deaminase domains of ADAR1 and ADAR2 exhibit high amino acid sequence similarity, possessing 39% sequence identity and 59% sequence similarity (61).

The crystal structure of the ADAR2 deaminase domain revealed a globular structure comprising 10 α-helices and 11 β-strands with intervening loops, measuring approximately 40 Å in diameter (58). This structure also confirmed the presence of a zinc ion that is buried in a pocket of the active site and coordinated by the conserved histidine and cysteine residues of the ZDD within the α2 and α3 helices. A structural element that distinguishes ADARs from ZDD-harboring CDAs is the presence of a loop bearing threonine 375, which sterically clashes with pyrimidines to obstruct their entry into the active site, and thus precludes ADAR deamination of cytidine to uridine. Another interesting feature revealed by the crystal structure of the ADAR2 deaminase domain is the presence of myo-inositol-1,2,3,4,5,6-hexakisphosphate (IP_6) bound deep in the catalytic core via extensive hydrogen bonding interactions with basic residues. IP_6 is required for ADAR activity as disruption of the IP_6 biosynthetic pathway in yeast prevents expression of ADAR (58). It is believed that IP_6 assists in proper folding of the carboxy terminus (58).

Characterization of the dsRBDs of ADAR2 via nuclear magnetic resonance (NMR) spectroscopy revealed the canonical “αβββα” dsRBD topology: a three-stranded antiparallel β-sheet with two α-helices on one side (62-67). Like the dsRBDs of most other proteins, ADAR2 dsRBDs recognize A-form RNA helices through many interactions of conserved residues with 2’-hydroxyl groups of the phosphodiester backbone (68,69). The NMR structure showed that the second dsRBD of ADAR2 interacts with 12 base pairs of dsRNA through contacts formed with two minor grooves and the intervening major groove (70). Although recognition of RNA duplexes by dsRBDs was originally thought to be mediated in a sequence-independent manner, the NMR

solution structure of ADAR2 dsRBDs complexed with the GluA2 substrate revealed that these dsRBDs make sequence-specific contacts with the minor groove (70). The unique features of dsRBDs within individual proteins may inform how different proteins select distinct dsRNA substrates. Substitution of the dsRBDs of ADAR2 with those of the dsRNA-activated protein kinase (PKR) results in a near-complete loss of editing, whereas mutation of select residues of the second dsRBD of ADAR2 affects the editing of only a subset of ADAR2 substrates (67,70,71). Moreover, deletion of the first or third dsRBD of ADAR1 significantly reduces editing efficiency, while deletion of the second dsRBD has little effect (53). Taken together, these data indicate that functional selectivity is largely dictated by ADAR dsRBDs.

An aspect of ADAR structural biology that remains contentious is the organization of ADAR monomers into oligomers. Though biochemical and fluorescence resonance energy transfer (FRET)-based experiments have confirmed that ADAR1 and ADAR2 can form homo- and heterodimers *in vitro* and *in vivo*, it is unclear if dimerization is necessary for enzymatic activity (72,73). One study has also reported that ADAR2 exists primarily as a monomer (74). Whether or not ADAR dimerization depends on RNA binding is also debatable (75-77).

ADAR catalytic mechanism

A mechanism for the hydrolytic deamination catalyzed by ADARs has long been proposed based on the mechanisms employed by similar enzymes such as CDAs and ADATs (78-80). Though mutagenic analyses and RNAs containing nucleoside analogs have been useful in probing the editing reaction, recent NMR and X-ray crystallographic characterization of human ADAR2 bound to dsRNA have further enriched the current understanding of ADAR structure-function relationships and have provided important insights into the editing mechanism (81,82).

In addition to dsRBD interactions, ADARs also make critical RNA contacts in regions 5’ and 3’ to the editing site via binding loops within the deaminase domain. The ADAR2 catalytic

domain contains two loops, loop 347-352 and loop 584-597, that bind 3' of the editing site (61,82). Each of these loops contain a basic residue (R348 and K594) that contact the RNA and decrease editing activity when mutated to alanine (82). The 5' binding loop comprises amino acids 454-477 that have an ill-defined structure in the absence of RNA but adopt an ordered conformation once bound to the substrate, suggesting that this region plays an important structural role (58,61). Unlike the 3' loops of ADAR2, which are conserved between either ADAR1 or ADAR3, the 5' loop differs substantially between members of the ADAR family, suggesting that the 5' loop may participate in ADAR-specific aspects of substrate selection or function (61).

Upon binding to a dsRNA substrate, ADARs access the target adenosine by flipping this base out of the RNA helix and into the active site of the enzyme—a mechanism similar to that employed by the DNA methyltransferase, HhaI (82,83). In ADAR2, the base-flipping loop includes a conserved glutamate (E) 488 (corresponding to E1008 in ADAR1) flanked by conserved glycines. This loop approaches the RNA helix from the minor groove side of the target adenosine where E488 intercalates into the helix, occupying the space vacated by the flipped-out adenosine (82). The role of E488 in helix penetration explains why this residue is flanked by flexible glycines that accommodate such a conformational change (84). Consistent with the notion that these glycines endow the ADAR base-flipping loop with conformational flexibility, screening of ADAR1 mutant libraries showed that only small residue substitutions were permitted at position 1007 (84). Mutation of this residue to an arginine (G1007R mutation) is associated with the inherited encephalopathy, Aicardi-Goutieres syndrome, further underscoring the critical function of the ADAR base-flipping loop (85). Other mutations in this loop serve to enhance ADAR catalytic activity. For example, Wang and colleagues showed that mutation of ADAR1 E1008 to a glutamine (E1008Q) or a histidine (E1008H) created enzymes that are more catalytically active than the wild-type protein (84). Similarly, screening of an ADAR2 mutant library revealed that an E488Q mutation created an ADAR2 hypermutant (86). Though wild-type ADAR2 and the E488Q mutant exhibit similar substrate binding affinities, the E488Q mutant induces a greater increase

in fluorescence of a 2-aminopurine (2-AP) modified dsRNA (86). As 2-AP fluorescence is quenched when buried within a duplex and increases upon release from this electronic environment, the increased 2-AP fluorescence induced by the E488Q mutant suggests that this mutant base-flips more efficiently than wild-type ADAR (86-88). Crystal structures of both the wild-type and E488Q mutant ADAR bound to dsRNA demonstrated that both proteins stabilize the flipped-out RNA conformation by hydrogen bonding with the complementary-strand base across from the flipped-out adenosine ("orphaned base"; Figure 1.2) (82). If E488 accomplishes this task by donating a hydrogen bond to the orphaned base, such an interaction would require E488 protonation (82). While the pKa of E488 is unknown, the catalytic rate enhancement exhibited by the E488Q mutant, which is fully protonated under physiologically relevant conditions, suggests that E488 may not be fully protonated at a physiologically relevant pH (82,86). The protonation of this residue is further explored in Chapter IV. It is also unknown whether E488 plays a role in activating the target adenosine for base-flipping or if this residue simply interacts with the orphaned base (61).

ADARs, as well as other nucleoside deaminases, use a catalytic mechanism in which zinc-activated water attacks the carbon bound to the amino group that departs by the end of the reaction (Figure 1.3) (56,89). Within the ADAR active site, the zinc ion is coordinated by conserved histidine and cysteine residues as well as a water molecule (58). ADAR2 E396 deprotonates this water molecule, generating a reactive zinc-hydroxide (55). This nucleophilic species then attacks C6 of the adenosine flipped into the active site, forming a high-energy intermediate with a tetrahedral center at C6 and disrupting the aromaticity of the purine ring (55). This type of reaction constitutes a Substitution, Nucleophilic, Aromatic (S_NAr) mechanism, and the high-energy species formed during S_NAr is referred to as the Meisenheimer intermediate (55). Because the Meisenheimer intermediate lacks the stability afforded by ring aromaticity, it is less stable than either adenosine or inosine. Kinetic studies of ADAR2 deamination using RNAs containing the adenosine analog 8-azaadenosine, which substitutes carbon with a more electronegative nitrogen

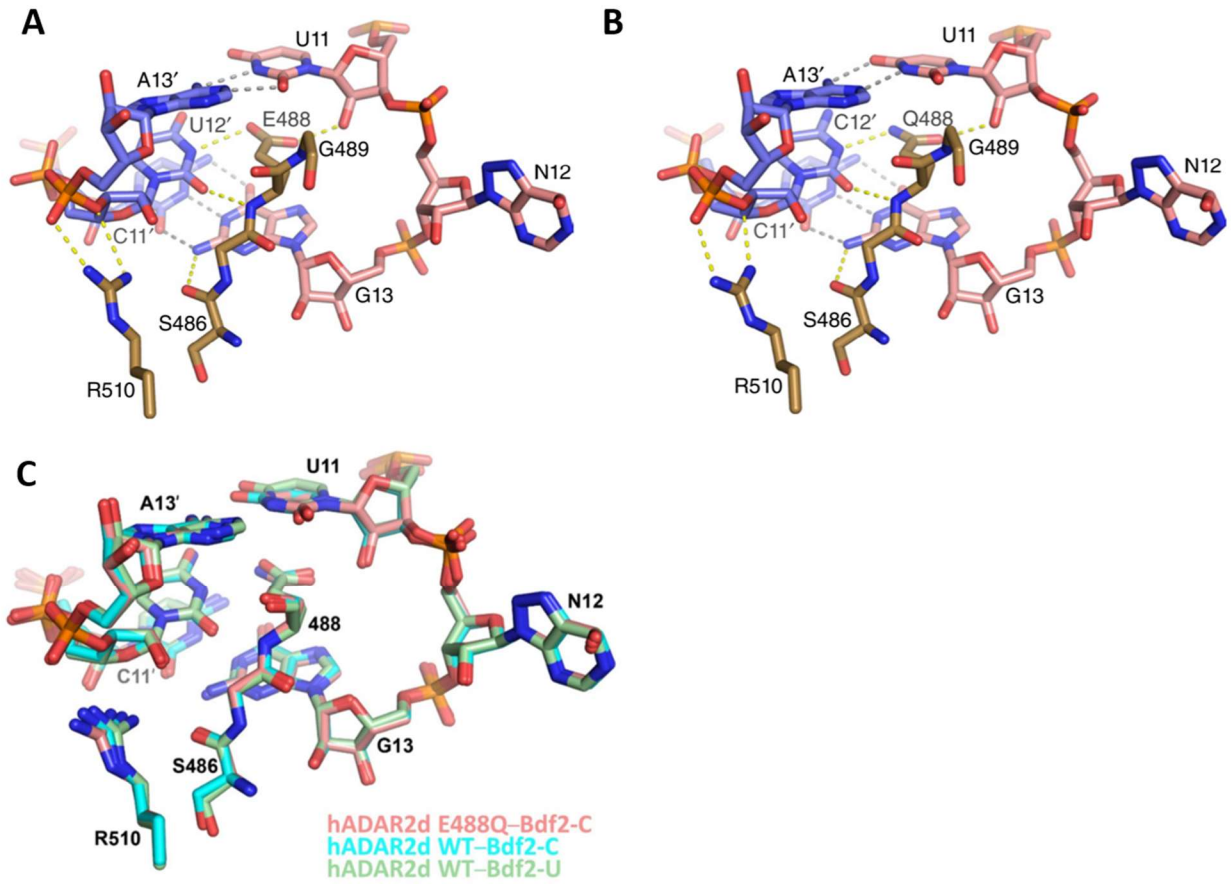

Figure 1.2. ADAR2 contacts with orphaned nucleotide. (**A**) The crystal structure of the wild-type human ADAR2 (hADAR2) helix penetrating residue, glutamate (E) 488, in complex with Bdf2 RNA containing a uridine opposite the editing site (Bdf2-U). The edited RNA strand is shown in pink, the complementary RNA strand is shown in blue, and ADAR deaminase domain residues are shown in brown. Dashed lines represent hydrogen bonding. (**B**) The crystal structure of the mutant hADAR2 helix penetrating residue, glutamine (Q) 488, in complex with Bdf2 RNA containing a cytidine opposite the editing site (Bdf2-C). Dashed lines represent hydrogen bonding, and colors are as in **A**. (**C**) Overlay of wild-type and E488Q mutant hADAR2 in complex with either Bdf2-U or Bdf2-C RNA. Adapted from Matthews et al., 2016 (82).

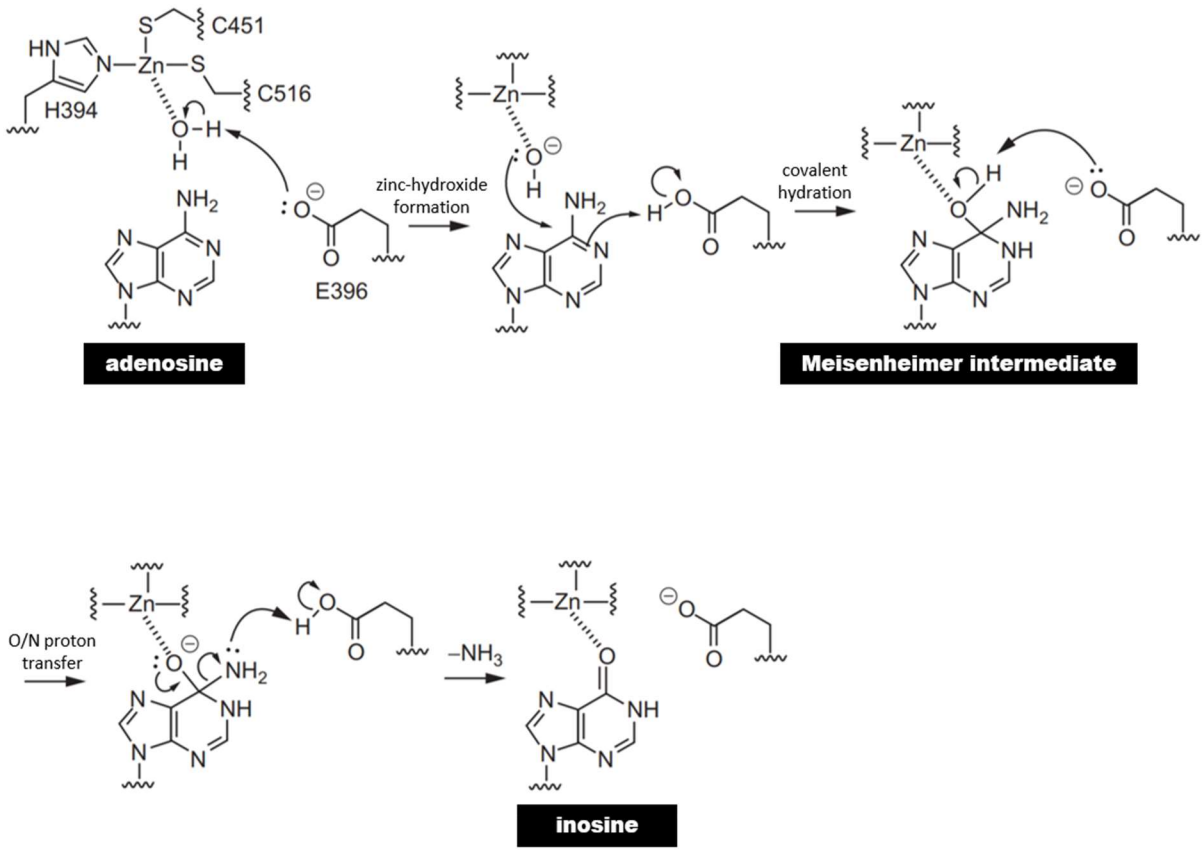

Figure 1.3. ADAR2 catalytic mechanism. Steps in the proposed ADAR2 deamination mechanism. Adapted from Wang et al., 2017 (61).

atom at the 8-position, indicate that hydration of the nucleoside is rate-limiting in the editing reaction (90,91).

Another nucleoside analog, 8-azanebularine, was used in x-ray crystallographic experiments to study the RNA-protein complex during base-flipping (82). Because the covalent hydrate of 8-azanebularine mimics the Meisenheimer intermediate, but lacks the C6 amino group, it cannot continue along the reaction pathway and traps the flipped-out conformation (82,91,92). Analysis of this structure revealed that six ADAR2 residues contact the flipped base: V351, T375, K376, E396, C451, and R455 (82). Three of these residues—T375, K376, and R455—contact the 5' and 3' phosphodiester groups of the flipped nucleotide, presumably to anchor the flipped base within the enzyme active site. E396, V351, and C451 directly contact the flipped nucleobase (61,82). Once the Meisenheimer intermediate is formed, E396 mediates a proton transfer from the C6 hydroxyl group to the C6 amino group (55). The protonated amino group then leaves as a molecule of ammonia, resulting in the formation of the product, inosine (55). Finally, the ADAR activity resets as inosine exits the active site, the RNA detaches from ADAR, and zinc binds another molecule of water (55).

Cis-regulatory elements for A-to-I editing

ADARs only perform hydrolytic deamination on dsRNAs, which may have perfect or imperfect complementarity between strands (23). Perfect duplexes exhibit non-selective editing of up to 50% of adenosine residues in both strands, while imperfect duplexes contain only one or a few adenosines that undergo site-specific deamination (93,94). Within imperfect duplexes, evolutionarily conserved structural elements such as bulges, terminal loops, internal loops, and base-pair mismatches can positively or negatively affect the extent of editing through distinct interactions with each ADAR (95-98). The structure of the 71-nucleotide stem loop containing one of the major editing sites in the GluA2 transcript ("R/G" site) has been determined in two fragments

by solution NMR (67,70). One of the fragments revealed the apical stem-loop structure: a rigid hairpin stabilized by hydrogen bonds and stacking interactions, and capped with a terminal GCUAA pentaloop (67). Modification or deletion of this pentaloop reduced the level of ADAR2-mediated editing. Analysis of the second fragment revealed that the structure surrounding the R/G site is a regular A-form helix despite the presence of several base-pair mismatches (70). Using a technique to monitor the protonation of adenine during a pH titration, it was shown that two adenines involved in A•C mismatches are protonated or partially protonated below pH 8.5, thereby forming A^+•C wobble pairs that minimally distort the A-form helix (70). Some evidence suggests that RNA tertiary structure also contributes to ADAR substrate recognition (99).

Aside from RNA structure, cis-active elements including the base opposite the target adenosine and flanking sequences play a role in modulating RNA editing. The target adenosine is commonly found in A:U pairs or A•C mismatches, but is rarely found opposite a guanosine or adenosine (61,100,101). In fact, when the opposing base is mutated from a pyrimidine to a purine, ADAR1 and ADAR2-mediated editing is drastically reduced (100). ADARs exhibit an opposite base preference because they interact with this position as it becomes orphaned during base-flipping of the target adenosine. When E488 in ADAR2 or E1008 in ADAR1 penetrate the RNA helix to stabilize the flipped-out conformation, these intercalating residues can form hydrogen bonds with a cytidine or uridine (82). However, a purine at the orphan base predicts a steric clash with the intercalating ADAR residue and therefore would decrease base-flipping efficiency (82).

Sequence context is another factor determining how particular adenosines within imperfect RNA duplexes are targeted for deamination by ADARs. ADAR1 and ADAR2 exhibit a 5’ nearest neighbor preference of U > A > C > G, and a 3’ nearest neighbor preference of G > C ~A > U and G > C > U ~A, respectively (86,102). ADARs lacking dsRBDs, as well as chimeric ADARs in which the ADAR1 and ADAR2 catalytic domains are exchanged, exhibit nearest neighbor preferences like those of wild-type ADARs (100,102). Interestingly, the ADAR2 E488Q mutant also exhibits similar preferences, but the hypermutant deaminates adenosine more

efficiently than the wild-type enzyme regardless of whether the target adenosine exists in a favored sequence context, 5'-UAG-3', or an unfavorable sequence context, 5'-GAC-3', where A represents the target adenosine (86). Taken together, these data suggest that the ADAR catalytic domain is essential in establishing 5' and 3' flanking sequence preferences. However, NMR structures of the GluA2 R/G stem-loop complexed with ADARs show that the dsRBDs also make sequence-specific contacts (70). Binding assays demonstrated that mutation of any of the bases recognized in a sequence-dependent manner by the dsRBDs decreases ADAR binding affinity (70). Furthermore, *in vitro* editing assays showed that mutation of any of the residues involved in making sequence-specific contacts also decrease editing activity (70).

Functional consequences of A-to-I editing

Advances in sequencing technology and omics research spurred the identification of millions of RNA editing sites in the transcriptomes of humans and other species (29). Editing events can be categorized into one of two major types: site-selective editing and hyper-editing (103-109). As discussed previously, the former affects one or few adenosines within an imperfect RNA duplex, while the latter involves the deamination of adenosine clusters within long, perfect or near-perfect RNA duplexes formed by base-pairing of inverted repeats. The frequency of editing at a given site depends upon the proportion of transcripts containing an inosine at that position within a sample, and ranges between 0-100% (the quantification of editing is discussed in more detail in Chapter II). Although hyper-editing constitutes the vast majority of editing events in the human transcriptome, the level of editing at each of these sites is generally low (104). By contrast, site-selective editing events in all vertebrates are rare but relatively efficient (110). Despite their differences, both types of editing contribute to transcriptome diversification through the creation of inosines that are recognized as guanosines by various cellular machines, and ultimately bear important consequences on many aspects of physiology (111,112).

RNA editing is widespread in humans owing to the primate-specific expansion of short interspersed nuclear elements (SINEs) called Alu sequences (113). Comprising approximately 10% of the human genome, Alu repeats are inverted sequences of ~300 base pairs that are primarily present within non-coding regions, especially UTRs and introns (113). Hyper-editing of Alu elements may regulate gene expression by creating or deleting splice sites, influencing RNA nuclear retention, and suppressing the synthesis of endogenous short interfering RNAs (111,114-118). The editing of Alu repeats has also been proposed as a mechanism to prevent retrotransposition of Alu sequences into the genome (105,112-114).

While the non-selective editing of Alu elements may influence gene expression, hyper-editing also plays an essential role in innate immunity. During pathogenic infections, cells recognize pathogen associated molecular patterns (PAMPs) using pattern recognition receptors (PRRs) whose signaling ultimately triggers innate immune responses (119). Upon viral infection, viral dsRNA genomes or replication intermediates are primarily detected by two cytosolic PRRs: retinoic acid-inducible gene I (RIG-I) and melanoma differentiation-associated protein 5 (MDA5) (119). These receptors then signal to mitochondrial antiviral signaling adaptor protein (MAVS), activating interferon signaling pathways (119). Interestingly, interferon production stimulates the transcription of the cytoplasmic ADAR1 p150 isoform, which in turn edits viral dsRNAs to produce both proviral and antiviral effects (43,120-122). Moreover, ADAR1-null mice exhibit elevated interferon signaling, failed liver hematopoiesis, and die during embryonic development (123). These phenotypes can be rescued with concurrent deletion of either MDA5 or MAVS, suggesting that ADAR1 hyper-edits endogenous, long dsRNAs to prevent activation of immune responses by host RNAs (124,125).

The site-selective editing of microRNAs (miRNAs) expands the regulatory capacity of this class of RNAs. MiRNAs are ~22-nucleotide non-coding RNAs generated from the processing of long, precursor miRNA hairpins by Drosha and Dicer enzymes (126). Mature miRNAs are then loaded into the RNA-induced silencing complex (RISC) where they bind with partial

complementarity to miRNA response elements (MREs) generally located within the 3'-UTRs of target mRNAs to promote mRNA degradation and/or inhibition of protein translation (126). Editing of precursor miRNA species can alter the processing of primary miRNA transcripts (pri-miRNAs) by Drosha or pre-miRNAs by Dicer; alternatively, editing can redirect miRNAs to different mRNAs by modifying the miRNA seed sequence which allows appropriate recognition of targeted mRNAs or the MREs within targeted mRNAs themselves (127-129).

One of the most well-studied functions of site-selective RNA editing is the alteration of codons within mRNAs. During translation, such editing events change codon:anticodon interactions. In contrast to the amino group at the 6-position of adenosine, which donates a hydrogen bond, the carbonyl group at the 6-position of inosine accepts a hydrogen bond—a feature reminiscent of the base-pairing properties of guanosine (130). Depending on the codon position to which editing introduces an inosine, interpretation of inosine as a guanosine by different tRNAs may result in non-synonymous amino acid substitutions during peptide synthesis (130). A recent investigation using an *in vitro* translation system and mass spectrometry confirmed that inosine is primarily decoded as a guanosine, although it may occasionally be decoded as uridine or adenosine (131). Studies also have shown that transcripts containing multiple inosine residues in close proximity may induce ribosome stalling and premature translation termination (130,131).

Evidence from studies of RNA editing for GluA2 transcripts further support the notion that inosine is decoded as guanosine during translation. Editing of a particular GluA2 site (Q/R site) changes a CAG codon to a CIG codon, which ultimately predicts a glutamine to arginine substitution within the pore loop domain of the encoded protein (27). AMPA receptors containing GluA2 subunits with a glutamine at the Q/R site are calcium permeable, but similar channels with an arginine at the same position are calcium impermeable (132). Consistent with the idea that GluA2 editing results in an amino acid substitution that alters calcium permeability of the ion channel, mice harboring an editing-incompetent GluA2 allele exhibit an excitotoxic phenotype,

developing epileptic seizures and dying by postnatal day 21 (133). Interestingly, ADAR2-null mice display a virtually identical phenotype (134). However, the seizures and early lethality exhibited by ADAR2-null mice are rescued by genomic encoding of guanosine at the Q/R site to yield solely arginine-containing GluA2 subunits (134). Taken together, these data not only suggest that inosine is decoded as guanosine *in vivo*, but also demonstrate that GluA2 editing by ADAR2 is absolutely essential for the normal development and function of the brain.

Beyond the Q/R site of GluA2, editing of numerous other transcripts predicts protein recoding events. Most of these recoding events affect the function of ADAR2 targets expressed in the brain, suggesting that such events are important for central nervous system function. For example, editing of five adenosines in $5HT_{2C}$ transcripts can change the identity of three amino acids within the second intracellular loop of the encoded G-protein coupled receptor. Combinatorial editing of these five sites gives rise to 32 different mRNA isoforms and 24 possible protein isoforms. In general, the extent of $5HT_{2C}$ editing is inversely correlated with the G-protein coupling efficiency and constitutive activity of the receptor (28). Another well-studied target of editing is the voltage-gated potassium channel, Kv1.1. Editing of transcripts encoding Kv1.1 affects inactivation kinetics of the encoded ion channel (135). While many recoding events alter the function of ion channels and neurotransmitter receptors expressed in the brain, other recoding events influence signaling mechanisms in various organ systems. One such example is the editing of transcripts encoding Caps1, which changes a genomically encoded glycine to a glutamate codon to promote dense core vesicle exocytosis (136). Yet another example is the editing-mediated conversion of an arginine to glycine codon in the mRNA encoding the transcription factor Gli1, which plays a role in the modulation of the Hedgehog signaling pathway (137).

Approximately 3% of human transcripts contain an editing site that predicts a protein recoding event, and only about 25 of these editing events are conserved within the mammalian lineage (138). Interestingly, squid, cuttlefish, and octopus extensively edit their transcripts to

generate increased diversity of the transcriptome and proteome, and it is believed that such transcriptomic plasticity in cephalopods is achieved at the expense of genome evolution (139). While cephalopod protein recoding via RNA editing appears to be adaptive, comparative genomic studies have suggested that such editing events in humans are generally neutral or nonadaptive (139,140). However, whether mammalian recoding events provide a functional advantage under altered physiologic conditions remains an active area of investigation.

Modulation of A-to-I editing

The identification of millions of editing sites across the transcriptomes of humans and other organisms spurred efforts to better understand spatiotemporal regulation of RNA editing profiles. A recent study analyzed the RNA "editome" across thousands of tissue samples collected from humans, non-human primates, and mice to survey the RNA editing landscape in mammals (141). Results from this study revealed that the overall level of editing between human tissues is similar, but comparing editing levels only in coding regions differentiates editomes among these various tissues. Arterial and brain tissues demonstrate the highest levels of editing, while skeletal muscle exhibits the lowest levels of editing. Principal component analysis of editomes across tissues from different species showed that editing levels more strongly correlated with species rather than tissue type, suggesting that species-specific *cis* regulatory elements play a larger role than tissue-specific *trans*-acting regulators in determining overall levels of editing. However, editing within coding regions relies more heavily on *trans*-regulation than editing in repetitive sequences. The same study also examined the developmental regulation of editing in several mouse tissues and found that editing in the fetal liver is greater than that in the brain between embryonic days 12 and 13, which is consistent with the timing of embryonic lethality and liver failure in ADAR1-null mice (123). Moreover, editing increases developmentally in the brain but not in other tissues.

In addition to normal spatiotemporal variation in editing, RNA editing levels vary with various physiologic or pathologic conditions. In 2015, three large-scale studies of RNA editing in various cancer types concluded that editing is generally elevated in the majority of examined cancers, and that this increased editing not only drives transcriptomic diversity in tumors, but is also associated with poor clinical prognosis (142-144). Because pathways that promote tumor growth are also involved in the regulation of hypoxic responses, the link between hypoxia and RNA editing also has been investigated. Several studies have reported increases in RNA editing in response to hypoxia (145-147). Another recent study found that ADAR1 promotes hypoxia signaling by inhibiting negative regulators of a key component of the hypoxia signaling network, hypoxia inducible factor-1α (148). Furthermore, *Drosophila* mutants with a dADAR loss-of-function mutation demonstrate increased vulnerability to oxygen deprivation and neuronal degeneration during aging (149).

Given the prevalence of editing events affecting transcripts expressed in the brain, it is not surprising that aberrant editing also is associated with neurological disorders. Decreased editing of the GluA2 Q/R site was found in patients with sporadic onset of progressive motoneuron degeneration in amyotrophic lateral sclerosis (ALS) (150). Conditional deletion of ADAR2 in mouse motor neurons causes a neurodegenerative phenotype similar to that in ALS, but can be rescued by genomic encoding of a guanosine at the Q/R site of GluA2 mRNAs (151). These data suggest that loss of ADAR2-mediated GluA2 editing may contribute to the neuronal excitotoxicity and cell death underlying ALS pathogenesis. Interestingly, hyperediting of the GluA2 R/G site has been reported in the hippocampus of patients with epilepsy (152). Several studies using rodent models of epilepsy also have demonstrated increased RNA editing in the brain (153,154). These findings prompted studies to examine now neural activity influences RNA editing. In general, neuronal depolarization increases editing while neuronal silencing decreases editing, and these activity-dependent changes involve changes in intracellular calcium (155,156). Taken together, these data indicate a role for RNA editing in the maintenance of neural excitability.

Evidence from studies in invertebrates further support a role for RNA editing in the control of neural excitability. Studies using *Drosophila* model systems have shown that ADAR overexpression or knockdown results in decreased or increased neuronal excitability, respectively (157). As discussed previously, cephalopods extensively edit transcripts to alter the function of many proteins, especially transporters and ion channels expressed in the nervous system. A seminal study by Garrett and Rosenthal demonstrated that polar and tropical octopuses differentially edit orthologous transcripts encoding Kv1.1 to alter the closing kinetics of this voltage-gated potassium channel (158). They found that polar octopuses edit a particular site (predicting an isoleucine-to-valine substitution at position 321) more highly than tropical octopuses. Importantly, the inclusion of a valine at residue 321 accelerates channel closure by destabilizing the open state. This mechanism in turn helps polar octopuses maintain rapid rates of neuronal firing at cold temperatures, which would otherwise prolong action potential duration and limit repetitive firing in poikilotherms. A similar inverse correlation between temperature and RNA editing also has been demonstrated in *Drosophila* (159).

Because editing can generate transcriptional and protein diversity through various mechanisms including the creation or alteration of splice sites, alteration of miRNA processing, and modification of the biophysical properties of proteins, it has been proposed that editing may be a dynamically regulated process that endows biological systems with functional plasticity (160). The normal spatiotemporal variation in RNA editing profiles may represent an epitranscriptional signature that helps to define the functional specialization of cells in a particular region or during a particular developmental period. Moreover, alterations of editing profiles in various pathological states or in response to altered physiological conditions implicates a role for RNA editing in the fine-tuning of cellular homeostatic or acclimatory responses. Though a few studies, mostly in invertebrates, have demonstrated dynamic modulation of RNA editing, it is unclear how such changes in editing are mediated and whether vertebrates are also capable of dynamically modifying RNA editing profiles in response to a physiologic stimulus.

To better understand the modulation of RNA editing, several comprehensive studies have investigated the relationship between ADAR expression and the extent of editing in different tissues and cell lines. The majority of these reports have concluded that ADAR expression levels are not well-correlated with RNA editing levels (141,161-164). Indeed, one study calculated that ADAR1 and ADAR2 respectively account for 20%, and 2.8% of variation in editing of repetitive sequences, and 6% and 25% of variation in editing of protein-coding sites (141). The catalytically inactive ADAR3 negatively regulates editing, presumably by competitive binding to ADAR1 and ADAR2 substrates. When all three ADARs are considered, ADAR expression accounts for more, but not all, variation in editing levels. Because ADAR expression cannot fully account for variation in editing, identification of other *trans*-acting regulators of editing has become an area of great interest. Among the first identified regulators of ADAR were peptidyl-prolyl isomerase NIMA interacting protein 1 (Pin1) and WW domain containing E3 ubiquitin protein ligase 2 (WWP2) (165). Pin1 promotes RNA editing of the GluA2 Q/R site by driving nuclear localization and stabilization of ADAR2, while WWP2 inhibits Q/R site editing by targeting ADAR2 for proteasomal degradation. Another negative regulator of ADAR is aminoacyl tRNA synthase complex-interacting multifunctional protein 2 (AIMP2) (141). AIMP2 has been shown to promote the degradation of ADAR1 and ADAR2, and its expression is abundant in skeletal muscle, which has the lowest editing levels of all human tissues (141). Recent work using a BioID-based approach to identify *trans*-regulators of RNA editing has revealed a role for all DZF-domain-containing proteins: ILF2, ILF3, STRBP, and ZFR (166). These DZF-domain containing proteins appear to exert their influence by binding to the same RNAs as ADARs. The *Drosophila* homolog of ZFR, Zn72D, is a positive regulator of editing, whereas ILF3 is a negative regulator (163,166). Though significant progress has been made in identifying *trans*-regulators of editing, there are likely many additional factors contributing to the complex modulation of RNA editing.

Summary

Adenosine-to-inosine RNA editing is a post-transcriptional mechanism for generating RNA and protein diversity and has a broad range of effects on various cellular pathways. Millions of editing sites have been discovered, and their discovery has prompted research on the *cis*- and *trans*-acting factors that modulate editing. Though some of the fundamental components involved in editing are known, including essential RNA sequence and structural features, aspects of ADAR structure and catalytic mechanism, and regulators of ADAR proteins, many molecular details and the functional outputs generated by cell-specific editing are ill-defined. Here, we investigate such previously unexplored topics in RNA editing:

In Chapter II, the methods used to quantify A-to-I editing are reviewed and compared. The approaches discussed in this chapter are used to analyze the extent of editing in subsequent chapters.

In Chapter III, we employ a cell-specific specific approach to investigate the *in vivo* modulation of $5HT_{2C}$ editing. We investigate how specific $5HT_{2C}$-mediated behaviors regulate—and are regulated by—particular $5HT_{2C}$ RNA editing profiles.

In Chapter IV, we investigate mechanisms by which ADAR catalytic activity can be modulated to influence the extent of site-specific editing.

Finally, in Chapter V the conclusions and future directions from the studies detailed in Chapters III and IV are discussed.

Chapter II

Quantitative Analysis of Adenosine-to-Inosine RNA editing

Introduction

The conversion of adenosine-to-inosine (A-to-I) by RNA editing is a post-transcriptional mechanism for increasing the diversity of the proteome and for modulating innate immune tolerance for host double-stranded RNAs formed by endogenous sequences (124,160). Common methods for the detection and quantification of A-to-I modifications have exploited the preferential base pairing of inosine with cytosine during reverse transcription (RT) to generate cDNA libraries or polymerase chain reaction (PCR) amplicons containing guanosine at the edited positions. These apparent guanosine (G) substitutions can be detected by various DNA sequencing methodologies. Pioneering studies on the RNA editing of transcripts encoding the GluA2 subunit of the α-amino-3-hydroxy-5-methyl-4-isoxazolepropionic acid (AMPA)-subtype of ionotropic glutamate receptor and the 2C-subtype of serotonin receptor ($5HT_{2C}$) determined editing levels using molecular cloning and Sanger sequencing strategies (27,28). RT-PCR amplicons were subcloned into plasmid or phage vectors, transformed or transduced into microbial hosts, and then purified from single clonal colonies or plaques before being subjected to Sanger sequencing. Although such clone-based sequencing provided information about the relative proportion of distinct RNA isoforms, the accuracy and precision of this approach was limited by the number of clones sequenced.

Next-generation sequencing (NGS) revolutionized almost all aspects of modern molecular biology and genetics, permitting more efficient, sensitive, and accurate identification and quantification of transcriptome-wide RNA editing events. Pyrosequencing emerged as the first major NGS technology, but was later supplanted by Illumina NGS platforms. Illumina platforms rely on sequencing by synthesis chemistry that effectively eliminate the erroneous base calls in homopolymeric sequences that were a common pitfall of pyrosequencing (167). A comparison of murine $5HT_{2C}$ RNA editing profiles generated by each of these NGS technologies revealed decreased accuracy and greater experimental variability for pyrosequencing than Illumina sequencing (168). As the most widely adopted NGS technology, Illumina platforms have been used in whole-transcriptome analyses as well as targeted RNA-sequencing studies. Although transcriptome profiling has been useful for identifying novel RNA editing sites, more targeted approaches increase the sequencing depth of transcripts expressed at low levels and therefore are better-suited to accurately quantify editing of specific sites (110,169). High-throughput strategies for targeted RNA sequencing leverage single- or dual-indexed library preparations to simultaneously quantify the editing of many editing targets across multiple samples (161,169).

Today, direct sequencing of RT-PCR products, by either Sanger sequencing or NGS, is the most common method of assessing RNA editing profiles (170). Quantification of editing by NGS data analysis requires a bioinformatic pipeline involving a comparison of target sequences to edited and non-edited reference sequences (108,171). RNA editing also can be determined from Sanger sequencing-derived electropherograms where edited positions appear as mixed A/G peaks, and the relative height of each peak is proportional to the number of transcripts containing A or G at that position within the complex RNA population of a given sample (102,172). As it is not possible to use Sanger sequencing to differentiate between editing permutations when a transcript contains more than a single editing site, it is often used as an orthogonal approach to validate NGS analysis (110). Here we describe and compare these methods for the quantification of RNA editing.

Materials

All reagents should be molecular biology grade and prepared using nuclease-free water (*see* **Note 1**). To minimize RNA degradation and PCR contamination, thoroughly and regularly clean laboratory benchtops and equipment with RNaseZap™ and DNA AWAY (*see* **Note 2**), autoclave glassware, use nuclease-free and sterile filter tips on pipettes, and wear gloves while handling reagents. Place RNA samples on ice during reaction setup and at -80°C for long-term storage. Thaw RNA samples on ice. All biohazardous materials should be disposed properly.

Although the methods described below are broadly applicable to quantify the editing of many sites that have been computationally or experimentally identified across different transcripts, cell types, and species, this example focuses on five editing events within serotonin 2C receptor transcripts isolated from the hypothalami of C57Bl/6J mice.

RNA isolation

1. Invitrogen™ TRIzol™ Reagent
2. Ultrasonic homogenizer
3. Chloroform
4. Isopropanol
5. 75% ethanol
6. Invitrogen™ TURBO™ DNase kit
7. Thermo Scientific™ Nanodrop™

Reverse Transcription-Polymerase Chain Reaction (RT-PCR)

1. Applied Biosystems™ High-Capacity cDNA Reverse Transcription kit: 10X RT buffer, 100 mM dNTP mix, 10X RT random primers, MultiScribe™ Reverse Transcriptase, RNase inhibitor
2. 2x Phusion® High-Fidelity Mastermix with HF Buffer

3. Sense and antisense target-specific primers: 10 μM stocks of each diluted in water
4. Sense and antisense universal primers: 10 μM stocks of each diluted in water
5. Exonuclease I (20,000 units/mL)
6. 20X sodium borate (SB) buffer: Measure 32g NaOH and 220g boric acid, and add water to a volume of 4 L.
7. Agarose gel: 1% agarose diluted in 1X SB buffer, with 0.2-0.5 μg/mL ethidium bromide
8. 6x DNA gel loading dye (containing bromophenol blue and xylene cyanol FF)
9. Promega Wizard® SV Gel and PCR Clean-Up System

Quantification of RNA editing

Analysis of Peak Heights from Sanger Sequencing Chromatograms

QSVanalyzer is a software application that provides relative peak height information for sequence variants from SCF, ABI, and Megabace trace files (173). The application runs on Microsoft Windows using the Microsoft.NET Framework version 2.0. Minimal hard disk space is required as the size of the application is 248 KB, and the total size of the output files generated in this example is about 300 KB. QSVanalyzer can be obtained from the Leeds Institute of Molecular Medicine website (http://dna-leeds.co.uk/qsv/download.php).

High-throughput Sequencing Analysis

We developed a workflow for processing high-throughput sequencing data using commodity hardware and a Linux/UNIX operating system, including CentOS7 and Ubuntu 18.04. The workflow is written in Python 2.7 and leverages SeqKit (174) and FqTools (175). To facilitate software environment management, we recommend using Anaconda2 to manage the required packages, including the aforementioned tools that are available via the Bioconda channel. To create the anaconda environment, first install Anaconda2 via https://www.anaconda.com/. Once

installed, open a terminal and execute the following commands to build the environment (note the %> indicates the command line prompt and # indicates the start of a comment):

```
%> conda create --name rna_editing python=2.7 # Create the conda environment
%> conda activate rna_editing # Activate the environment
%> conda install -c bioconda seqkit # Install SeqKit
%> conda install -c bioconda fqtools  # Install FqTools
%> conda install -c bioconda fastx_toolkit # Install fastx_toolkit
%> pip install pandas matplotlib jupyter # Install packages using PIP
```

Alternatively, an Anaconda2 environment file is available https://gitlab.com/jpcartailler/analysis-of-rna-editing-hts-data/blob/master/rna_editing.yaml which can be used via the following command to reproduce the environment:

```
%> conda env create -f rna_editing.yaml
```

Methods

RNA isolation

1. Collect tissue sample in a 1.5 ml polypropylene tube and add 1 mL of Trizol reagent per 50-100 mg of tissue (*see* **Note 3**).
2. Homogenize the sample in TRIzol reagent by sonication at ~140 watts for 2-10 s (*see* **Note 4**).
3. Add 200 µL of chloroform (per 1 mL of TRIzol reagent used in Step 1) to the homogenized sample and shake the tube vigorously for 15 s; incubate for 2-3 min.
4. Centrifuge the sample at 12,000 x g for 15 min at 4°C. The sample will separate into three distinct phases upon centrifugation.

5. Carefully remove the sample from the centrifuge without disturbing phases. Using a P200 micropipette, aspirate only the aqueous (top) layer and transfer the liquid to a new 1.5 ml polypropylene tube (*see* **Note 5**). Discard the organic (pink) and interphase (white) layers.
6. To the isolated aqueous layer, add 0.5 mL isopropanol (per 1 mL of TRIzol reagent used in Step 1). Mix thoroughly by inverting the tube 3-5 times. Incubate at room temperature for 10 min.
7. Centrifuge the sample at 12,000 x g for 10 min at 4°C to precipitate the RNA.
8. Carefully decant or aspirate the isopropanol away from the RNA pellet. Resuspend the pellet with 1 mL 75% ethanol (per 1 mL of TRIzol reagent used in Step 1), and vortex briefly for 1-2 s.
9. Centrifuge the sample at 12,000 x g for 5 min at 4°C.
10. Carefully aspirate the ethanol away from the RNA pellet.
11. Allow the RNA pellet to dry for 5 minutes, and then use a P10 micropipette to carefully aspirate any residual ethanol, if necessary.
12. Resuspend the RNA in 20-50 µL of nuclease-free water.
13. Using a Nanodrop™, measure the concentration of the RNA sample.
14. Dilute an aliquot of the sample to 200 ng/µL (*see* **Note 6**).
15. Add one-tenth sample volume of TURBO DNase™ buffer. Add 1 µL of TURBO DNase™ per 50 µL reaction and disperse by gently flicking the side of the tube. Incubate the reaction at 37°C for 30 minutes.
16. Add one-fifth volume of DNase inactivation reagent, and disperse by flicking the tube once per minute for 5 min.
17. Centrifuge at 10,000 x g for 2 minutes.
18. Using a P10 micropipette, carefully aspirate the RNA sample without collecting any of the pelleted inactivation reagent and transfer into a new 1.5 ml polypropylene tube.

Reverse Transcription-Polymerase Chain Reaction (RT-PCR)

Reverse Transcription

1. In a 0.2 mL PCR strip tube, prepare a 20 µL reverse transcription reaction according to Table 2.1 (*see* **Note 7**)
2. Run thermocycling program according to Table 2.2 (*see* **Note 8**)

Polymerase Chain Reaction

1. If possible, design target-specific sense and antisense primers flanking an edit site in separate exons to avoid amplification of genomic DNA and to generate amplicons between 75 and 300 base pairs in length (*see* **Note 9**). For multiplex analyses of multiple RNA samples, add unique sequences to the 5'-ends of the target-specific sense and antisense primers during primer design. This approach allows amplification of each transcript with only two target-specific primers, followed by amplification with a set of "universal" primers allowing incorporation of index sequences and adapter sequences required for the Illumina NGS platform. In this example, we add T3 (ATTAACCCTCACTAAAGGGA) and T7 (TAATACGACTCACTATAGG-G) RNA polymerase promoter sequences to the 5'-ends of the sense and antisense primers, respectively.
2. Design universal primers that include one of two Illumina adapter sequences at the 5'-end, followed by a unique 6-nucleotide barcode, and sequences complementary to either T3 or T7 RNA polymerase promoter at the 3'-end (Figure 2.1.).
3. In a PCR strip tube, prepare PCR reaction according to Table 2.3.
4. Run thermocycling program according to Table 2.4
5. Remove unincorporated primers by adding 1 µL exonuclease I, and incubate at 37°C for 20 min.
6. Incubate the reaction at 80°C for 20 min. to inactivate exonuclease I.

7. Add 1 µL each of 10 µM sense and antisense universal primers.
8. Run thermocycling program according to Table 2.5 (*see* **Note 10**)

Gel Electrophoresis and Clean-up

1. Add DNA gel loading dye to the PCR reaction and mix well by pipetting up and down several times.
2. Load the entire reaction onto a 1% agarose gel and resolve samples by electrophoresis in 1X SB buffer at 300 V until bottom dye band (bromphenol blue) migrates off the bottom of the gel.
3. Wearing amber-filtered goggles, image the gel using a blue light DNA transilluminator. Check that the amplicon is the correct size and that no bands are present in the RT- samples (indicative of PCR contamination), and then carefully use a single-edge razor blade to cut out the agarose containing the desired amplicon(s).
4. Purify the amplicons using Promega Wizard® SV Gel and PCR Clean-Up System according to manufacturer's instructions.

Sequencing

1. Sanger sequence RT-PCR amplicon with reverse primer (*see* **Note 11**). Output should be collected in the '.ab1' chromatographic file format.
2. Subject "library-ready" RT-PCR amplicons to Illumina high-throughput sequencing.

Table 2.1: Reverse transcription reaction setup

Reagent	Volume (µL)	
	+ Reverse Transcriptase (RT+)	-Reverse Transcriptase (RT-)
10X RT buffer	2	2
100 mM dNTP mix	0.8	0.8
10X RT random primers	2	2
MultiScribe™ Reverse Transcriptase	1	0
RNase inhibitor	1	1
RNA (200-1000 ng)	variable	variable
Water	to 20 µL	to 20 µL

Table 2.2: Reverse transcription thermocycling protocol

Step #	Temperature (°C)	Time
1	25	10 min
2	37	60 min
3	85	5 min
4	4	∞

Table 2.3: PCR setup for amplification using target-specific primers

Reagent	Volume (µL)
Target-specific sense primer (10 µM)	1
Target-specific antisense primer (10 µM)	1
2x Phusion® High-Fidelity Mastermix with HF Buffer	25
cDNA	5
Water	18

Table 2.4: Thermocycling protocol for PCR using target-specific primers

Step #	Temperature (°C)	Time
1	98	30 sec
2	98	10 sec
3	55	30 sec
4	72	45 sec
5	Repeat steps 2-4	4x
6	4	∞

Table 2.5: Thermocycling protocol for PCR using universal primers

Step #	Temperature (°C)	Time
1	98	15 sec
2	56	30 sec
3	72	60 sec
4	Repeat steps 1-3	24x
5	4	∞

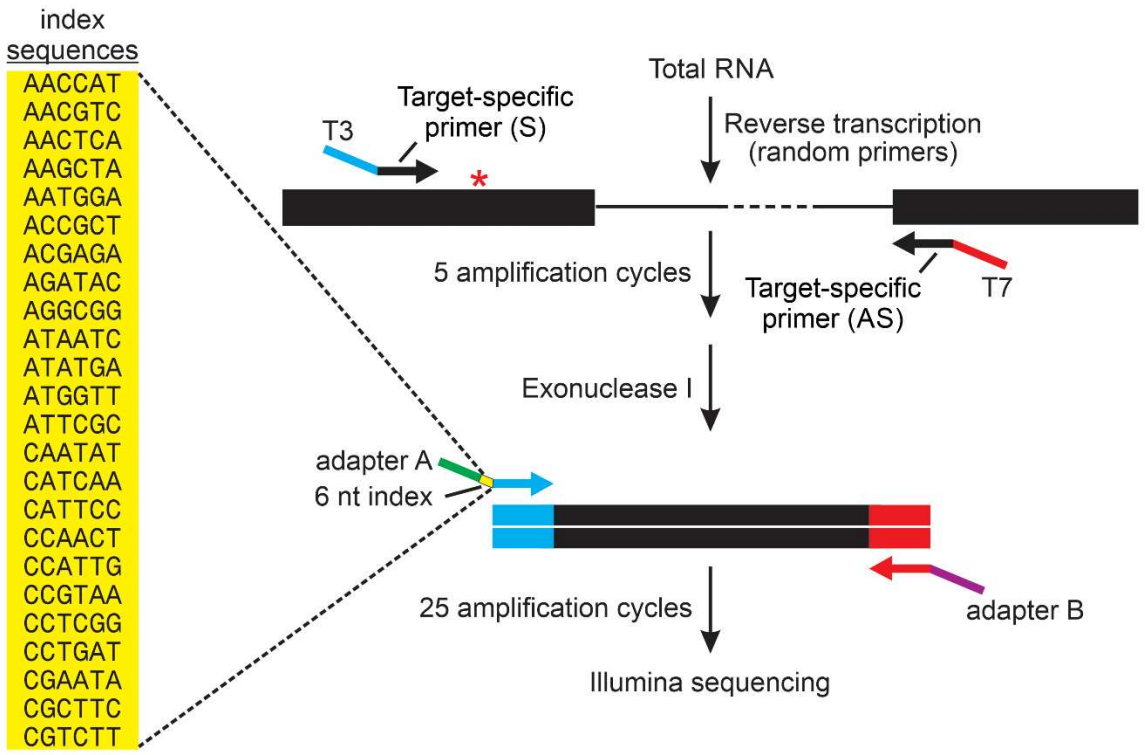

Figure 2.1. Next-generation sequencing strategy for multiplex quantification of RNA editing profiles. A schematic diagram is presented for RT-PCR amplification of a region of an mRNA target flanking an A-to-I editing site (✱). In general, target-specific primers are designed in adjacent exons containing either T3 (blue) or T7 (red) RNA polymerase promoter sequence extensions for the sense and antisense primers, respectively. These primers are used for PCR amplification (5 cycles) before digestion of the remaining single-stranded primers using Exonuclease I. A second round of amplification (25 cycles) is performed with universal primers in which the oligonucleotide contains sequences matching the T3 promoter, one of 24 unique 6-nt index sequences (yellow) for sample identification, as well as an adapter sequence (Adapter A; green) or sequences matching the T7 and an adapter sequence (Adapter B; purple) for library preparation and high-throughput single-end sequencing on the Illumina platform.

Quantification of RNA Editing

Analysis of Peak Heights from Sanger Sequencing Chromatograms

1. Create a folder containing all the .ab1 traces to be analyzed (*see* **Note 12**)
2. Open a single .ab1 file from the folder created in the previous step by going to File > Open in QSVanalyzer.
3. Once the trace is opened, go to QSV analysis > Select nucleotide
4. Click on the position of the editing site within the chromatogram trace. Edited positions will appear as T/C mixed peaks in the sequence of the antisense strand. The “QSV information” window will automatically appear. One of the peaks will be designated as “Gene A” and the other will be designated as “Gene B” (*see* **Note 13**). Verify that the 5’- and 3’-flanking sequences are correct.
5. Select all six reference bases (*see* **Note 14**). T/C peak heights at the edited position will be adjusted relative to the heights of the reference peaks.
6. If only a single editing site is to be analyzed, select Create web pages and images, click Add, and then press Run batch. If more than one position is to be analyzed, select Add, then select Find. A “QSV image” window will automatically open showing an abbreviated trace with the 5’ and 3’ flanking sequences on either side of the editing site bisected by a vertical red line. Close the “QSV image” window, then close the “QSV information” window, and repeat Steps 4-6 until all sites for analysis within the chromatogram have been added (*see* **Note 15**). When all sites have been selected, select Create web pages and images and then press run batch in the “QSV information” window (*see* **Note 16**). In the “Browse for folder” window that automatically opens, select the folder created in Step 1 and click OK. A “QSV_data” subfolder will be created. This subfolder contains a web page with peak height information for each editing site within the trace file folder (*see* **Note 17**).

7. Go to the QSV_data subfolder and open the web page for each editing site (*see* **Note 18**). For each trace, record the relative peak height data for “Variant A” and “Variant B” under the “Trace images and peak heights” section of the web page.
8. Calculate the percentage of transcripts containing an edited nucleotide editing by using the peak heights obtained from Step 7 as shown (*see* **Note 19**):

$$\%\ editing = \frac{\text{C peak height}}{\text{T peak height + C peak height}} \times 100$$

High-throughput Sequencing Analysis

1. Clone or download the software repository from https://gitlab.com/jpcartailler/analysis-of-rna-editing-hts-data. Enter this working directory.
2. (if set up, activate the anaconda environment)
3. Place your FastQ file in the data/ directory and ensure that it is in GZIP format.
4. Enter the src/ directory and create a file called config.yaml, which contains all the configuration parameters expected from the workflow script. The “targets” represent specific genes targeted in the analysis, since more than one may have been sequenced and need to be demultiplexed. In this example, there is only one target.

```
paths:
    data: ../path/to/sample.fastq.gz
    results: ../results
targets:
    5HT2C:
        name: Mus musculus 5-hydroxytryptamine (serotonin) receptor 2C (mRNA)
        analysis_criteria:
            seqkit_degenerate: no # allow degenerates
            seqkit_max_mismatch: 0 # no mismatch
        sequences:
            barcodes:
                sample_1: AACGTC
                sample_2: ATATGA
                sample_3: CGTCTT
            promoter: GCTGGACCGGTATGTAGCA
            # reference -- sequence(s) of variants to search for within reads
            reference:
                # seq_help: editing site (A/G) indicated with |
                # seq_help: |-|---||----|----------------------------------------
                sequence_1: ATACGTAATCCTATTGAGCATAGCCGGTTCAATTCGCGGACTAAGGCCATCATGAA
                sequence_2: GTACGTAATCCTATTGAGCATAGCCGGTTCAATTCGCGGACTAAGGCCATCATGAA
```

```
    sequence_3: ATGCGTAATCCTATTGAGCATAGCCGGTTCAATTCGCGGACTAAGGCCATCATGAA
    (etc...)
    sequence_32:GTGCGTGGTCCTGTTGAGCATAGCCGGTTCAATTCGCGGACTAAGGCCATCATGAA
# variant_position -- nucleotide position where RNA editing var...
variant_position: 13
# variant_extended_by_nt -- for exact matching, number of nucle...
variant_extended_by_nt: 20
```

5. Execute the workflow from the src/ directory:

```
%> python workflow.py
```

6. Then, execute the bash scripts generated from the workflow.py output:

```
%> bash workflow_step1.bash

%> bash workflow_step2.bash
```

7. The results/ directory will have files in .seq format, for each barcode and sequence target (in this case, 3 barcodes and 32 sequences per barcode)

```
results/job-01.5HT2C.AACGTC.sequence_1.seq

results/job-01.5HT2C.AACGTC.sequence_2.seq

results/job-01.5HT2C.AACGTC.sequence_3.seq

...

results/job-01.5HT2C.AACGTC.sequence_32.seq
```

8. Within the results/ directory, run the following command to quantify the number of reads per barcode-sequence combination.

```
%> wc -l results/statistics_barcode_search_exact/*.seq
```

9. These results can then be tabulated manually into a worksheet.

Results and Discussion

Comparison of Sanger sequencing and NGS strategies

In agreement with previous reports (176), the levels of RNA editing measured by peak height analysis and high-throughput sequencing do not differ significantly (Figure 2.2). While Sanger sequencing-derived methods of RNA editing quantification can be used to confirm the extent of editing determined by high-throughput sequencing, the accuracy of peak height analysis

may be compromised when sequencing chromatograms are noisy or when levels of editing are very low (<5%). High-throughput sequencing analysis offers an additional benefit over peak height analysis in that it can differentiate between editing permutations of multiple sites within a single RNA transcript (Figure 2.3).

Notes

1. To prepare all reagents, stocks, and reactions directly contacting nucleic acids (RNA samples, primer stocks, PCR reactions, etc.), we recommend using commercially available autoclaved, 0.22 μM sterile filtered, nuclease- and protease-free water. All other materials (SB buffer, agarose gels, etc.) can be prepared using high-quality laboratory water (e.g. Milli-Q® water).
2. To prevent RNA degradation and PCR contamination, we recommend working with RNA and DNA samples in a dedicated PCR hood equipped with a UV sterilizer. Do not work in the hood while the UV light is on.
3. For very small samples such as tissue punches, homogenize the sample in 300 μL of Trizol, and then perform a scaled-down RNA extraction procedure through Step 5 of Subheading 3.1. Follow the directions in the RNeasy® Micro Kit handbook beginning at Step 4 of the handbook protocol for purifying total RNA from animal and human tissues.
4. Only sonicate enough so that the sample is homogenous and no particulates are visible. Additional sonication may result in RNA degradation.
5. Be careful not to transfer any of the interphase layer when aspirating the aqueous layer. Collection of the interphase into the RNA sample increases the risk of genomic DNA contamination during subsequent RT-PCR amplification.

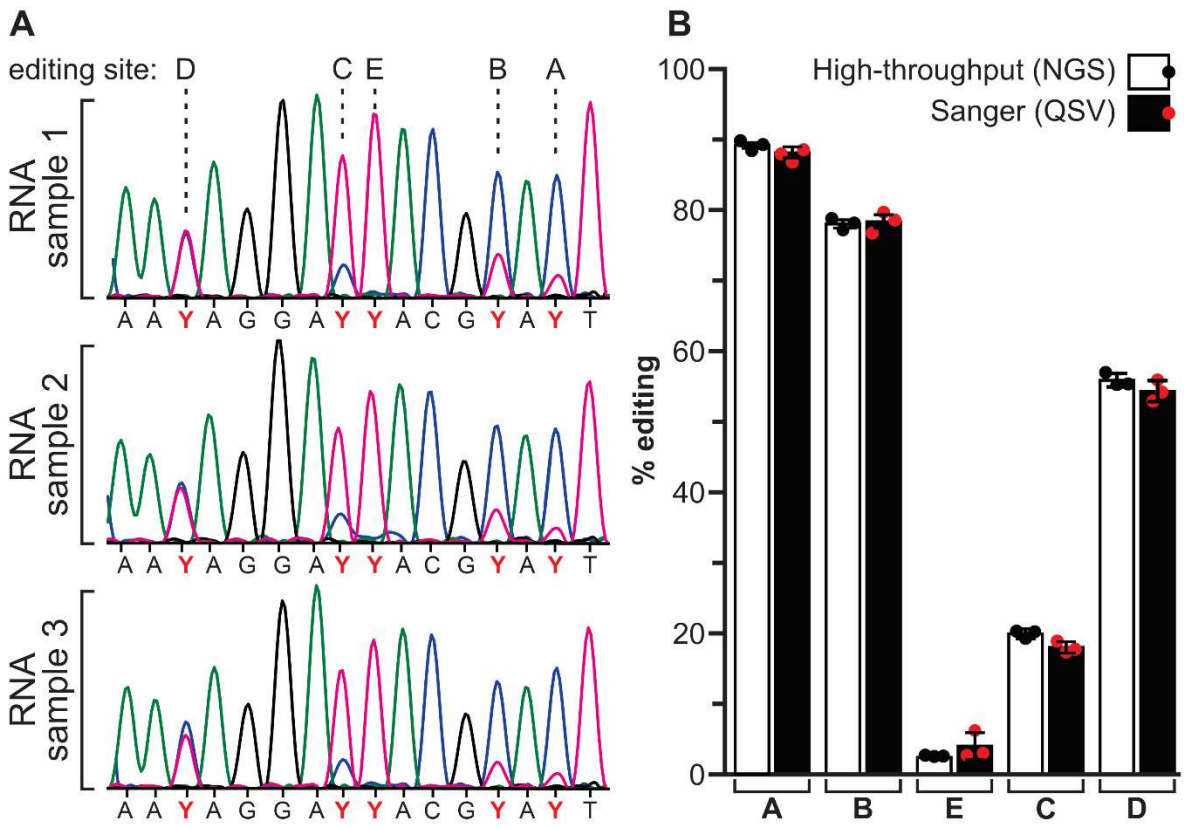

Figure 2.2. Analysis of hypothalamic $5HT_{2C}$ RNA editing profiles in C57Bl/6J mice. **A)** Representative electropherogram traces from Sanger sequencing of cDNAs generated from hypothalamic RNA (n = 3) are presented. The position of the editing sites (A-E) are shown and the mixed T/C peaks from the antisense strand are designated as pyrimidine (Y). **B)** Comparisons of RNA editing quantification using high-throughput (NGS) and Sanger (QSV) sequencing revealed no significant differences; mean ± SEM, n = 3.

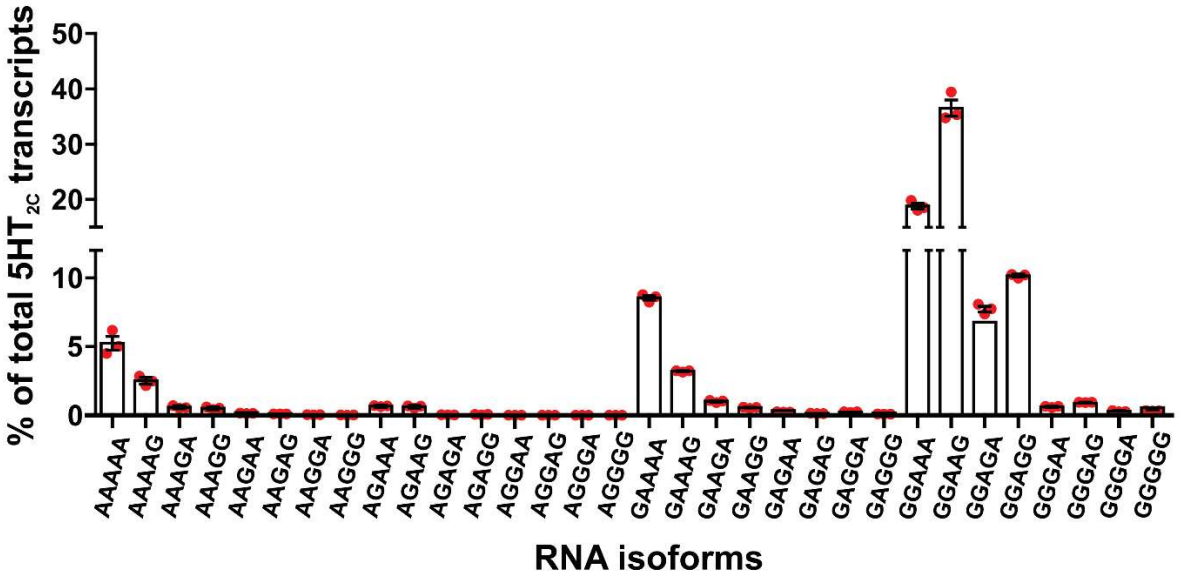

Figure 2.3. Quantification of $5HT_{2C}$ RNA editing profiles in mouse hypothalamus using high-throughput sequencing. The relative expression for all possible $5HT_{2C}$ isoforms generated by RNA editing are represented as the percentage of total $5HT_{2C}$ sequence reads; mean ± SEM, n = 3. The 32 possible permutations of A-to-I editing are designated according to the presence of either an adenosine (A) or guanosine (G) at each of the five distinct editing sites within the analyzed cDNA library (e.g. AAAAA = non-edited, GGGGG = fully-edited).

6. Only sonicate enough so that the sample is homogenous and no particulates are visible. Additional sonication may result in RNA degradation.
7. Be careful not to transfer any of the interphase layer when aspirating the aqueous layer. Collection of the interphase into the RNA sample increases the risk of genomic DNA contamination during subsequent RT-PCR amplification.
8. If it is not possible to dilute the sample to 200 ng/µL, add 2-3 µL DNase directly to the sample.
9. When synthesizing cDNA, it is important to include a negative control that lacks reverse transcriptase (RT-) to assess PCR contamination from genomic DNA and cDNA products within the laboratory environment.
10. Reverse transcription at 37°C can be carried out for 2 hours to increase the cDNA yield of low-abundance transcripts.
11. Amplicon size and relative positions of multiple editing site(s) within a single transcript will determine whether single-read or paired-end reads are required during Illumina sequencing
12. PCR cycle number may be increased to amplify low-abundance transcripts, however, increasing cycle number may increase potential errors introduced by PCR.
13. The antisense primer used for Sanger sequencing should anneal at least 50 base pairs downstream of the editing site(s) because the first ~30 base pairs of sequence are generally of poor quality. It is important to generate antisense Sanger sequencing reads because subsequent QSV analysis depends on relative peak heights, and T/C peak heights are more consistent than A/G peak heights(102).
14. Include only high-quality Sanger sequencing data in the QSV analysis. Ensure that all electropherograms to be analyzed have high signal-to-noise ratios (i.e., electropherograms should be virtually free of “background” peaks; double peaks should

only appear at the edited positions). Include all replicates for a single transcript in the same folder.

15. Usually the variant with the larger peak height will be designated as “Gene A,” and the minor variant will be designated as “Gene B.” Occasionally, QSVanalyzer will miscall the minor variant. If this happens, manually enter the correct nucleotide into the “Gene B” box.
16. We recommend including all six upstream bases as reference bases, even if one or more of them are edited nucleotides.
17. It is necessary to click Find before selecting additional nucleotides, but this step may be omitted after addition of the first nucleotide.
18. QSV information window may be accessed at any time by going to QSV analysis > QSV ratios
19. Image (.png) and spreadsheet (.xls) files are also created for each analysis, but are not used in the analysis here.
20. Web pages for each edit site are automatically named in the following format: “QSV_data_5’ flanking sequence_Variant A_Variant B_3’ flanking sequence_-1-2-3-4-5-6_.htm,” where the 5’ and 3’ flanking sequences are the 10 nucleotides up- and downstream of the edit site, Variant A and Variant B are the nucleotide variants at the edit site, and the trailing numbers are reference bases. Web pages may be renamed if desired.
21. Although web page output files created by QSVanalyzer include relative adjusted peak heights and peak height ratios for each trace, we have found that calculating % editing using uncorrected peak heights provides a more reliable estimate of % editing as determined by high-throughput sequencing.

Chapter III

Interplay between the central modulation of feeding behavior and serotonin 2C receptor RNA editing

Introduction

Serotonin (5-Hydroxytryptamine; 5HT) is a monoaminergic neurotransmitter involved in the homeostatic control of feeding behavior and metabolism. The actions of 5HT are mediated by specific interaction with multiple 5HT receptor subtypes (177-180). Genetic and pharmacological studies have demonstrated a role for the 2C-subtype of serotonin receptor ($5HT_{2C}$) in the serotonergic modulation of central feeding pathways (181-192). Activation of this G-protein coupled receptor on pro-opiomelanocortin (POMC) neurons in the arcuate nucleus of the hypothalamus (ARC) produces G_q-mediated stimulation of phospholipase C (PLC) signaling to release α-melanotropin (αMSH), the endogenous agonist of melanocortin receptors (193-195). Second-order neurons in the paraventricular nucleus expressing melanocortin 4 (MC4) receptors activate in response to αMSH binding, thereby promoting satiety and decreasing food intake (182,184,185,196). In contrast, inverse agonism of MC4 receptors by Agouti-Related Peptide (AgRP), released from a separate population of neuropeptide Y (NPY)-expressing neurons in the ARC, increases feeding (197). The significant contribution of 5HT signaling in the modulation of feeding circuits has made the serotonergic system an attractive target for obesity therapeutics. A substituted amphetamine that causes the release of serotonin [d-fenfluramine (d-fen)] onto $5HT_{2C}$ receptors in the ARC was widely prescribed in the 1990s for the treatment of obesity, but was later withdrawn due to off-target $5HT_{2B}$-mediated cardiovascular complications (198-200). Nevertheless, the therapeutic efficacy of d-fen stimulated research on the role of the $5HT_{2C}$ receptor in food intake. Recently, it was found that $5HT_{2C}$-null mice exhibit hyperphagia, adult-onset obesity, and type 2 diabetes, and are insensitive to the anorectic effects of d-fen (190). Interestingly, selective reactivation of $5HT_{2C}$ receptor expression on POMC neurons of $5HT_{2C}$-null

mice, rescues normal feeding, energy homeostasis and d-fen responsiveness (185). An increased understanding of the crucial role that $5HT_{2C}$ plays in feeding behavior and energy balance has led to the recent development of an FDA-approved selective $5HT_{2C}$ receptor agonist (Lorcaserin) for the treatment of obesity. Despite this progress, questions remain regarding the relationship between feeding-related pathologies and the modulation of $5HT_{2C}$ receptor function on POMC neurons.

RNA transcripts encoding the $5HT_{2C}$ receptor undergo up to five adenosine-to-inosine (A-to-I) editing events that occur within a 13-base pair span of exon 5. These editing events predict alterations in the identity of three amino acids within the second intracellular loop of the receptor to generate as many as 24 receptor isoforms from 32 edited mRNA species (Figure 3.1A-B). Functional comparisons in heterologous expression systems between the non-edited (INI) and the fully-edited (VGV) $5HT_{2C}$ isoforms revealed a 40-fold decrease in $G_{q/11}$-protein coupling efficiency and decreased coupling to other signaling pathways (Figure 3.1C) (28,201). In addition, cells expressing more highly edited $5HT_{2C}$ receptors (e.g. VSV and VGV) demonstrate considerably reduced (or absent) constitutive activity in the absence of ligand compared to cells expressing the non-edited isoform (201). Recent evidence implicates post-transcriptional processing of $5HT_{2C}$ transcripts in the pathogenesis of eating disorders including Prader-Willi Syndrome (PWS), a maternally imprinted human disorder resulting from a loss of paternal gene expression on chromosome 15q11–13 (REF). Mice solely expressing the fully edited $5HT_{2C}$ receptor (VGV) phenocopy several clinical features of PWS including early hypophagia and hypotonia, followed by post-weaning hyperphagia (202). Despite these data, it remains unknown whether and how $5HT_{2C}$ RNA editing patterns in POMC neurons are regulated.

Heterogeneous $5HT_{2C}$ expression across tissues and within different cell types have hampered efforts to understand how $5HT_{2C}$ RNA processing contributes to the modulation of specific circuits or behaviors. Previous studies of $5HT_{2C}$ RNA processing have relied upon broad overexpression, gross manipulation, or whole-tissue analyses of specific $5HT_{2C}$ isoforms. Here,

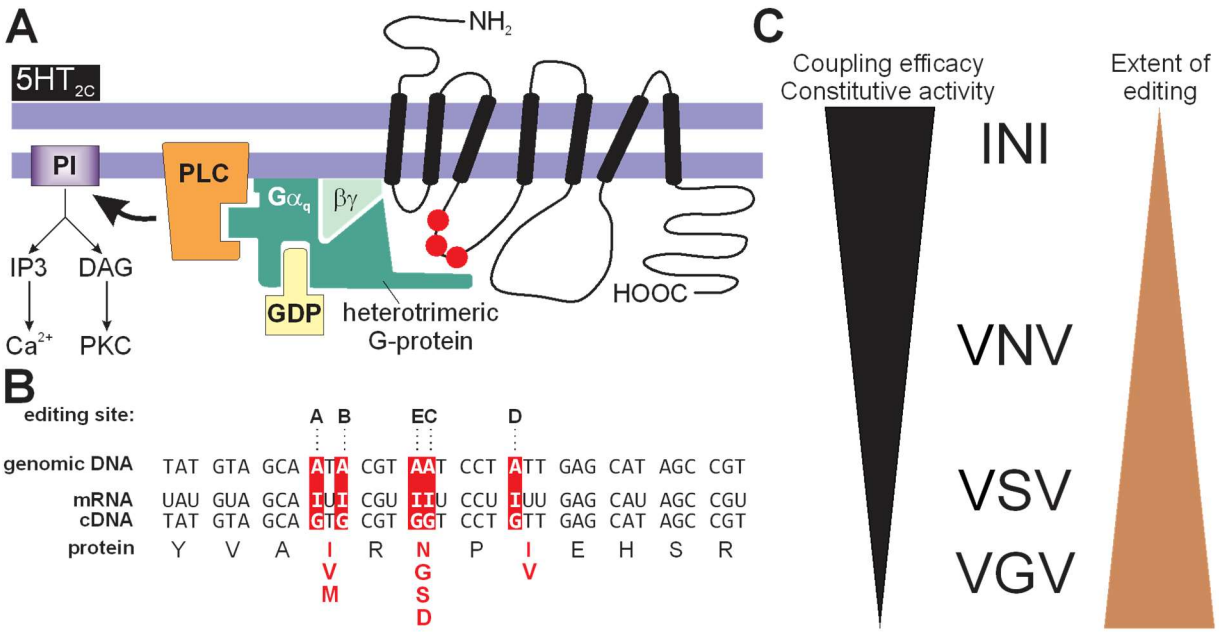

Figure 3.1. Post-transcriptional processing of $5HT_{2C}$ transcripts. (**A**) A schematic representation of the predicted topology for $5HT_{2C}$ receptor is presented together with the major intracellular signaling pathway. The approximate positions of amino acid alterations within the second intracellular loop that result from RNA editing events are indicated with red circles. (**B**) Nucleotide and predicted amino acid sequence alignments between $5HT_{2C}$ genomic, mRNA and cDNA sequences; nucleotide discrepancies resulting from RNA editing events and predicted alterations in amino acid sequence are indicated in inverse and red lettering, respectively. (**C**) The inverse relationship between the extent of $5HT_{2C}$ RNA editing and properties of the $5HT_{2C}$ receptor (coupling efficacy and constitutive activity) is shown. Three-letter abbreviations indicating the amino acid alterations resulting from RNA editing denote the $5HT_{2C}$ receptor isoform.

we have taken advantage of genetically-modified mouse models in which $5HT_{2C}$ expression is selectively enriched in POMC neurons to assess the $5HT_{2C}$ transcriptional profile under normal physiological conditions as well as conditions in which normal energy balance is challenged by diet or exercise. Our results indicate that the $5HT_{2C}$ RNA editing profile in POMC neurons is significantly altered in response to these metabolic perturbations. We also have engineered two mutant mouse models for future studies that can be crossed with a POMC:Cre line to generate mice that will selectively express either the INI or VGV $5HT_{2C}$ isoform in POMC neurons.

Materials and Methods

Generation of 2C/POMC mice. A previously developed mouse strain in which a loxP-flanked transcriptional blocker (loxTB) was inserted between exons 3 and 4 of the *Htr2c* gene to ablate $5HT_{2C}$ expression (Htr2c^{tm1Jke}/J) was crossed to a transgenic mouse line expressing Cre recombinase under the control of the *Pomc1* promoter [Tg(Pomc-cre)1^{Lowl}/J] (185). The genotypes of mutant offspring were determined using standard polymerase chain reaction (PCR) protocols 29720 (Htr2c<tm1Jke>) and 22392 (generic Cre) provided by The Jackson Laboratory (www.jax.org) . Double-mutant "2C/POMC" mice were those animals determined to be hemizygous for Cre recombinase and hemizygous or homozygous for the loxTB.

Diet manipulation. For high-fat diet experiments, 5-week old 2C/POMC animals were provided with regular chow diet (10% kcal% fat; Research Diets D12450K) or a high-fat (45% kcal% fat; Research Diets D12451) diet for 20 weeks. Weights were monitored and recorded weekly. For calorie restriction experiments, 8-12 week old 2C/POMC animals were provided either *ad libitum* access to a standard chow diet or a 40% reduction in total caloric intake for ten days or until mice lost more than 20% of their starting weight. Calorie-restricted mice were fed immediately before the onset of the dark cycle to minimize disruption of circadian rhythms (203). The weights of mice in calorie restriction experiments were monitored daily.

Voluntary exercise. 8-12 week old 2C/POMC animals were housed with or without access to a running wheel for one month. Wheel running activity was monitored using ClockLab software (Actimetrics, Evanston, IL).

Analysis of RNA editing. Hypothalami dissected from mouse brains were homogenized in 1 mL Trizol Reagent (Invitrogen) according to manufacturer instructions. DNA was removed from RNA samples using the rigorous DNase treatment procedure outlined in the Turbo™ DNase kit (Invitrogen). cDNA was prepared from 1 µg of DNase-treated RNA sample using the High-Capacity cDNA Reverse Transcription kit (Applied Biosystems). When preparing cDNA, a control reaction lacking reverse transcriptase was prepared in parallel for each RNA sample to ensure PCR amplification did not result from contaminating genomic DNA. For each sample, $5HT_{2C}$ PCR amplicons were generated and subjected to high-throughput sequencing for quantitative analysis of RNA editing, as described previously (161).

In situ hybridization. Mice were anesthetized using isofluorane and then cervically dislocated before decapitation. Whole brains were extracted and washed briefly in ice-cold PBS before embedding the tissue in optimum cutting temperature (OCT; Tissue-Tek®). Embedded tissue was frozen at −80°C for at least 12 hours prior to sectioning. 14 µM sections were cut at −20°C using a cryostat and mounted onto SuperFrost® Plus slides (Fisherbrand™). Slides were immediately stored at −80°C before further processing. To perform *in situ* hybridization, the RNAscope® fluorescent assay (Advanced Cell Diagnostics) was performed using probes for $5HT_{2C}$ (Mm-Htr2c-C3) and POMC (Mm-Pomc-C2) according to manufacturer instructions.

Mouse genome engineering on the $Htr2c^{tm1Jke}$/J background. A homology-directed repair (HDR) CRISPR/Cas9-based approach was used to generate mice in which the five edited adenosine residues within exon 5 were mutated on the $Htr2c^{tm1Jke}$/J background (185). 3-4 week old superovulated female $Htr2c^{tm1Jke}$/J mice were mated with male stud mice overnight. The following morning, female mice were collected and single-cell zygotes were retrieved for microinjection of recombinant Cas9 protein, single guide RNA (sgRNA), and a single-stranded DNA

(ssDNA) repair oligo. A guide RNA (TTGAACCGGCTATGCTCAATAGG, where the underlined nucleotides represent the protospacer adjacent motif) was used to target Cas9 to induce a double-stranded DNA break near the editing cassette in exon 5 of the Htr2c gene. The 180 base-pair single-stranded DNA repair template included mutations changing target adenosines to guanosines, as well as three silent mutations to create a SacII restriction site for screening and genotyping purposes:

ATTTCACTAGATGTGCTATTTTCAACTGCGTCCATCATGCACCTCTGCGCCATATCGCTGGA

CCGGTATGTAGCA**G**T**C**CG**CGG**TCCT**G**TTGA**A**CATAGCCGGTTCAATTCGCGGACTAAGGCC

ATCATGAAGATTGCCATCGTTTGGGCAATATCAATAGgtaattatacctggccatag,

where bolded letters represent mutated nucleotides, underlined letters represent the SacII restriction site, uppercase letters represent exonic sequence, and the lowercase letters represent intronic sequence.

A non-homologous end joining (NHEJ) CRISPR/Cas9-based approach was used to generate a separate mouse line in which a portion of intron 5 of the *Htr2c* gene was deleted on the Htr2c^{tm1Jke}/J background (185). Single-cell zygotes were collected as described above, but were microinjected with Cas9 protein and two guide RNAs used to induce two double-stranded breaks in intron 5 of the *Htr2c* gene: ACCTGGCCATAGAATTGCAGCGG and TGTTACCAGTCGACGTCTGTAGG, where the underlined nucleotides represent the protospacer adjacent motif (PAM).

All zygotes were transferred to pseudopregnant female mice immediately following microinjection. F0 founders were screened by Sanger sequencing of genome-derived PCR amplicons flanking the edited region to verify the desired mutation.

Results

Molecular characterization of mice that express $5HT_{2C}$ selectively in POMC neurons.

Our laboratory, and those of our collaborators, have demonstrated that systemic disruption of normal $5HT_{2C}$ RNA processing patterns alters feeding and energy homeostasis in mice (202,204,205). Here we have investigated whether manipulation of energy balance dynamically modifies patterns of $5HT_{2C}$ RNA editing selectively in POMC neurons. Although protein recoding via dynamic alterations in RNA processing has long been proposed as a mechanism to provide homeostatic systems with response flexibility, evidence to support this hypothesis in mammals is lacking. Previous attempts to examine dynamic changes in RNA editing profiles from bulk tissue samples have largely proven futile (161,206,207). Many of these studies relied upon population-averaged assays that failed to capture the functional and transcriptional heterogeneity of unique subpopulations within complex networks. As the hypothalamus comprises a number of distinct $5HT_{2C}$-expressing cell populations, not all of which are involved in the regulation of energy balance, ensemble measurements have the potential to mask biologically meaningful changes in $5HT_{2C}$ RNA processing occurring in a small number of cells. Accordingly, we hypothesized that experience-dependent alterations in $5HT_{2C}$ RNA processing occur only within those $5HT_{2C}$-expressing cells directly involved in modulating relevant responses.

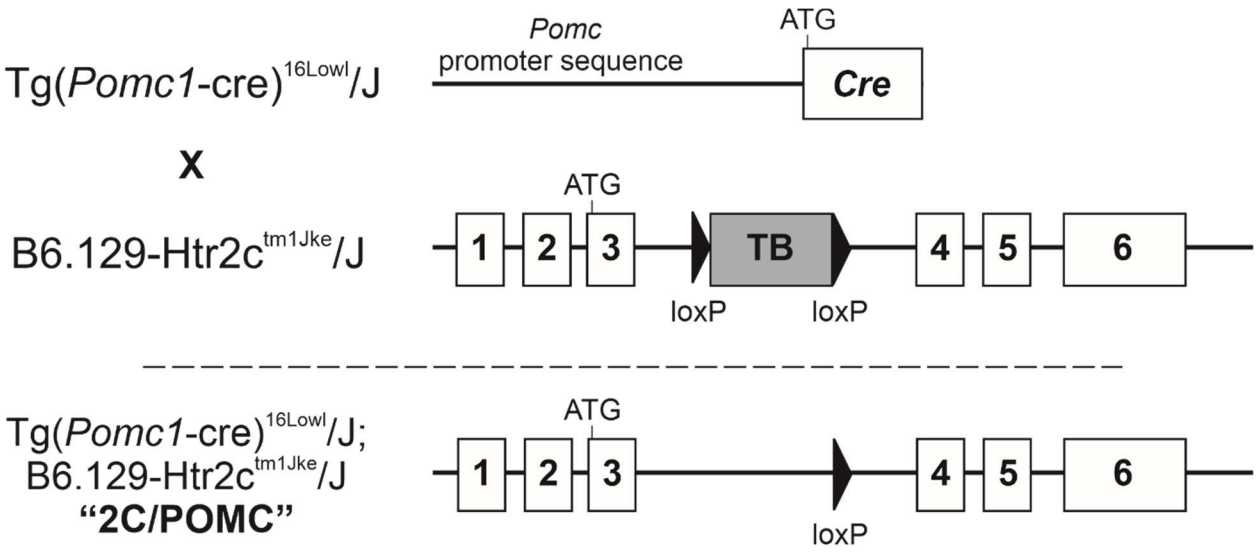

Figure 3.1. Genetic strategy for the selective expression of $5HT_{2C}$ in POMC neurons. Mice expressing a Cre recombinase transgene under the control of the *Pomc1* promoter (POMC:Cre; *top*) were crossed to a transgenic line carrying a loxP-flanked transcriptional blocker (TB) in intron 3 of the endogenous *Htr2c* locus (*middle*) to generate mice that should express $5HT_{2C}$ in POMC neurons in an otherwise $5HT_{2C}$-null background ("2C/POMC"; *bottom*).

To test this hypothesis, we have taken advantage of previously characterized mice designed to express $5HT_{2C}$ receptors solely in this neuronal subpopulation (2C/POMC mice) (185). These mice were generated using POMC:Cre-dependent recombination of a loxP-flanked transcriptional blocker in intron 3 of the endogenous *Htr2c* locus (Figure 3.1). Selective re-expression of $5HT_{2C}$ in POMC neurons is sufficient to normalize the hyperphagia, obesity, hyperleptinemia, and diabetes associated with $5HT_{2C}$-null animals (185). Given the particular behavioral and molecular phenotypes of 2C/POMC mice, we have exploited this unique genetic model to isolate POMC-neuron specific $5HT_{2C}$ transcripts without the need for further transcript enrichment. Before initiating these studies, we used fluorescent *in situ* hybridization to examine the Cre-dependent expression of $5HT_{2C}$ RNA in the arcuate nucleus of 2C/POMC and control mice (Figure 3.2). Results from this analysis revealed that wild-type animals showed $5HT_{2C}$ RNA expression in both POMC and non-POMC expressing neurons. Unexpectedly, our results also revealed that $5HT_{2C}$ expression is enriched in, but not restricted to, POMC neurons in 2C/POMC mice. Furthermore, RNA profiling studies showed a unique hypothalamic $5HT_{2C}$ editing signature in 2C/POMC mice relative to control animals (Figure 3.3). High-throughput sequencing analysis of $5HT_{2C}$ editing profiles revealed sharp differences between the two samples, including a 5-fold decrease in expression of the non-edited (INI) $5HT_{2C}$ isoform in 2C/POMC mice. The simplest interpretation of these data is that the $5HT_{2C}$ editing profile in POMC neurons is distinct from population-averaged $5HT_{2C}$ editing in whole hypothalamus.

$5HT_{2C}$ RNA editing profiles change minimally in response to perturbations in central feeding pathways.

The maintenance of energy homeostasis requires rapid and dynamic expression of genes in metabolic pathways to predict and respond to fluctuations in energy. Modulation of protein function by post-transcriptional processing is poised to offer such dynamic fine-tuning, and

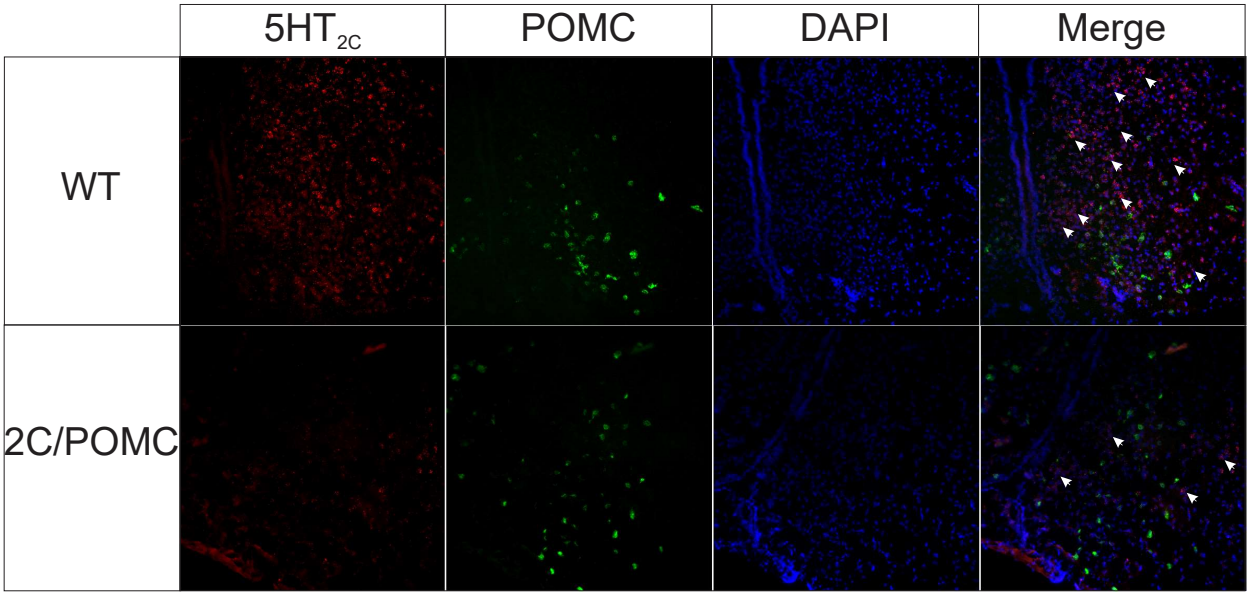

Figure 3.2. *In situ* characterization of 2C/POMC mice. Widefield images (20X) of the arcuate nucleus in wild-type and 2C/POMC mice. Fluorescent *in situ* hybridization reveals expression of POMC (green) and $5HT_{2C}$ (red); cell nuclei are stained with DAPI (blue). White arrows indicate $5HT_{2C}$ expression in cells that do not express POMC. $5HT_{2C}$ expression is enriched in, but not restricted to, POMC neurons in 2C/POMC mice.

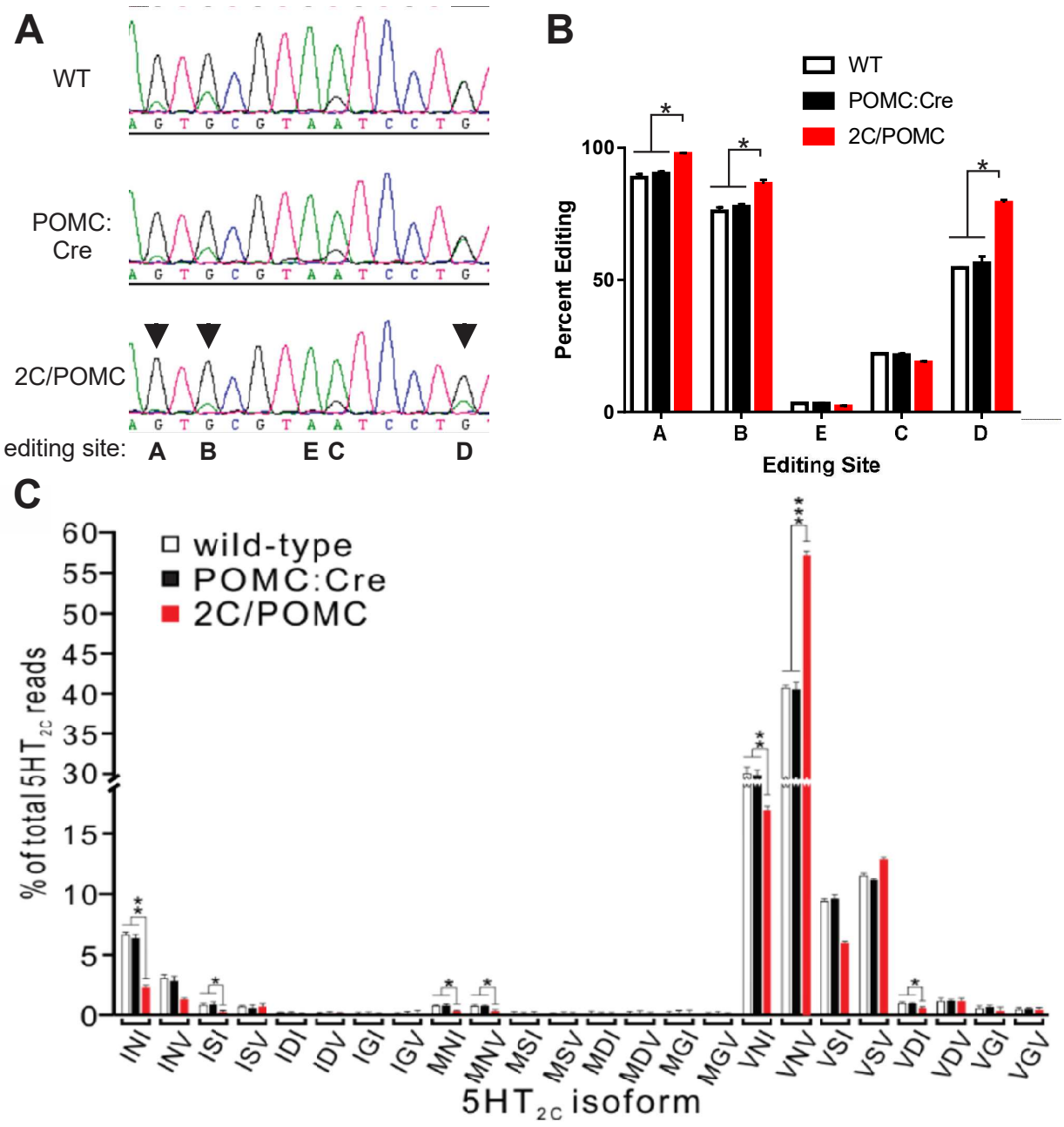

Figure 3.3. Characterization of hypothalamic $5HT_{2C}$ editing profiles. (**A**) Electropherogram traces obtained from Sanger sequencing of $5HT_{2C}$ RT-PCR amplicons; edited positions A-E are indicated beneath the traces at their respective positions. Arrows indicate editing sites that differ between 2C/POMC and control mice. (**B**) The extent of editing at each $5HT_{2C}$ site; mean ± SEM, n = 3 animals/condition; *p ≤ 0.05. (**C**) Encoded $5HT_{2C}$ protein isoforms (three-letter abbreviation) resulting from RNA editing are represented as percentage of total $5HT_{2C}$ sequence reads; mean ± SEM, n = 3 animals/condition; *p ≤ 0.05, **p ≤ 0.01, ***p ≤ 0.001.

bypasses time-consuming and energetically costly transcriptional and translational regulatory mechanisms. Several lines of evidence suggest that several factors involved in RNA processing are themselves regulated by energy status. For example, insulin signaling in pancreatic β-cells upregulates the expression of the splicing factor SRSF1, which in turn induces alternative splicing of the insulin receptor (208). The expression and activity of the RNA editing enzyme ADAR2 is also metabolically regulated in pancreatic cells (207). Despite some similarities in gene expression between neurons and pancreatic β-cells (209), energy-dependent alterations in RNA editing have not been detected in whole brain. It remains possible, however, that whole brain analyses lack the power to detect changes occurring only within energy-sensitive neurons in the brain. To address this possibility, we have focused on examining RNA processing of $5HT_{2C}$ in POMC neurons using the above-described mouse models (2C/POMC). Accordingly, we have manipulated the diet and exercise regimen of these models to assess whether $5HT_{2C}$ RNA processing adjusts in response to metabolic perturbations in an effort to maintain systemic energy homeostasis.

2C/POMC mice were randomly assigned to one of three diet groups: standard, high-fat (HFD), or calorie-restricted (CR). For HFD studies, singly housed, 5-week old mice were given *ad libitum* access to either a standard (control) diet (4.3% fat; Research Diets D12451K) or a nutritionally-matched HFD (45% fat; Research Diets D12451) for 20 weeks and food consumption was measured daily. For CR experiments, singly housed, 8- to 12-week old mice were calorically restricted to 60% of average daily consumption for 10 days or until mice lost 20% of their original body weight. CR mice were fed immediately before the onset of the dark cycle to minimize disruption of circadian rhythms (203). Analyses of hypothalamic $5HT_{2C}$ RNA editing profiles in 2C/POMC mice fed a HFD revealed no differences in editing compared to controls, even though the weights of HFD mice were significantly higher than those of controls at the end of the 20-week diet manipulation (Figure 3.4). In contrast, 2C/POMC mice under CR exhibited a small but significant increase in editing at the B- and D-sites of $5HT_{2C}$ compared to

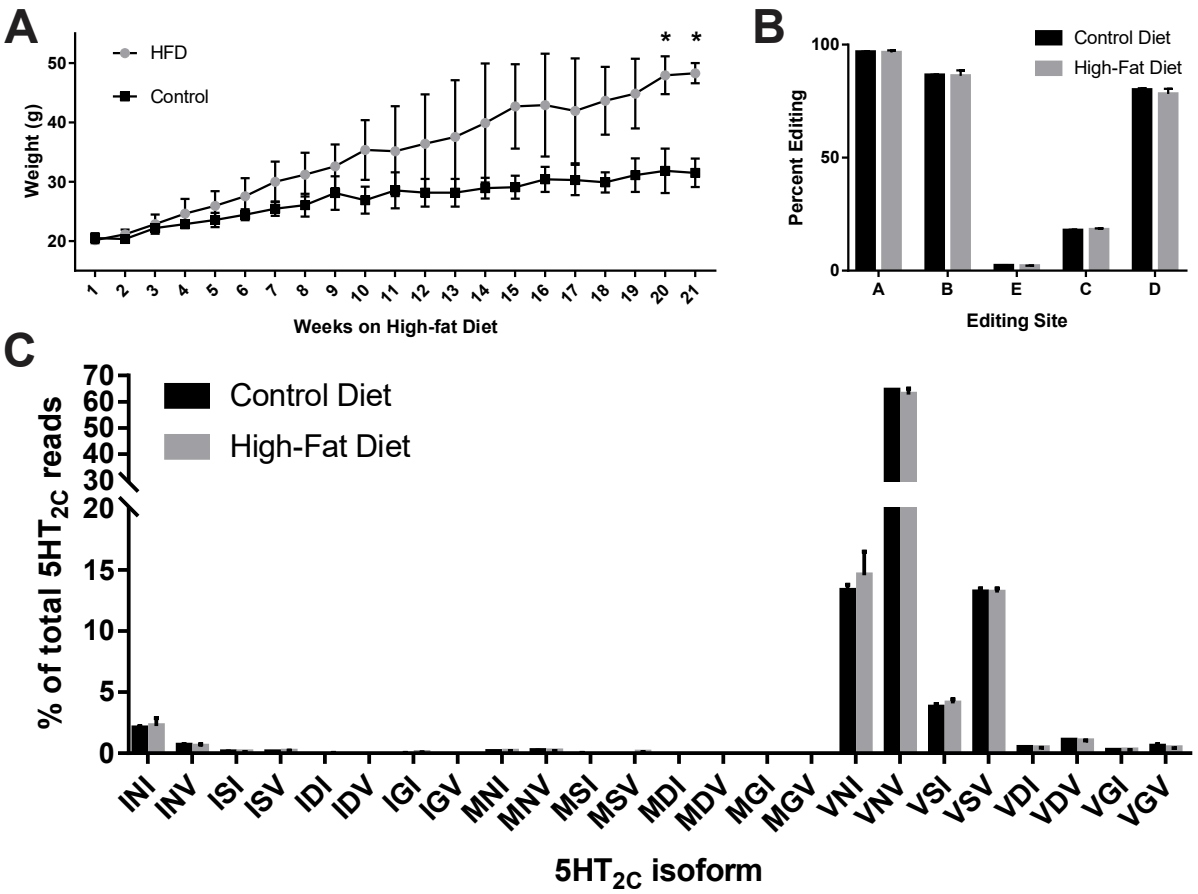

Figure 3.4. $5HT_{2C}$ editing profiles in response to high-fat diet. (**A**) 5-week old 2C/POMC animals were provided with regular chow diet (black bars) or a high-fat (45% kcal from fat) diet (grey bars) for 20 weeks; mean ± SEM (n = 3 animals/ condition) were statistically compared by unpaired t-test; *p ≤ 0.05. (**B**) The extent of editing at each $5HT_{2C}$ site; mean ± SEM, n = 3 animals/condition. (**C**) Encoded $5HT_{2C}$ protein isoforms (three-letter abbreviation) resulting from RNA editing are represented as percentage of total $5HT_{2C}$ sequence reads; mean ± SEM, n = 3 animals/condition.

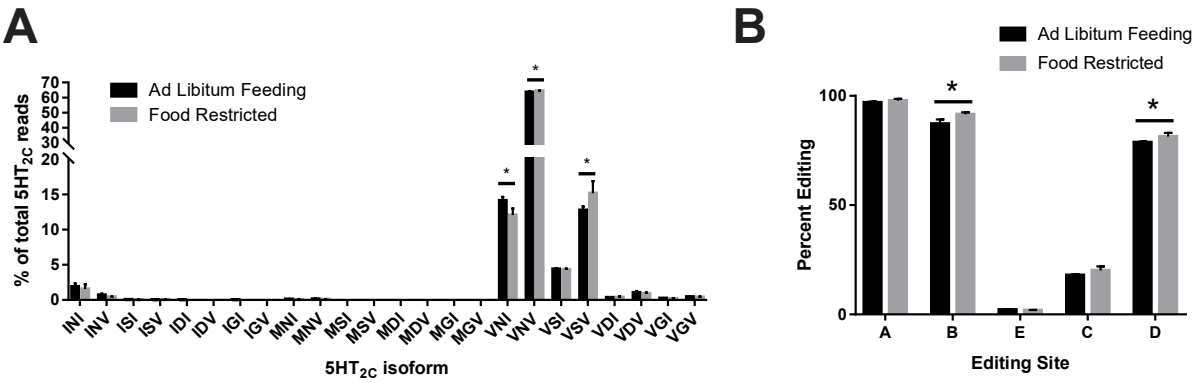

Figure 3.5. $5HT_{2C}$ editing profiles in re-sponse to calorie restriction. 8-12 week old 2C/POMC animals were provided either ad libitum ac-cess to regular chow diet (black bars) or a 40% reduction in total caloric intake (grey bars) for ten days or until mice lost more than 20% of starting weight. (**A**) Encoded $5HT_{2C}$ protein isoforms (three-letter abbreviation) resulting from RNA editing are represented as percentage of total $5HT_{2C}$ sequence reads; mean ± SEM, n = 3 animals/condition; *p ≤ 0.05. (**B**) The extent of $5HT_{2C}$ editing for each site; mean ± SEM, n = 3 animals/condition; *p ≤ 0.05.

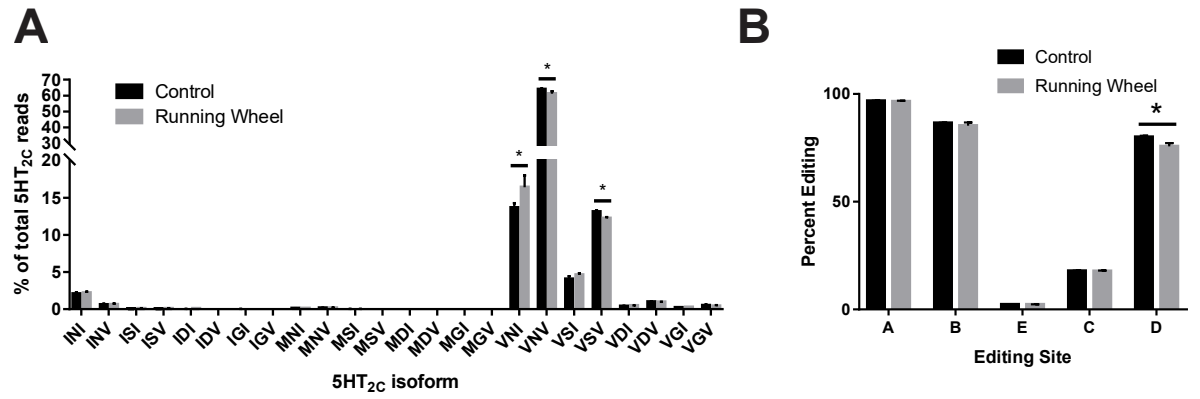

Figure 3.6. $5HT_{2C}$ editing profiles in response to voluntary exercise. 8-12 week old 2C/POMC animals were housed with (black bars) or without (grey bars) access to a running wheel for one month. (**A**) Encoded $5HT_{2C}$ protein isoforms (three-letter abbreviation) resulting from RNA editing are represented as percentage of total $5HT_{2C}$ sequence reads; mean ± SEM, n = 3 animals/condition; *p ≤ 0.05. (**B**) The extent of editing at each $5HT_{2C}$ site; mean ± SEM, n = 3 animals/condition, *p ≤ 0.05.

animals with *ad libitum* access to food (Figure 3.5). The increase in D-site editing appeared to result from an increase in the expression of $5HT_{2C}$ transcripts encoding the VNV and VSV receptor isoforms at the expense of transcripts encoding the VNI protein isoform. In addition to diet, exercise also regulates the metabolic and serotonergic systems (210,211). Therefore, we used a voluntary exercise paradigm to assess the functional dynamics of $5HT_{2C}$ RNA processing in POMC neurons. Relative to controls, exercised mice revealed a small but significant decrease in editing at the $5HT_{2C}$ D-site (Figure 3.6), which resulted from an increase in the expression of $5HT_{2C}$ transcripts encoding the VNI protein isoform at the expense of transcripts encoding the VNV and VSV protein isoforms.

Generation of mice containing $5HT_{2C}$ alleles encoding a single $5HT_{2C}$ isoform.

$5HT_{2C}$-null mice exhibit hyperphagia, adult-onset obesity and type 2 diabetes, and are insensitive to the anorectic effects of d-fen (190), yet selective reactivation of $5HT_{2C}$ receptor expression (solely in POMC neurons) rescues these deficits, reinforcing the importance of $5HT_{2C}$ expression in this specific neuronal subpopulation for the regulation of feeding and metabolism (185). To determine if distinct, edited $5HT_{2C}$ isoforms selectively expressed in POMC neurons can rescue the feeding and metabolic derangements observed in $5HT_{2C}$-null animals, we have generated mice that can be bred with mutant animals bearing a POMC:Cre transgene to generate progeny solely expressing the fully-edited or non-edited $5HT_{2C}$ isoforms in POMC neurons.

To generate mice that possess alleles encoding solely the fully-edited $5HT_{2C\text{-}VGV}$ isoform, we have taken advantage of a CRISPR/Cas9-based approach in which the five edited adenosine residues within exon 5 were mutated to guanosine moieties in the previously developed mouse strain where a loxP-flanked transcriptional blocker was inserted between exons 3 and 4 of the *Htr2c* gene to ablate $5HT_{2C}$ expression ($Htr2c^{tm1Jke}$/J) (185). Single-cell $Htr2c^{tm1Jke}$/J embryos were co-injected with the humanized *S. pyogenes* Cas9 enzyme and a chimeric guide RNA (sgRNA)

targeted to a selected locus of the *Htr2c* gene (212,213), in addition to a sense single-stranded oligodeoxynucleotide (ssODN) containing the desired $5HT_{2C\text{-}VGV}$ sequence flanked by homology arms corresponding to the target insertion site (Figure 3.7A). Embryos were transferred to pseudopregnant dams and allowed to develop normally. Offspring were screened by Sanger sequencing of genome-derived PCR amplicons flanking the edited region to verify the desired mutation. Analysis of Sanger sequencing electropherograms confirmed that several F0 pups acquired the desired mutation. These mice were then backcrossed to wild-type C57BL/6J mice to segregate any mosaic insertion/deletions (indels) or off-target modifications and to verify germline transmission of the targeted mutations in N1 pups. Screening of N1 mice by Sanger sequencing confirmed germline transmission of the desired mutation (Figure 3.7B).

Using a similar approach, we also generated a mutant mouse line on the $Htr2c^{tm1Jke}$/J background that introduced an allele solely encoding the non-edited $5HT_{2C\text{-}INI}$ isoform. Generation of this mutant mouse line required deletion of a portion of intron 5 rather than the simple adenosine to guanosine transitions necessary to encode the fully-edited $5HT_{2C\text{-}VGV}$ variant. Previous studies have demonstrated that A-to-I editing of $5HT_{2C}$ transcripts is dependent upon an extended duplex structure formed by imperfect inverted repeats flanking the editing sites and a region of intron 5, and that mutation of an intronic segment directly across from the editing sites was sufficient to disrupt the necessary duplex structure and ablate editing at all sites within the $5HT_{2C}$ pre-mRNA (Figure 3.8A) (28,214-216). To generate such a model on the $Htr2c^{tm1Jke}$/J background, we employed a non-homologous end joining (NHEJ) CRISPR/Cas9-based approach using two guide RNAs to induce two double-stranded breaks in intron 5 of the *Htr2c* gene and delete the intervening region (Figure 3.8B). F0 pups harboring this deletion were backcrossed to wild-type C57BL/6J mice to generate N1 pups. Screening of N1 mice by Sanger sequencing confirmed germline transmission of the desired mutation (Figure 3.8C).

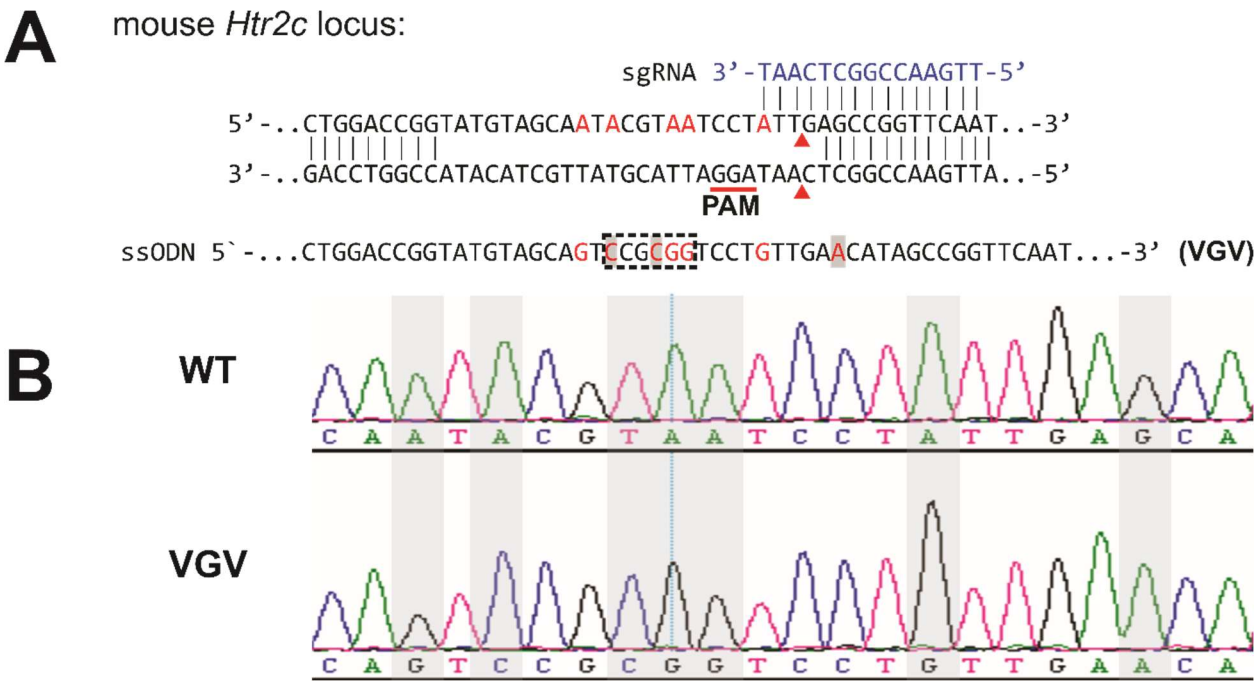

Figure 3.7. Generation of B6.129-Htr2c^{tm1Jke}/J mice containing 5HT$_{2C}$ alleles encoding the fully edited 5HT$_{2C}$ isoform. (**A**) Schematic diagram depicting the selected CRISPR guide RNA (sgRNA) used to direct Cas9 nuclease to produce a double-stranded break (red arrowheads) at the candidate 5HT$_{2C}$ locus within exon 5 of the *Htr2c* gene on the B6.129-Htr2c^{tm1Jke}/J background; RNA editing sites are show in red with bold lettering; PAM: protospacer adjacent motif (NGG) required for Cas9 cleavage. The donor template (ssODN) for homology-directed repair that was used to introduce guanosines at the editing sites (red lettering), as well as several silent mutations (red lettering with grey highlighting) to generate a SacII restriction site (dashed box) for screening and genotyping purposes, is shown. (**B**) Electropherogram traces of 5HT$_{2C}$-derived RT-PCR products generated from wild-type (WT) and mutant mice with alleles encoding the fully edited 5HT$_{2C}$ isoform (VGV). Nucleotides that were targeted using the strategy described in (**A**) are highlighted in grey.

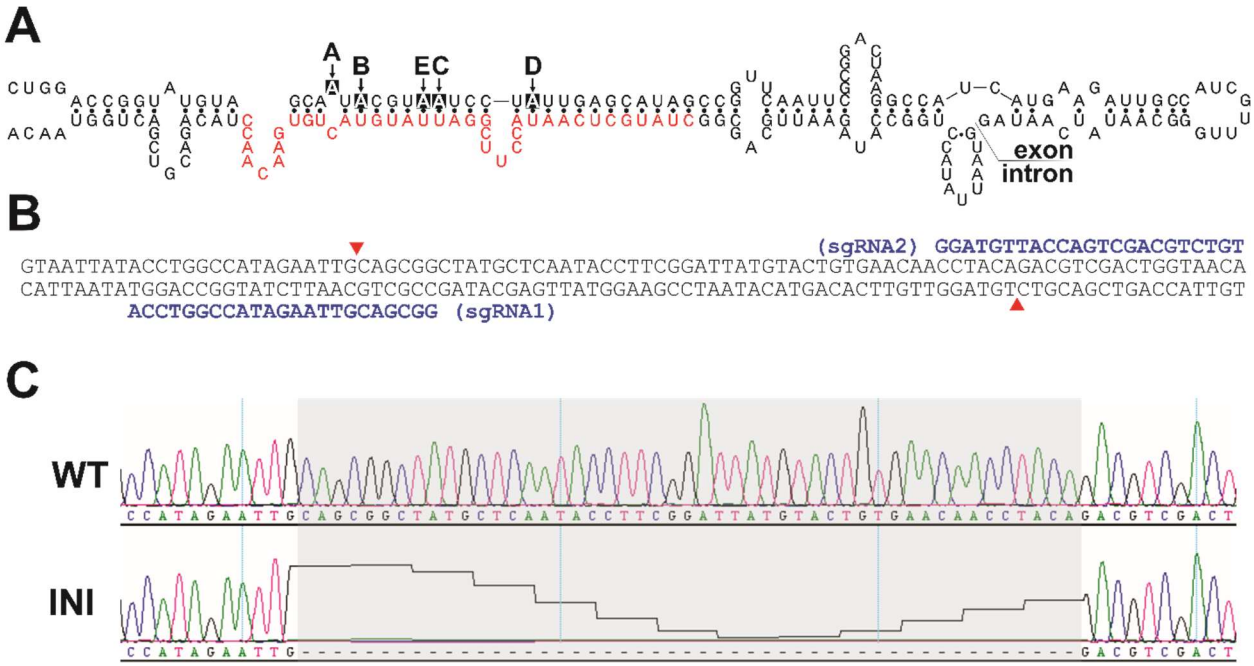

Figure 3.8. Generation of B6.129-Htr2c^{tm1Jke}/J mice containing 5HT$_{2C}$ alleles encoding the non-edited 5HT$_{2C}$ isoform. (**A**) Schematic diagram depicting the predicted duplex structure required for A-to-I editing within 5HT$_{2C}$ pre-mRNAs with the five editing sites (A-E; inverse lettering). The minimal sequence (editing site complementary sequence) in intron 5 that must be deleted to disrupt the duplex is shown in red lettering. (**B**) Nucleotide sequence of a portion of the Htr2c gene (intron 5) indicating the position of two sgRNAs and the predicted Cas9 cleavage sites to introduce double-stranded breaks (red arrows). (**C**) Electropherogram traces of 5HT$_{2C}$-derived RT-PCR products generated from wild-type (WT) and mutant mice with alleles encoding the non-edited 5HT$_{2C}$ isoform (INI). Nucleotides that were targeted using the strategy described in (**B**) are highlighted in grey; dashed lines in Sanger sequencing readout indicate deleted nucleotides in the aligned sequences.

Discussion

The expression of $5HT_{2C}$ receptors on POMC neurons is essential for the maintenance of energy homeostasis. Though transcripts encoding $5HT_{2C}$ receptors undergo critical RNA processing events, how $5HT_{2C}$ RNA editing shapes, or is shaped by, energy balance is unknown. Here, we have used a transgenic mouse model to examine $5HT_{2C}$ transcriptional profiles selectively in POMC neurons and have assessed whether or not $5HT_{2C}$ RNA editing changes in response to diet manipulation and exercise. Our results show that while $5HT_{2C}$ expression is selectively enriched in, but not limited to, POMC neurons in 2C/POMC mice, these animals demonstrate a distinct hypothalamic $5HT_{2C}$ RNA editing signature compared to control animals, suggesting that the $5HT_{2C}$ editing profile in POMC neurons is distinct from population-averaged $5HT_{2C}$ editing in whole hypothalamus. However, it remains possible that deletion of $5HT_{2C}$ in most cells, except POMC neurons, may have resulted in compensatory alterations in $5HT_{2C}$ RNA profiles in 2C/POMC mice relative to controls. Nevertheless, we probed $5HT_{2C}$ RNA editing in 2C/POMC mice following various metabolic manipulations. Our data show that high-fat diet does not change $5HT_{2C}$ RNA editing in POMC neurons. However, caloric restriction and exercise have opposing effects on $5HT_{2C}$ RNA editing in POMC neurons, respectively causing increased and decreased editing. The magnitude of these effects is relatively small, changing D-site editing by less than five percent. These changes in site-specific editing are caused by alterations in the relative expression of transcripts encoding the three major $5HT_{2C}$ isoforms expressed in 2C/POMC mice: VNV, VNI, and VSV. The mechanism underlying these changes in editing are unknown, and it is also unknown whether these metabolic perturbations alter editing of other ADAR substrates. It is intriguing to speculate however, that the increased editing observed in calorie-restricted mice increases the expression of more highly edited $5HT_{2C}$ protein isoforms, which in turn decreases $5HT_{2C}$ activity to inhibit POMC neurons, thereby promoting energy consumption.

To determine how distinct, edited $5HT_{2C}$ isoforms expressed in POMC neurons regulate energy balance, we have generated mice that can be bred with POMC:Cre mutant animals to generate progeny solely expressing the fully-edited or non-edited $5HT_{2C}$ isoforms in POMC neurons. Though additional work is necessary to generate double-mutant mice expressing $5HT_{2C\text{-}INI}$ or $5HT_{2C\text{-}VGV}$ on the 2C/POMC background, we anticipate that the $5HT_{2C\text{-}INI}$-expressing model will rescue the hyperphagia, hyperleptinemia, maturity-onset obesity and type II diabetes observed in $5HT_{2C}$-null mice, whereas the $5HT_{2C\text{-}VGV}$-expressing model will phenocopy several characteristics of Prader-Willi syndrome that overlap with the feeding abnormalities observed in $5HT_{2C}$-null animals (185,190).

Chapter IV

Regulation of RNA Editing by Intracellular Acidification

Modified from: Malik et al. Regulation of RNA Editing by Intracellular Acidification. *Nucleic Acids Research* (under review, 2020).

Introduction

Dynamic and rapidly coordinated gene expression relies upon various post-transcriptional mechanisms that modify RNA sequence, structure, and stability (6). Prevalent among more than one hundred RNA processing events that shape the transcriptional landscape is the conversion of adenosine to inosine (A-to-I) by RNA editing (9,103). It has been predicted that the human transcriptome contains as many as one-hundred million A-to-I editing sites, comprising selectively edited adenosines in protein-coding regions as well as hyper-edited adenosine clusters in non-coding, repetitive sequences such as short interspersed nuclear elements (SINEs) (103,104,141). A-to-I editing is generally identified as adenosine to guanosine (A-to-G) discrepancies during comparisons of genomic and cDNA sequences due to the base-pairing of cytidine to inosine (like guanosine) during reverse transcriptase-mediated first-strand cDNA synthesis. Many cellular machines also recognize inosine as guanosine, indicating that A-to-I editing constitutes functional A-to-G substitutions that can modulate diverse pathways involved in innate immunity, RNA splicing, RNA interference, and protein recoding (111,217).

The specificity and frequency of A-to-I editing are dictated by both *cis*- and *trans*-acting regulatory elements. *Cis*-acting factors such as RNA sequence context influence the extent of site-specific A-to-I conversion, but the formation of an extended region of double-stranded RNA (dsRNA) by intramolecular base-pairing is paramount for editing (92,93,102). The major *trans*-regulatory factors are the editing enzymes themselves, referred to as adenosine deaminases acting on RNA (ADARs), which catalyze the deamination of adenosine residues within dsRNA

substrates (111). Two active members of the vertebrate ADAR family, ADAR1 and ADAR2, each contain multiple copies of a dsRNA binding domain (dsRBD) and a carboxyl-terminal adenosine deaminase domain (55). The RNA editing reaction involves three main steps: 1) ADAR binding to the dsRNA substrate, 2) flipping the targeted adenosine out of the RNA duplex into the enzyme active site, and 3) hydrolytic deamination at position 6 of the purine ring (86).

Expression of ADAR1 and ADAR2 is ubiquitous but enriched in the brain along with inosine-containing mRNAs (218,219). Interestingly, many editing-dependent recoding events in mRNAs occur within transcripts critical for nervous system function. The extent of editing for these RNAs varies spatiotemporally and carries functional consequences for encoded proteins including changes in calcium permeability through GluA2 subunit-containing AMPA receptors, alterations in inactivation dynamics for the Kv1.1-subtype of voltage-gated potassium channel, and modulation of G-protein coupling efficacy and constitutive activity for the 2C-subtype of serotonin receptor ($5HT_{2C}$) (28,133,135,141). Furthermore, alterations in ADAR1 or ADAR2 expression have been shown to result in neurobehavioral phenotypes, as well as embryonic or early postnatal lethality, in animal models (39,42,134,220,221). Dysregulation of RNA editing in humans has been implicated in disorders of innate immunity and nervous system function including Aicardi-Goutières syndrome, epilepsy, suicide, amyotrophic lateral sclerosis, and schizophrenia (85,150,152,222,223). Taken together, these data not only demonstrate an important role for A-to-I editing in numerous physiological systems, but also suggest that editing may be regulated to produce transcriptional plasticity that can endow biological systems with adaptive capacities in the face of changing environmental or physiologic conditions (158,160).

In mammals, several proteins regulate ADAR stability and subsequent RNA editing. The coordinate action of a positive regulator, Pin1, and a negative regulator, WWP2, modulate ADAR2 expression through post-translational interactions (165). AIMP2 also inhibits editing by decreasing ADAR protein levels (141). Although these *trans*-acting regulators provide a mechanism for editing regulation by modulating ADAR stability, studies spanning the past decade have

consistently concluded that changes in ADAR protein expression do not fully account for differences in the extent of A-to-I conversion (141,161-164,224,225). Accordingly, it is likely that other factors modulate ADAR activity, rather than protein expression, to alter the extent of editing for ADAR substrates.

Recent studies of the structural basis for ADAR base-flipping have revealed the importance of a highly conserved glutamate (E1008 in ADAR1 and E488 in ADAR2) residing in the deaminase domain of the enzyme (82). This residue stabilizes the flipped-out conformation of the RNA duplex, presumably by occupying the space vacated by the flipped-out adenosine and hydrogen bonding with the complementary-strand orphaned base. Consistent with the idea that this glutamate requires protonation to stabilize the altered nucleic acid conformation, an enhancement in base-flipping and deamination rate is observed when this glutamate is mutated to a glutamine (E1008Q and E488Q in ADAR1 and ADAR2, respectively), which is fully protonated at physiologically relevant pH (84,86). These findings indicate that protonation of this glutamate may be critical for optimal catalytic activity and may alter the overall rate of ADAR catalysis during pH shifts in the cell.

To determine if editing is regulated by such changes in pH, we have employed a cell culture model system in which we analyzed ADAR1 or ADAR2-mediated editing of transfected minigene-derived RNAs subjected to acidic or more physiologically normal pH conditions. We also have performed *in vitro* studies to examine both editing kinetics and ADAR base-flipping in response to changes in pH. Finally, we have investigated how such changes in pH that occur in a cell culture model of hypoxia might affect the extent of site-selective A-to-I conversion. Our results show that RNA editing increases upon acidification, and that these effects are at least partially explained by enhanced base-flipping and deamination rate of ADARs at decreased pH.

Materials and Methods

Plasmids for transfection. cDNAs encoding mouse ADAR1 (p110) or rat ADAR2 were subcloned into mammalian expression vectors as previously described (28). To generate ADAR-Q mutants, E1008Q and E488Q mutations were respectively introduced to wild-type ADAR1 and ADAR2 plasmids using the QuikChange II Site-Directed Mutagenesis kit (Agilent Technologies), where the polymerase chain reaction (PCR) reactions were supplemented with 4% DMSO. Plasmids encoding human $5HT_{2C}$, mouse GluA2, and human Gli1 minigenes, containing the minimum sequences required for editing, were subcloned into either the pRC-CMV or pcDNA3 mammalian expression vectors (Thermo-Fisher) (28,46,226).

Cell culture. HEK293T cells were maintained in high-glucose Dulbecco's Modified Eagle Medium (DMEM, Gibco) supplemented with 10% heat inactivated fetal bovine serum (Gibco) and 1% 10,000 µg/ml penicillin-streptomycin (Gibco) and incubated in a humidified chamber at 37°C and 5% CO_2. Twenty-four hours prior to transfection, cells were seeded in 6-well plates (for RNA analysis) or 100 mm dishes (for protein analysis). Cells in 6-well plates were transiently co-transfected with 1 µg ADAR1, ADAR1-E1008Q (ADAR1-Q), ADAR2, or ADAR2-E488Q (ADAR2-Q) as well as 1 µg of one of the substrate minigene-expressing plasmids (*as described above*) using Fugene 6 (Promega) according to manufacturer's instructions. Cells in 100 mm dishes were transiently co-transfected with 3 µg of ADAR1 or ADAR2 expression plasmids, as well as 3 µg of the $5HT_{2C}$ minigene-containing plasmid using Fugene 6 according to manufacturer's instructions. Twenty-four hours after transfection, cells were washed with 1x Dulbecco's phosphate-buffered saline (DPBS) and incubated with high-glucose DMEM containing 3.7 mg/mL $NaHCO_3$ (for control samples) or high-glucose DMEM containing a reduced concentration of $NaHCO_3$ (either 2, 1.5, 1, 0.5, 0.17, or 0 mg/mL $NaHCO_3$ for experimental samples) for an additional 1, 3, 6, 12, or 24 hours at 37°C and 5% CO_2. Following this 24-hour incubation, a pH meter was used to measure the pH of the cell culture medium immediately after removing dishes from the tissue culture incubator.

The establishment of acidic culture medium via reduced $NaHCO_3$ concentration is similar to that previously reported by Kondo and colleagues (227,228).

Niclosamide treatment. HEK293T were seeded into 6-well plates and co-transfected with ADAR1 or ADAR2 and $5HT_{2C}$ expression vectors as described above. Twenty-four hours after transfection, cells were washed with 1x DPBS and incubated with high-glucose DMEM containing 3.7 g/L $NaHCO_3$ and treated for 6 hours with either 5 μM niclosamide (diluted from a freshly prepared 10 mM stock solution in DMSO) or an equivalent volume of DMSO.

Cell culture hypoxia. HEK293T were seeded into 6-well plates and co-transfected with ADAR1 or ADAR2 and $5HT_{2C}$ expression vectors as described above. Twenty-four hours after transfection, cells were washed with 1x DPBS and incubated with high-glucose DMEM containing 3.7 g/L $NaHCO_3$. Cells exposed to normoxic conditions were placed in the tissue culture chamber at 37°C and 5% CO_2 for 24 hours. Induction of hypoxia was achieved by subjecting cells to a 1% O_2/5% CO_2/94% N_2 environment within a modular incubator chamber (STEMCELL Technologies) placed inside the tissue culture chamber for 24 hours, as described previously (229). The pH of the cell culture medium was measured immediately following normoxic or hypoxic treatment.

Analysis of RNA editing from HEK293T cells. Total RNA was extracted from HEK293T cells using 1 mL Trizol Reagent (Invitrogen) according to manufacturer's instructions. DNA was removed from RNA samples using the Turbo™ DNase kit (Invitrogen), and following the rigorous DNase treatment procedure, cDNA was prepared from 1 μg of DNase-treated RNA sample using the High-Capacity cDNA Reverse Transcription kit (Applied Biosystems). When preparing cDNA, a control reaction lacking reverse transcriptase (-RT) was prepared in parallel for each RNA sample to ensure the absence of genomic DNA contamination. For each sample, PCR amplicons were generated and subjected to high-throughput sequencing for quantitative analysis of RNA editing, as described previously (161). The target-specific primers used to generate PCR amplicons are presented in Table 4.1.

Western blotting. HEK293T were seeded into 100 mm plates and co-transfected with ADAR1 or ADAR2 and $5HT_{2C}$ expression vectors as described above. Twenty-four hours after transfection, cells were washed with 1x DPBS and incubated with high-glucose DMEM containing 3.7 or 0 g/L $NaHCO_3$ for 24 hours. HEK293T whole cell lysates were prepared using RIPA lysis and extraction buffer (Thermo-Fisher). 20 µg of each sample was resolved by electrophoresis on a 4-20% gradient SDS-PAGE gel and then transferred to a nitrocellulose membrane using a Trans-Blot® SD semi-dry transfer cell (Bio-Rad). After blocking the membrane with Intercept PBS blocking buffer (LI-COR) for 1 hour, the membrane was probed using either a mouse ADAR1 monoclonal antibody (sc-73408, Santa Cruz; 1:1000 dilution) or an affinity-purified rat ADAR2 antiserum (Exalpha Biologicals; 1:375 dilution), as well as a polyclonal affinity-purified β-actin antibody (sc-1616-R, Santa Cruz; 1:1000 dilution). ADAR1 and β-actin signals were detected using IRDye secondary antibodies (LI-COR; 1:20,000 dilution), and ADAR2 signals were detected using Alexa Fluor® 790 light-chain specific anti-sheep IgG secondary antibody (Jackson ImmunoResearch; 1:50,000). All blots were imaged using an Odyssey CLx infrared imaging system (LI-COR) and quantified using Image Studio Lite (LI-COR).

pHrodo intracellular pH indication. HEK293T cells were seeded on poly-L-lysine- and laminin-coated 35-mm glass bottom dishes (MatTek Life Sciences). Twenty-four hours later, cells were washed with Live Cell Imaging Solution (LCIS) and incubated for 30 minutes with 2 µL of pHrodo Red AM Intracellular pH Indicator (Invitrogen) diluted in 20 µL of PowerLoad concentrate and added to 2 mL of pre-warmed LCIS. Cells were then washed in DPBS and incubated for 6 hours at 37°C and 5% CO_2 with high-glucose DMEM lacking phenol red and containing either 0 or 3.7 g/L $NaHCO_3$. Plates were then removed from the cell culture incubator and 2 µL of BioTracker™ 488 Nuclear Dye (Sigma-Aldrich) were added directly to the cell culture medium and incubated at 37°C for 10 minutes. Immediately following this incubation, z-stack images were captured using a Zeiss LSM 510 META Inverted confocal microscope. pHrodo Red and

BioTracker™ 488 were excited at 543 nm and 488 nm, respectively. The average pHrodo Red fluorescence intensity per cell was quantified using Fiji image processing software.

General biochemical procedures. Unless otherwise stated, all regents were purchased from commercial sources (Fisher Scientific or Sigma Aldrich) and were used without further purification. Reagents for *in vitro* transcription, *in vitro* editing, and PCR amplification were purchased from: Promega: Access RT-PCR kit, RQ1 DNase free RNase; Qiagen: Gel Extraction kit; Zymo Research: DNA Clean & Concentrator kit; Syd Labs: Spin columns for PCR product clean up; New England BioLabs: Molecular-biology-grade bovine serum albumin (BSA), and RNase inhibitor. SDS-polyacrylamide gels were visualized with a Molecular Dynamics 9400 Typhoon phosphorimager. Data were analyzed with Molecular Dynamics ImageQuant 5.2 software. All MALDI analyses were performed at the University of California, Davis Mass Spectrometry Facilities using a Bruker ultrafleXtreme MALDI TOF/TOF mass spectrometer. Oligonucleotide masses were determined with Mongo Oligo Calculator v2.08. Unless otherwise noted, oligonucleotides were purchased from either Dharmacon or Integrated DNA Technologies.

Purification of oligonucleotides. All oligonucleotides for biochemical experiments were purified by denaturing polyacrylamide gel electrophoresis (PAGE) and visualized by UV shadowing. Oligonucleotides extracted from the gel using the crush and soak method for 16 h at 4 °C into 0.5 M NH_4OAc and 1 mM EDTA. Polyacrylamide fragments were removed using a 0.2 µm pore size cellulose acetate membrane filter (Corning). Oligonucleotides were precipitated from 75% ethanol containing 75 mM NaOAc at -70°C for 2 hours. The resulting pellet was dried under vacuum and resuspended in nuclease free water.

***In vitro* transcription and preparation of editing target RNA.** Target RNA was transcribed from a DNA template with the MEGAScript T7 Kit (ThermoFisher). DNA digestion was performed using RQ1 RNase-free DNase (Promega). The DNase-treated RNA product was purified by 4% PAGE as described above. Purified $5HT_{2c}$ target RNA (180nM) was added to 1X TE buffer and 100 mM NaCl, heated to 95 °C for 5 min, and slowly cooled to room temperature.

Protein overexpression and purification of ADAR2 constructs. Human ADAR2 deaminase domain (ADAR2d), wild-type human ADAR2, and human ADAR2-E488Q were expressed and purified as previously described (230). Purification was carried out by lysing cells in buffer containing 20 mM Tris-HCl, pH 8.0, 5% glycerol, 1 mM 2-mercaptoethanol, 750 mM NaCl, 35 mM imidazole, and 0.01% Nonidet P-40 using a French press. Cell lysate was clarified by centrifugation (39,000 x g for 1 h). Lysate was passed over a 3 mL Ni-NTA column, which was then washed in 3 steps with 20 mL lysis buffer, wash I buffer (20 mM Tris-HCl, pH 8.0, 5% glycerol, 1 mM 2-mercaptoethanol, 750 mM NaCl, 35 mM imidazole, 0.01% Nonidet P-40), wash II buffer (20 mM Tris-HCl, pH 8.0, 5% glycerol, 1mM 2-mercaptoethanol, 35 mM imidazole, 500 mM NaCl), and eluted with 20 mM Tris-HCl, pH 8.0, 5% glycerol, 1 mM 2-mercaptoethanol, 400 mM imidazole, 100 mM NaCl. Fractions containing the target protein were pooled and concentrated to 30-80 μM for use in biochemical assays. Purified wild-type ADAR2 was stored in 20 mM Tris-HCl pH 8.0, 100 mM NaCl, 20% glycerol and 1 mM 2-mercaptoethanol at -70°C. Protein concentrations were determined using BSA standards visualized by SYPRO orange staining of SDS-polyacrylamide gels.

Protein Overexpression and Purification of ADAR1 p110. MBP-tagged human ADAR1 p110 construct was cloned into a pSc vector using standard PCR techniques (74). The generated construct (yeast codon optimized) consisted of an N-terminal MBP-tag, a tobacco etch virus (TEV) protease cleavage site followed by human ADAR1 p110 gene. The obtained clone was transformed in *S. cerevisiae* BCY123 cells and overexpressed as described previously (230). Purification was carried out by lysing cells in lysis/binding buffer containing 50 mM Tris-HCl, pH 8.0, 5% glycerol, 5 mM 2-mercaptoethanol, 1000 mM KCl, 0.05% NP-40 and 50 μM $ZnCl_2$ using a microfluidizer. Cell lysate was clarified by centrifugation (39,000 x g for 50 min). Lysate was passed over a 2 mL NEB amylose column (pre-equilibrated with binding buffer), which was then washed in 2 steps with 50 mL binding buffer followed by 100 mL wash buffer (50 mM Tris-HCl, pH 8.0, 5% glycerol, 5 mM 2-mercaptoethanol, 500 mM KCl, 0.01% NP-40 and 50 μM $ZnCl_2$) and

eluted with buffer containing 50 mM Tris-HCl, pH 8.0, 10% glycerol, 5 mM 2-mercaptoethanol, 500 mM KCl, 0.01% NP-40, 50 μM $ZnCl_2$, and 20 mM maltose. Fractions containing the target protein were pooled and dialyzed against a storage buffer containing 50 mM Tris-HCl, pH 8.0, 400 mM KCl, 0.5 mM EDTA, 0.01% NP-40, 10% glycerol and 1 mM tris(2-carboxy-ethyl)phosphine. Dialyzed protein was concentrated to 2-50 μM and stored as aliquots at -70 °C until further use in biochemical assays. Protein concentrations were determined using BSA standards visualized by SYPRO orange staining of SDS-polyacrylamide gels.

Deamination Assay with ADAR2d, ADAR2, and ADAR1 p110. Deamination assays were performed under single-turnover conditions in 15 mM Tris-HCl (pH 7.0 to 8.5) or 15 mM Bis-Tris-HCl (pH 6.0 to 7.0), 3% glycerol, 60 mM KCl, 1.5 mM EDTA, 0.003% Nonidet P-40, 3 mM $MgCl_2$, 160 U/mL RNAsin, 1.0 μg/mL yeast tRNA, 10 nM RNA, and 75 nM ADAR2d or wild-type ADAR2. Each reaction solution was incubated at 30 °C for 30 min before the addition of enzyme. Reactions were then incubated at 30 °C for varying times prior to quenching with 190 μL 95°C water and heating at 95 °C for 5 min. Reaction products were used to generate cDNA using RT-PCR (Promega Access RT-PCR System). The target-specific primers used to generate these PCR amplicons are presented in Table 4.2. DNA was purified using a DNA Clean & Concentrator kit (Zymo) and subjected to Sanger Sequencing using an ABI Prism 3730 Genetic Analyzer at the UC Davis DNA Sequencing Facility. The sequencing peak heights were quantified in 4Peaks v1.8. Data were fit to the equation $[\mathrm{P}]t = 0.9[1 - e^{-k_{\mathrm{obs}} * t}]$ for ADAR2 and $[\mathrm{P}]t = 0.6[1 - e^{-k_{\mathrm{obs}} * t}]$ for ADAR1 p110 where $[\mathrm{P}]t$ is percent edited at time t, and k_{obs} is the observed rate constant. Each experiment was carried out in triplicate where the k_{obs} reported is the average of each replicate ± standard deviation. Statistical significance between groups was determined by one-way ANOVA using Prism software (Graph Pad). For the ADAR1 p110 enzyme, deaminations were performed as above with the following modifications: The final reaction solution for ADAR1 p110 contained 15 mM Tris-HCl (pH 7.0 to 8.5) or 15 mM Bis-Tris-HCl (pH 6.0 to 7.0), 4% glycerol, 26 mM KCl,

40 mM potassium glutamate, 1.5 mM EDTA, 0.003% Nonidet P-40, 160 U/mL RNAsin, 1.0 μg/mL yeast tRNA, and 10 nM RNA, and 150 nM ADAR1 p110.

Preparation of Duplex Substrates for Base-Flipping Analysis. Oligonucleotides previously described for use in ADAR2 base-flipping analysis were purchased from Dharmacon (86). RNAs were purified by 18% PAGE as previously described. PAGE purified top and bottom strands were annealed for a final concentration of 30 μM edited strand, 45 μM guide strand, 30 mM Tris-HCl, 6% glycerol, 120 mM KCl, 3 mM EDTA, 0.006% NP-40, and 0.6mM DTT. The mixture was heated to 95°C for 5 min, and slowly cooled to room temperature.

Base-flipping assay using a fluorescent RNA substrate. Fluorescence measurements were performed using a CLARIOstar microplate reader and a Nunc MaxiSorp 384-well black bottom plate. Excitation was at 320 nm and fluorescence emission was scanned from 340 to 430 nm with 0.2 nm resolution. Spectra were obtained for solutions containing 2.5 μM RNA, with or without 10 μM ADAR2, in 36 mM Tris-HCl (pH 7.0 to 8.5) or Bis-Tris-HCl (pH 6.0 to 7.0), 7% glycerol, 142 mM KCl, 3.6 mM EDTA, 0.007% NP-40, and 0.7 mM DTT at room temperature (78). The background fluorescence of the enzyme buffered at each pH was subtracted from the spectrum of the complex, and the background fluorescence of the buffer alone at each pH was subtracted from the RNA. Each spectrum is an average of three independent measurements that were LOWESS fit in Prism software (GraphPad). The fluorescence intensity values at λ_{max} were used to determine the fluorescence enhancement by ADAR in the formula FE = ($FI_{ADAR\text{-}RNA}$-FI_{RNA})/FI_{RNA} where FE is fluorescence enhancement, and FI values are the fluorescence intensity of samples containing either RNA or RNA in the presence of ADAR2. Fluorescence enhancement values were normalized so that the value of $FI_{ADAR\text{-}RNA}$ at pH 7.5 corresponds to 1.

Table 4.1. Target-specific primers for quantitative analysis of RNA editing in transfected cells

Transcript	Sense or Antisense	Primer Sequence
$5HT_{2C}$	Sense	5'- ATT AAC CCT CAC TAA AGG GAC GCT GGA TCG GTA TGT AGC A -3'
	Antisense	5'- TAA TAC GAC TCA CTA TAG GGC GTC TGT ACG TTG TTC ACA GTA C -3'
GluA2 (Q/R, +3, +4, +60, and +88 sites)	Sense	5'- ATT AAC CCT CAC TAA AGG GAA TAG TCT CTG GTT TTC CTT GGG -3'
	Antisense	5'- TAA TAC GAC TCA CTA TAG GGA GCT GGT GAC ATC TTT ATG GTG -3'
GluA2 (sites +241 through +271)	Sense	5'- ATT AAC CCT CAC TAA AGG GAG TTG ATC AGG TGT TTC CCT GGT -3'
	Antisense	5'- TAA TAC GAC TCA CTA TAG GGC GAT CTA AAA TCG CCC ATT TTC CC -3'
Gli1	Sense	5'- ATT AAC CCT CAC TAA AGG GAG GAC AGA ACT TTG ATC CTT ACC TCC -3'
	Antisense	5'- TAA TAC GAC TCA CTA TAG GGC ATA TAG GGG TTC AGA CCA CTG -3'

Table 4.2. Target-specific primers for quantitative analysis of *in vitro* RNA editing

Transcript	Sense or Antisense	Primer Sequence
$5HT_{2C}$	Sense	5'- TGG GTA CGA ATT CCC ACT TAC GTA CAA GCT T -3'
	Antisense	5'- AGA ACC CGA TCA AAC GCA AAT GTT AC- 3'
Gli1	Sense	5'- CAG AAC TTT GAT CCT TAC CTC C -3'
	Antisense	5'- CAT ATA GGG GTT CAG ACC ACT G -3'

Results

Intracellular acidification increases RNA editing

Kinetic analyses of ADAR activity in which a conserved glutamate in the deaminase domain was mutated to a glutamine, which is fully protonated under normal conditions, revealed enzyme hyperactivity (82,84,86). These observations suggest that editing activity by wild-type ADARs may be enhanced when the intracellular proton concentration is increased beyond that normally observed under control conditions. To determine the effects of cellular acidification on RNA editing, minigene constructs encoding the minimum essential RNA duplexes required for editing of $5HT_{2C}$, GluA2, and Gli1 transcripts (Figure 4.1A) were transiently co-expressed with either ADAR1 or ADAR2 in a human embryonic kidney (HEK293T) cell line, followed by quantitative analysis of site-selective A-to-I conversion. For these studies, the pH of the cell culture medium was adjusted to either pH 7.4 (control) or pH 6.7 (acidic) by manipulation of the bicarbonate concentration, which affects the buffering capacity of the media in the 5% CO_2 incubator environment. Acidification significantly increased ADAR1 and ADAR2-mediated editing of numerous sites within the examined transcripts (Figure 4.1B-D), although the magnitude of the effect was both site-dependent and dependent upon the specific ADAR acting upon it. To further examine these effects using a more complex RNA target, we used a high-throughput sequencing-based approach to quantify the 32 transcriptional permutations arising from combinatorial editing at up to five sites within $5HT_{2C}$ transcripts (sites A, B, E, C, and D). Results from this analysis showed that acidification significantly increased the expression of several more highly edited $5HT_{2C}$ RNA isoforms at the expense of less edited RNA species (Figure 4.2).

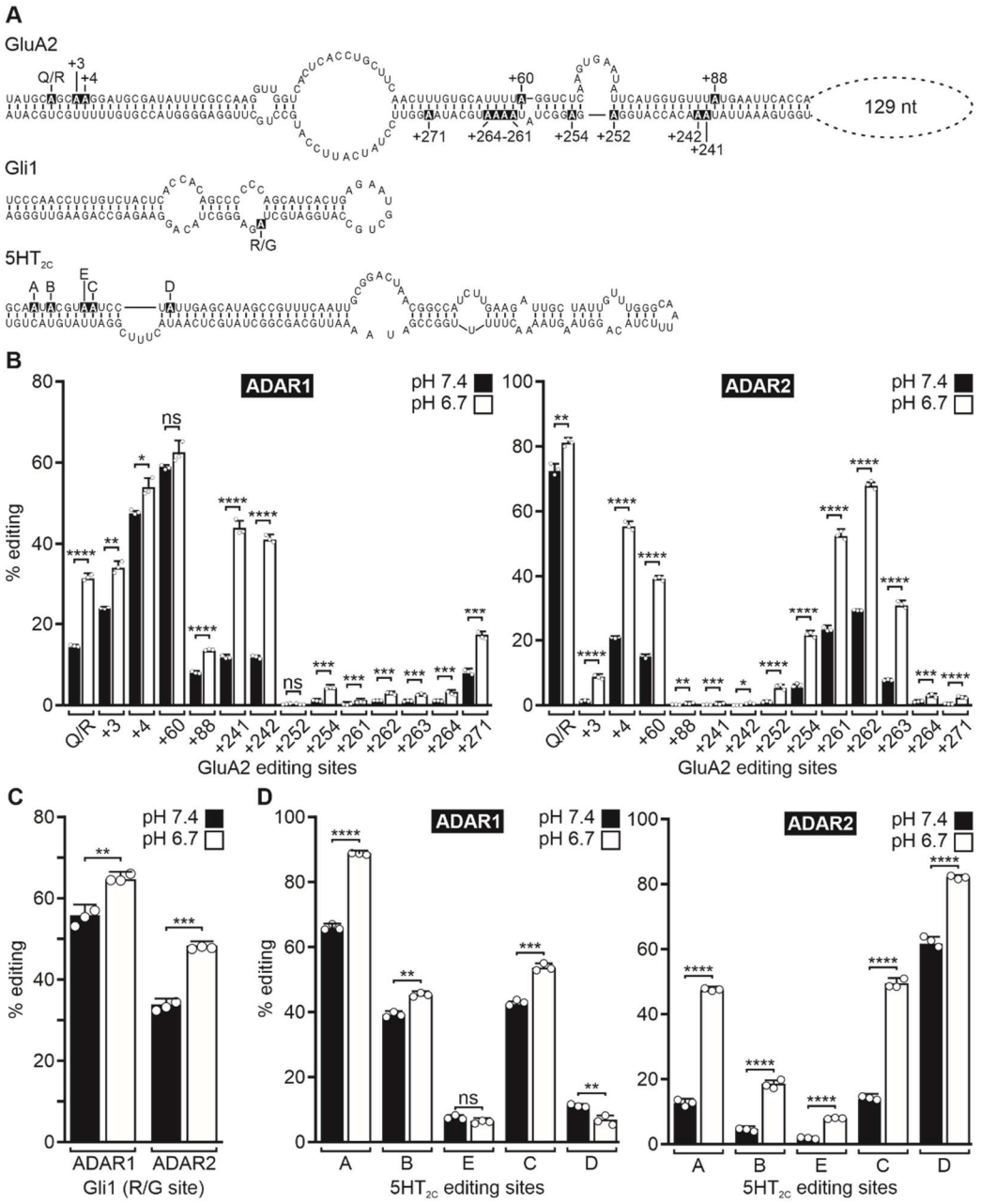

Figure 4.1. Effects of cellular acidification on A-to-I editing. (**A**) The predicted secondary structures of GluA2, Gli1, and $5HT_{2C}$ minigene-derived RNA transcripts is presented; editing sites are indicated in inverse lettering; nt = nucleotides. (**B-D**) Quantification of site-selective ADAR1 or ADAR2-mediated editing in minigene-derived RNAs from HEK293T cells incubated with control media (pH 7.4) or under acidic conditions (pH 6.7). Results for 24-hour editing assays for GluA2 and $5HT_{2C}$, and 6-hour editing assays for Gli1 are shown. Plotted values are the means of three biological replicates (○) ± standard deviation. Statistical significance between groups for each site in GluA2 and $5HT_{2C}$ transcripts was determined using the Holm-Sidak t-test for multiple comparisons; statistical significance between groups for the Gli1 R/G site was determined using an unpaired t-test with Welch's correction; *p ≤ 0.05; **p ≤ 0.01; ***p ≤ 0.001; ****p ≤ 0.0001; ns, not significant.

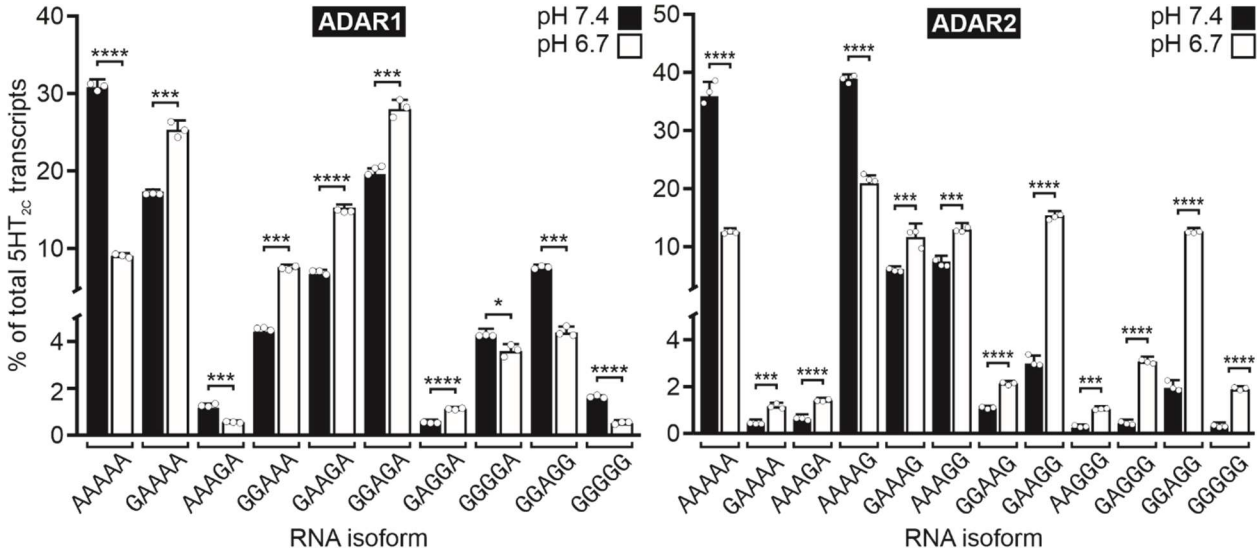

Figure 4.2. Quantification of $5HT_{2C}$ RNA editing profiles. The relative expression of $5HT_{2C}$ RNA isoforms constituting ≥1% of total $5HT_{2C}$ transcripts is presented. Permutations of editing are designated by the presence of adenosine (A) or guanosine (G) residues at sites A-E within the sequenced cDNA library (AAAAA = non-edited; GGGGG = fully edited). Plotted values are the means of three biological replicates (○) ± standard deviation. Statistical significance between groups for each $5HT_{2C}$ isoform was determined using the Holm-Sidak t-test for multiple comparisons; *$p \leq 0.05$; ***$p \leq 0.001$; ****$p \leq 0.0001$.

To examine pH-dependent increases in RNA editing as a function of time, we quantified the A-to-I modification of $5HT_{2C}$ transcripts by ADAR1 or ADAR2 over a time course from 1 to 24 hours (Figure 4.3 and Figure 4.4). We chose $5HT_{2C}$ RNA for these studies because it contains multiple editing sites that are recognized by both ADARs, though previous studies have shown that ADAR1 preferentially edits the A- and B-sites, and ADAR2 preferentially edits the D-site (28). The extent of editing for all five $5HT_{2C}$ sites was increased significantly under acidic conditions for most time points. For several sites, a significant increase in editing at pH 6.7 (acidic) compared to pH 7.4 (control) could be observed in as little as one hour and continued to increase over control levels over the entire 24-hour time period. Interestingly, ADAR1 editing of the A-site as well as ADAR2 editing of several sites appeared to increase logarithmically under acidic conditions, whereas the time-dependent increases in editing under control conditions appeared more linear. We also examined pH-dependent alterations in Gli1 editing at two timepoints, 6 and 24 hours (Figure 4.1C and Figure 4.5). Acidification-induced increases in editing at the R/G site were observed only at the earlier timepoint. Interestingly, the absence of increased editing at reduced pH for the R/G site at 24 hours was concurrent with increased editing at additional adenosine residues within the Gli1 transcript, many of which exhibited increased editing upon acidification. These results indicate that editing of the R/G site reached its endpoint by 24 hours and further suggest that the rate of catalysis for this site is more rapid than for other Gli1 sites.

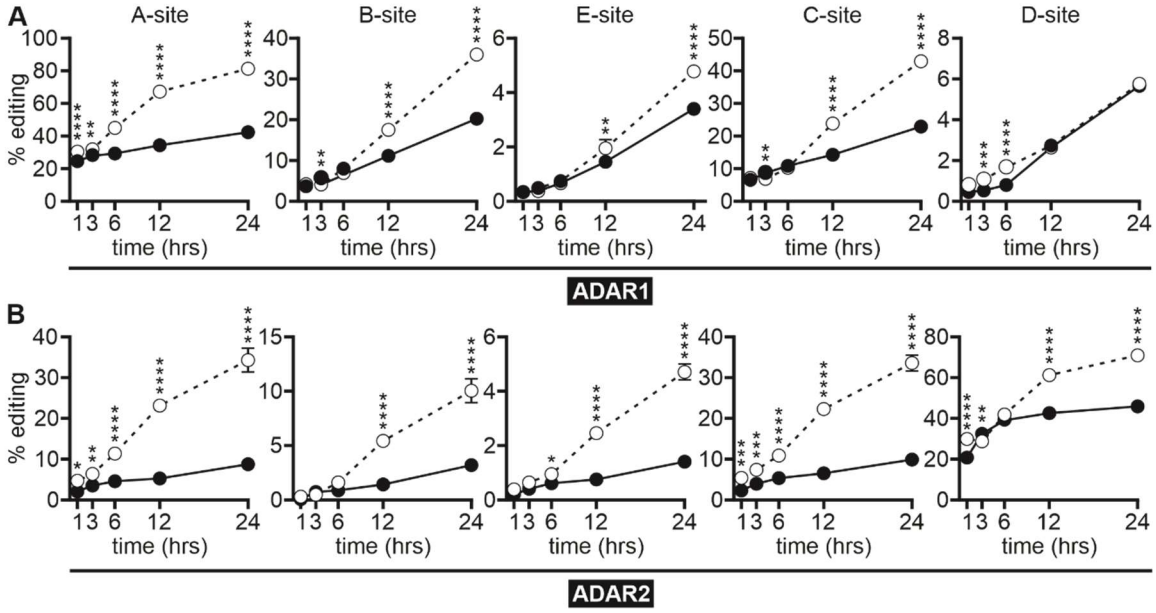

Figure 4.3. Time course for site-selective editing of $5HT_{2C}$ transcripts at reduced pH. (**A**) A comparison of the extent of ADAR1 or (**B**) ADAR2-mediated editing for $5HT_{2C}$ transcripts at control (pH 7.4, —●—) or acidic pH (pH 6.7, ---○---) after 1, 3, 6, 12, or 24 hours is presented. Plotted values are the means of three biological replicates ± standard deviation. Statistical significance between groups at a given time point was determined using Sidak's multiple comparisons test; *p ≤ 0.05; **p ≤ 0.01; ***p ≤ 0.001; ****p ≤ 0.0001.

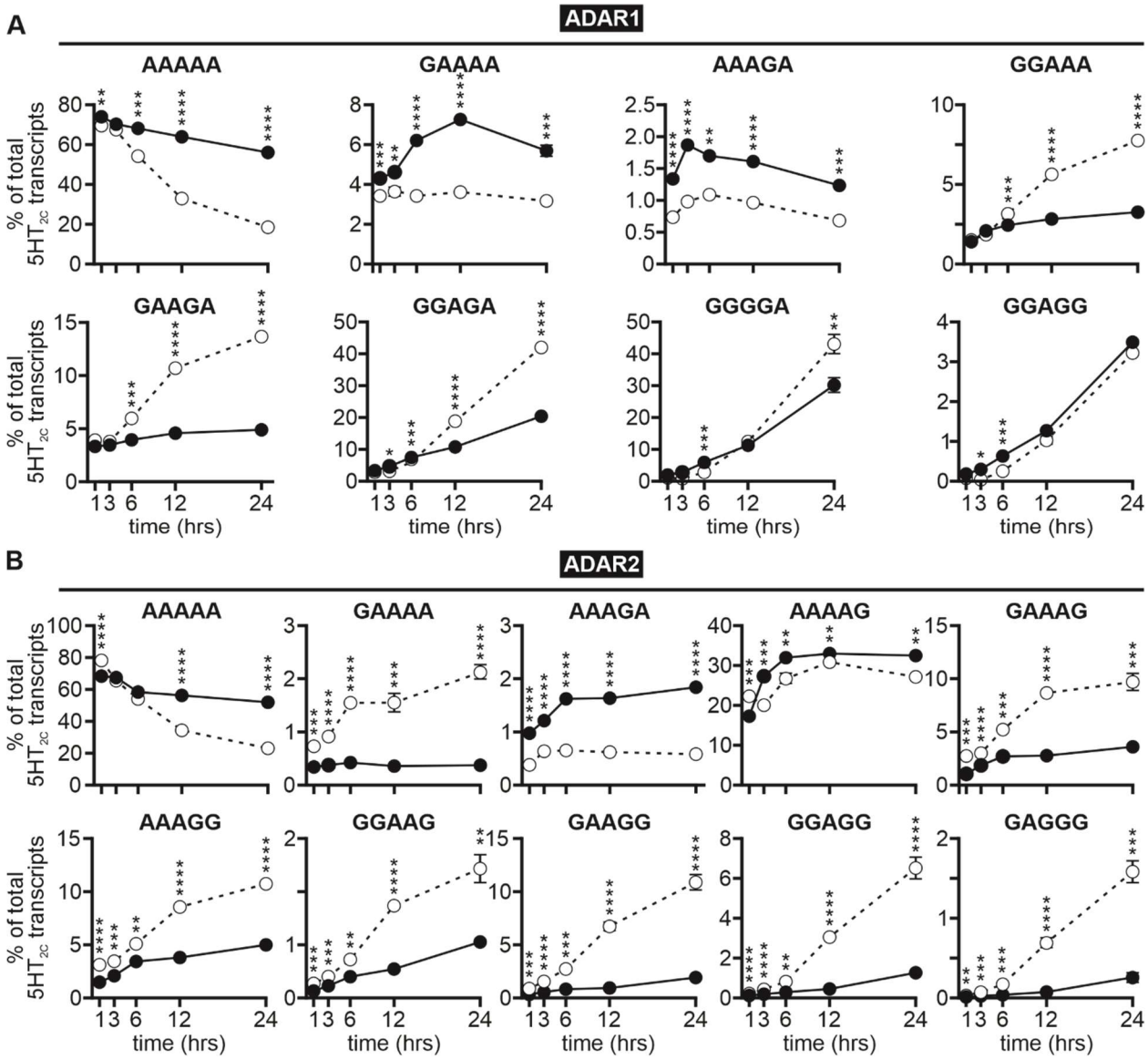

Figure 4.4. Time course for the expression of $5HT_{2C}$ RNA editing isoforms at reduced pH. (**A**) Relative expression of $5HT_{2C}$ RNA editing isoforms (constituting ≥1% of total $5HT_{2C}$ transcripts) generated by ADAR1 or (**B**) ADAR2-mediated editing at control (pH 7.4, —●—) or acidic pH (pH 6.7, ---○---) after 1, 3, 6, 12, or 24 hours is presented. Permutations of editing are designated by the presence of adenosine (A) or guanosine (G) residues at sites A-E within the sequenced cDNA library (AAAAA = non-edited; GGGGG = fully edited). Plotted values are the means of three biological replicates ± standard deviation. Statistical significance between groups at a given time point was determined using Sidak's multiple comparisons test; *p ≤ 0.05; **p ≤ 0.01; ***p ≤ 0.001; ****p ≤ 0.0001.

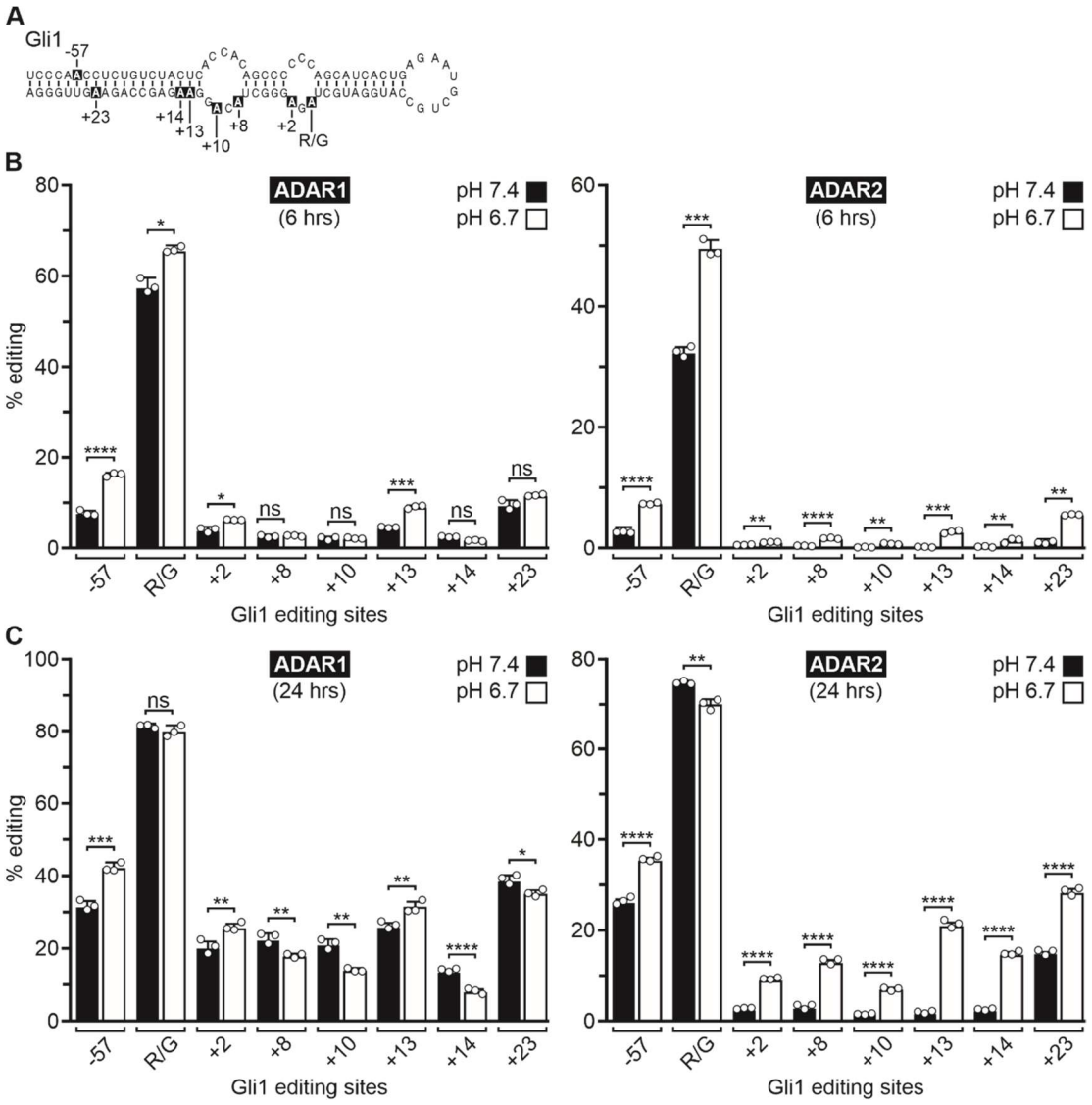

Figure 4.5. Time-dependent editing of Gli1 transcripts at reduced pH. (**A**) The predicted secondary structure of the Gli1 minigene-derived transcript is presented; editing sites are indicated in inverse lettering. (**B**) Quantification of ADAR1 or ADAR2-mediated Gli1 editing from HEK293T cells incubated with control media (pH 7.4) or under acidic conditions (pH 6.7) for 6 hours. (**C**) Quantification of the extent of ADAR1 or ADAR2-mediated Gli1 editing from HEK293T cells incubated with control media (pH 7.4) or under acidic conditions (pH 6.7) for 24 hours. Plotted values are the means of three biological replicates (each replicate is shown as ○) ± standard deviation. Statistical significance between groups for each Gli1 site was determined using the Holm-Sidak t-test for multiple comparisons; *p ≤ 0.05; **p ≤ 0.01; ***p ≤ 0.001; ****p ≤ 0.0001; ns, not significant.

To further examine how RNA editing is affected by alterations in pH, we analyzed ADAR1 or ADAR2-mediated editing of $5HT_{2C}$ transcripts over a pH range from 6.7 to 7.4 that was established by varying the concentration of bicarbonate in the cell culture medium between 0 and 3.7 mg/mL $NaHCO_3$ (Figure 4.6A). ADAR1 editing at the A-, B-, and C-sites, as well as ADAR2 editing at all five sites, showed incremental increases in editing with decreasing pH (Figure 4.7A-B; statistical analysis of Figure 4.7A-B shown in Figure 4.6B; and Figure 4.8). The largest stepwise increase in pH-dependent ADAR1 editing was observed between pH 7.4 and 7.3, whereas the largest stepwise increase in pH-dependent ADAR2 editing was observed between pH 6.9 and 6.8.

To verify that changing the bicarbonate concentration to manipulate the extracellular pH concomitantly produced changes in intracellular pH, we used a fluorescent pH indicator, pHrodo Red, whose fluorescence intensity is inversely correlated with intracellular pH. pHrodo fluorescence significantly increased upon incubation with the acidic cell culture medium (pH 6.7) (Figure 4.7C). This highly fluorescent pHrodo Red signal colocalized with a vital nuclear dye (BioTracker 488), indicating acidification of the nucleus, which is thought to be the major site of ADAR localization and RNA editing (231,232). To verify that the observed increases in RNA editing resulted from decreased pH rather than cellular mechanisms associated with altered extracellular bicarbonate levels, we employed an alternative method to induce intracellular acidification by treating cells with niclosamide, which has previously been shown to trigger intracellular acidification in the absence of extracellular acidification (233). Significant increases in ADAR1-mediated editing of the A-, B-, and C-sites as well as ADAR2-mediated editing of the B- and C-sites were observed upon 6-hour treatment with 5 μM niclosamide compared to vehicle-treated controls (Figure 4.7D-E).

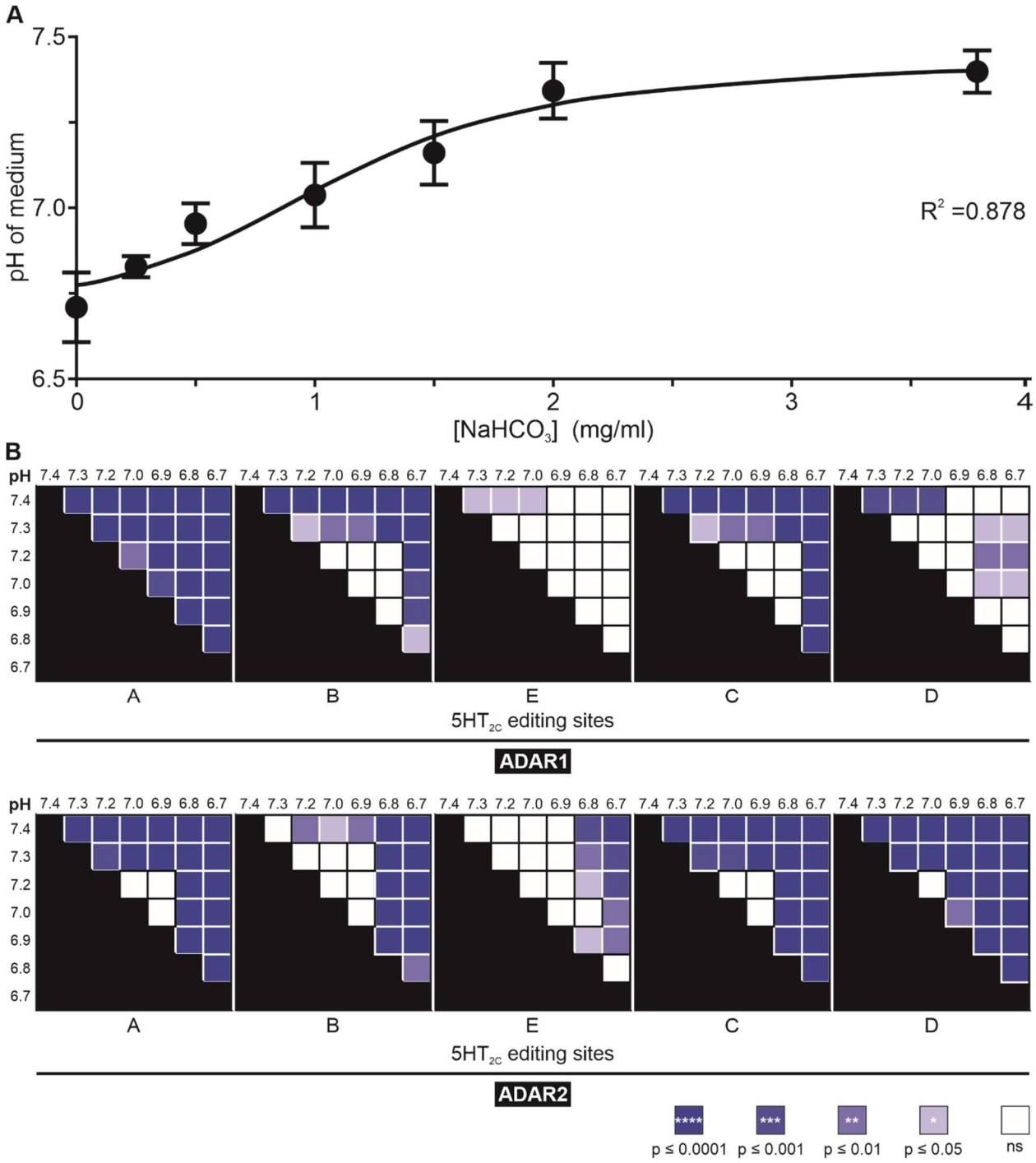

Figure 4.6. Effects of varying pH on site-selective $5HT_{2C}$ RNA editing. (**A**) The relationship between bicarbonate ($NaHCO_3$) concentration and the pH of cell culture medium after a 24-hour incubation at 37°C and 5% CO_2 is shown. Plotted values are the means of five independent pH measurements ± standard deviation. (**B**) Pairwise statistical comparisons for quantitative analyses of site-specific $5HT_{2C}$ editing at pH 6.7-7.4 (as presented in **Figure 3A-B**) are shown. Statistical significance was determined using two-way ANOVA with Tukey's multiple comparisons test.

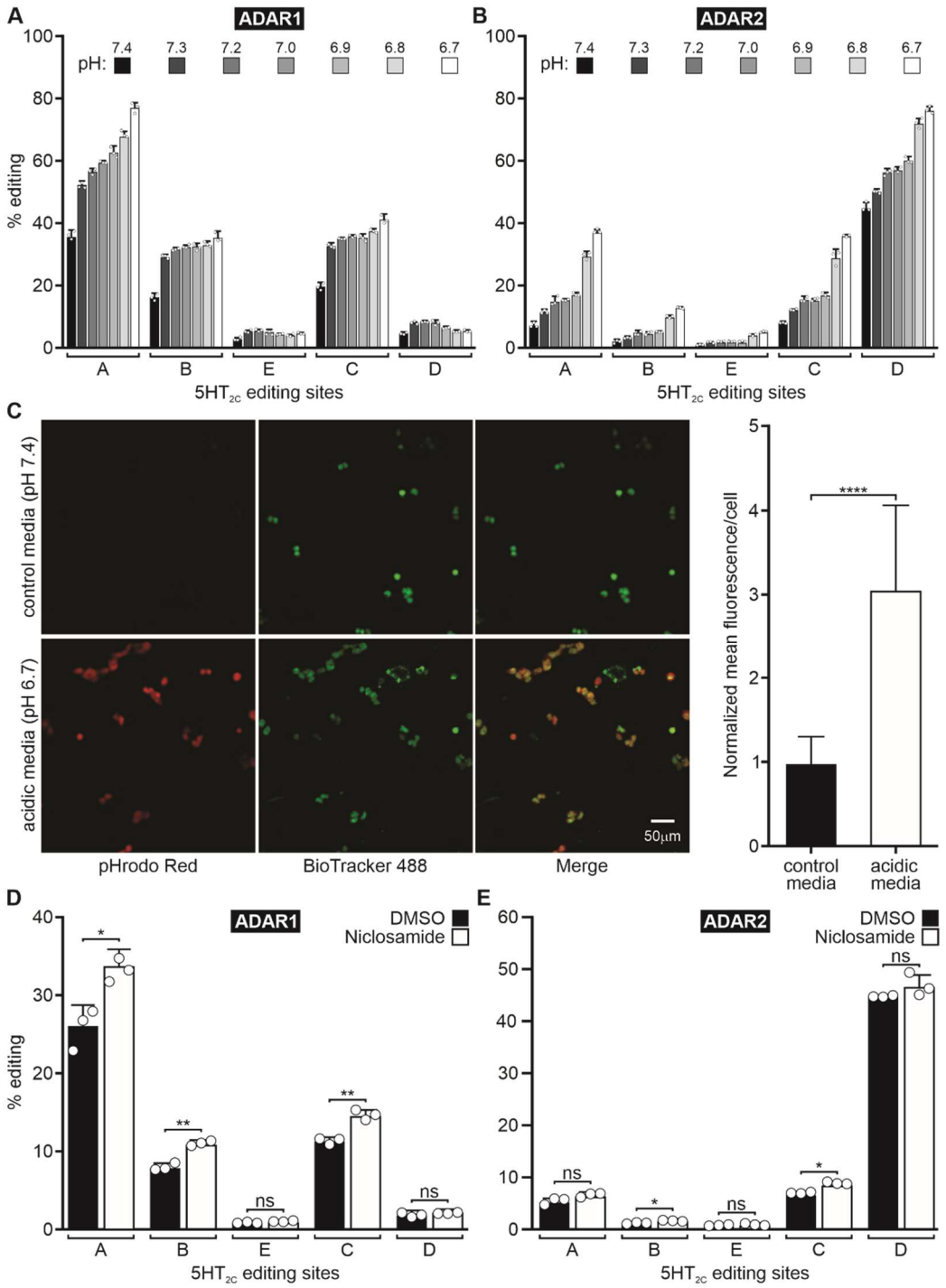

Figure 4.7. Effects of various pH manipulations on A-to-I editing. (**A**) Quantification of ADAR1 or (**B**) ADAR2-mediated $5HT_{2C}$ editing across a pH range from 6.7 to 7.4. Plotted values are the means of three biological replicates (○) ± standard deviation. (**C**) Representative 20x confocal images of live HEK293T cells incubated with control media (pH 7.4; *top*) or acidic media (pH 6.7; *bottom*) and double labelled with pHrodo Red AM Intracellular pH Indicator and BioTracker 488 Green Nuclear Dye (*left*); normalized mean pHrodo Red fluorescence intensity per cell is presented (*right*). Means ± standard deviation (n = 115 control cells from three independent

experiments and n = 106 acidic cells from three independent experiments) were compared by using the unpaired t-test with Welch's correction; ****p < 0.0001. (**D**) Quantification of the extent of ADAR1 or (**E**) ADAR2-mediated $5HT_{2C}$ editing from cells treated with DMSO (vehicle) or 5 μM niclosamide. Plotted values are the means of three biological replicates (○) ± standard deviation. Statistical significance between groups for each $5HT_{2C}$ site was determined using the Holm-Sidak t-test for multiple comparisons; *p ≤ 0.05; **p ≤ 0.01; ns, not significant.

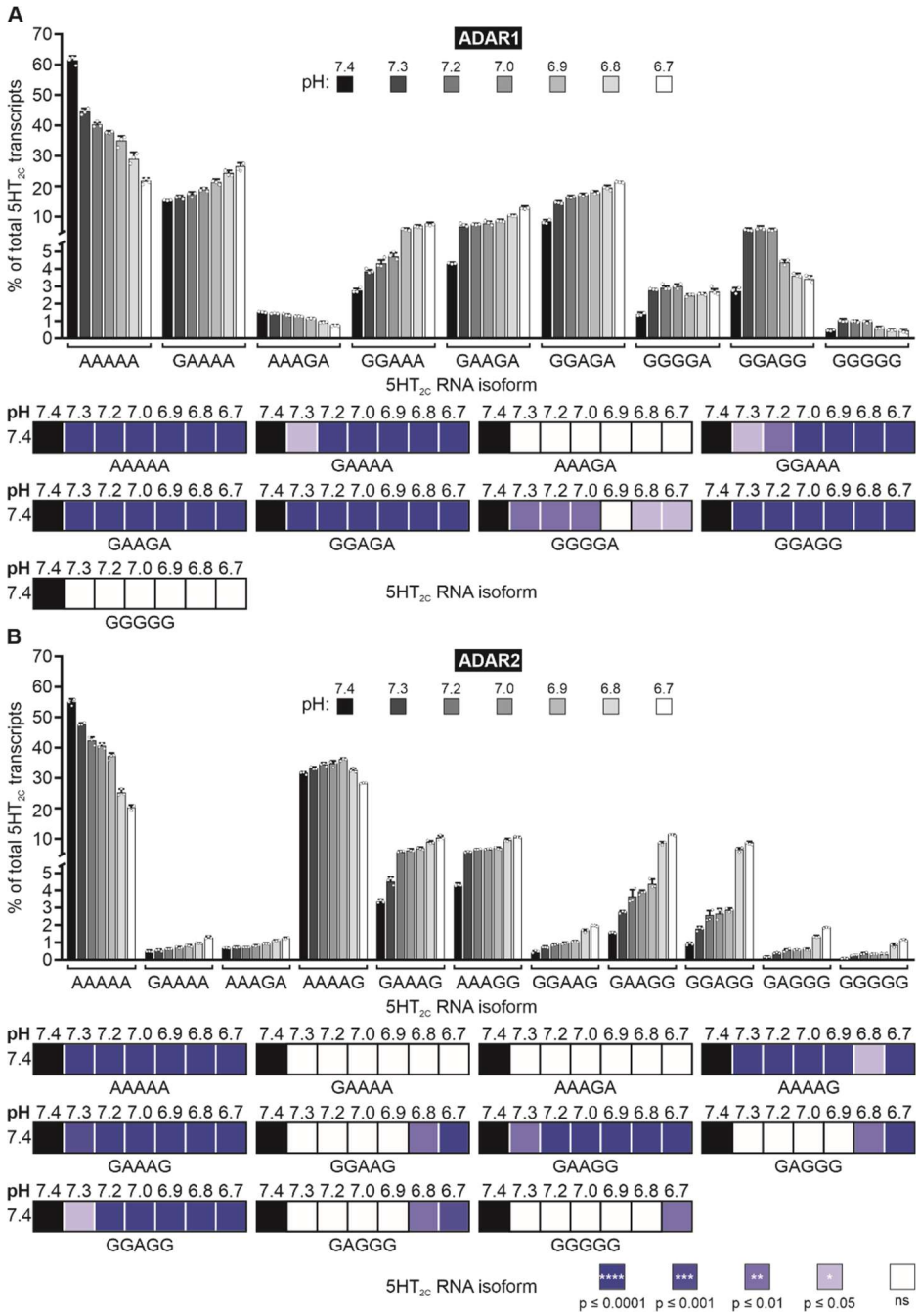

Figure 4.8. Expression of 5HT$_{2C}$ RNA editing isoforms at varying pH. (**A**) Relative expression of 5HT$_{2C}$ RNA isoforms (constituting ≥1% of total 5HT$_{2C}$ transcripts) generated by ADAR1- or (**B**) ADAR2-mediated editing at varying pH (*top*); Pairwise statistical comparisons for quantitative analyses of relative 5HT$_{2C}$ isoform expression. 5HT$_{2C}$ isoform expression at each pH is compared to the percentage of that isoform at pH 7.4 (*bottom*). Permutations are designated by the presence of adenosine (A) or guanosine (G) residues at sites A-E within the sequenced cDNA library (AAAAA = non-edited; GGGGG = fully edited). Plotted values on graphs are the means of three biological replicates (○) ± standard deviation. Statistical significance was determined using two-way ANOVA with Dunnett's multiple comparisons test.

Although numerous studies have concluded that differences in steady-state ADAR protein levels do not fully account for differences in the cell- and region-specific RNA editing profiles, previous studies in cell culture model systems have shown a correlation between editing and ADAR expression levels (43,141,161-164,224,225,234). To determine whether the reductions in extracellular pH that promoted increased editing affected ADAR protein levels in transfected cells, ADAR expression from HEK293T cells co-transfected with ADAR1 or ADAR2 and the $5HT_{2C}$ minigene were quantified after a 24-hour incubation with cell culture medium under control (pH 7.4) or acidic (pH 6.7) conditions. Quantitative western blotting analyses revealed significant increases in both ADAR1 and ADAR2 protein expression upon cellular acidification (Figure 4.9), suggesting that pH-dependent increases in ADAR protein could be responsible for the increases in editing observed at reduced pH.

The RNA editing reaction is intrinsically pH-sensitive

While increases in RNA editing produced by acidification in HEK293T cells could result from increased ADAR expression, other molecular mechanisms could also be responsible including activation of various pH-regulated signaling pathways, or the effects of pH on RNA structure and the intrinsic pH sensitivity of ADAR function. To directly investigate this last possibility, *in vitro* editing assays were performed to quantify deamination rate constants (k_{obs}) at varying pH (from pH 6.0 to pH 8.5) using purified, recombinant ADAR protein and an *in vitro* transcribed $5HT_{2C}$ substrate. For most sites examined, an inverse correlation between deamination rate and pH between pH 6.5 and 8.5 was observed. For example, ADAR1 deamination of the A-site was most efficient at pH 6.5 (Figure 4.10A). Similarly, ADAR2 deamination of the A-, B-, and C-sites also was most efficient at pH 6.5 and pH 7.0 (Figure 4.10B). The rate of editing for these sites is about 1.5- fold less efficient at pH 7.5 than at either pH 7.0 or pH 6.5. To assess whether the observed differences in catalytic rate resulted from changes in

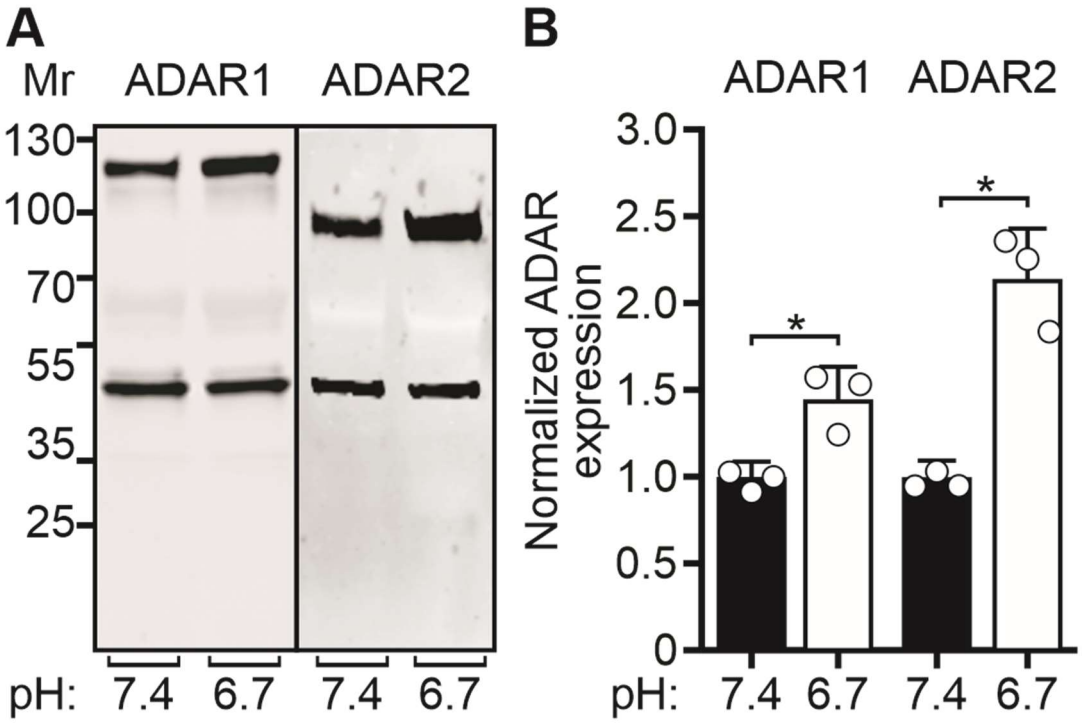

Figure 4.9. ADAR protein expression in response to cellular acidification. (**A**) Representative Western blots for ADAR1 (110 kDa) and ADAR2 (80 kDa) protein expression from HEK293T cells incubated with control (pH 7.4) or acidic media (pH 6.7); β-actin (43 kDA) was used as a loading control. (**B**) Quantification of ADAR1 and ADAR2 protein expression normalized to the β-actin loading control is presented. Plotted values are the means of three biological replicates (○) ± standard deviation. Statistical significance between groups was determined using the unpaired t-test with Welch's correction; *$p \leq 0.05$.

pH-dependent stability of ADAR proteins, the melting temperature of recombinant ADAR2 protein was quantified using SYPRO Orange, a dye that increases in fluorescence intensity upon thermal denaturation of the protein (235). Results from this ThermoFluor analysis revealed that ADAR2 was relatively stable from pH 6.5 to pH 8.5, with a melting temperature of ~53°C across this range (Figure 4.10C). At pH 6.0 however, the melting temperature of the ADAR2 protein was significantly decreased, an instability that paralleled the observed reduction in catalytic rate for $5HT_{2C}$ editing sites (Figure 4.10A-C).

Taken together, these *in vitro* data demonstrate that the RNA editing reaction is intrinsically pH-sensitive, a property that may arise through changes in ADAR-substrate binding or catalysis at reduced pH. To exclude the possibility that the observed increase in editing rates resulted from enhanced ADAR2-substrate binding via the double-stranded RNA binding domains (dsRBDs), the pH-sensitivity of the ADAR catalytic domain alone was assessed by taking advantage of the efficient editing of Gli1 by the ADAR2 deaminase domain (ADAR2d) lacking dsRBDs (226). ADAR2d deaminated the Gli1 R/G site 40- to 130-fold more efficiently under acidic conditions than at pH 7.5, with k_{obs} = 3.1 min^{-1} ± 0.2 at pH 6.5 and k_{obs} = 0.023 min^{-1} ± 0.006 at pH 7.5 (Figure 4.10D). ADAR2d deaminated the Gli1 +23 site 40- to 600-fold more efficiently under acidic conditions than at pH 7.5, with k_{obs} = 0.91 min^{-1} ± 0.2 at pH 6.5 and k_{obs} = 0.0015 min^{-1} ± 0.00067 at pH 7.5 (Figure 4.10D). These data indicate that RNA editing can be facilitated under acidic conditions independently of substrate interactions with the ADAR dsRBD

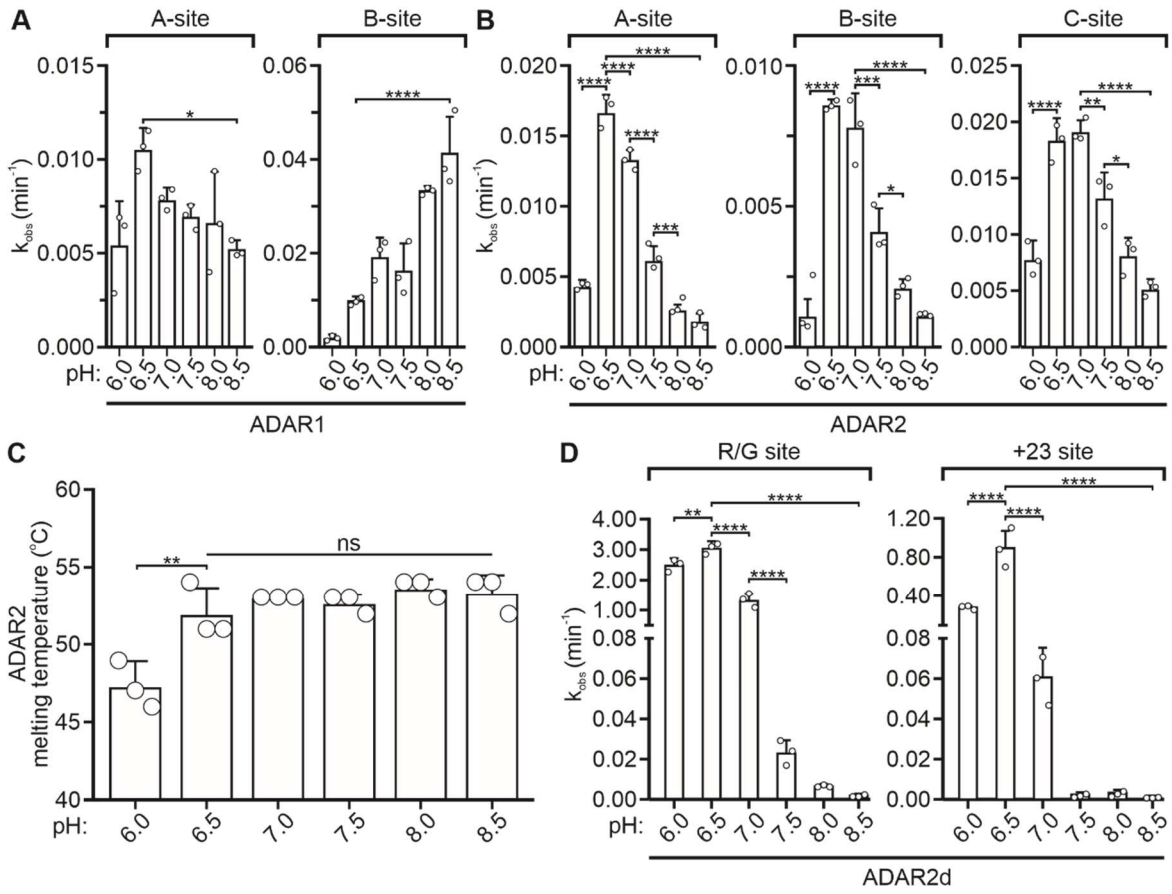

Figure 4.10. Effect of varying pH on *in vitro* A-to-I editing. (**A**) Rate of *in vitro* ADAR1- or (**B**) ADAR2-mediated $5HT_{2C}$ editing at half-pH intervals from 6.0 to 8.5. Plotted values are the means of three technical replicates (○) ± standard deviation. Statistical significance between groups was determined using one-way ANOVA with Tukey's multiple comparisons test; *p ≤ 0.05; **p ≤ 0.01; ***p ≤ 0.001; ****p ≤ 0.0001. (**C**) Quantification of ADAR2 melting temperature across the pH range used for *in vitro* editing experiments. Plotted values are the means of three technical replicates (○) ± standard deviation. Statistical significance between groups was determined using one-way ANOVA with Tukey's multiple comparisons test; **p ≤ 0.01; ns, not significant. (**D**) Rate of *in vitro* ADAR2d-mediated Gli1 editing. Plotted values are the means of three technical

Protonation of a conserved glutamate residue in the ADAR base-flipping loop partially accounts for increases in RNA editing at acidic pH

A recent investigation of the structural basis for base-flipping by ADAR2 revealed the importance of a highly conserved glutamate, E488 (corresponding to E1008 in ADAR1), residing in the deaminase domain of the enzyme (82). This residue stabilizes the flipped-out conformation of the RNA duplex, presumably by occupying the space vacated by the flipped-out adenosine and hydrogen bonding with the complementary-strand orphaned base (Figure 4.11A-B and Figure 4.12). Mutant ADAR proteins bearing a glutamate-to-glutamine substitution at this residue (ADAR1-Q and ADAR2-Q) exhibit increased catalytic activity via enhanced base-flipping (12,31,32). As this glutamine is fully protonated under normal physiologic conditions at pH 7.4, these observations are consistent with the idea that the corresponding glutamate residue in wild-type ADARs requires protonation to support RNA stabilization during the base-flipping step in catalysis (Figure 4.11A-B). To further examine how base-flipping is modulated by ADAR protonation, we compared base-flipping for ADAR2 and ADAR2-Q proteins as a function of pH using a 2-aminopurine (2-AP)-modified GluA2 transcript to measure 2-AP fluorescence intensity, which has been shown previously to correlate with base-flipping (78,86). The fluorescence intensity observed with the ADAR2-Q mutant was greater than that exhibited with the wild-type ADAR2 protein at each pH, confirming that ADAR2-Q has enhanced base-flipping abilities (Figure 4.11C). However, a differential pH dependence between wild-type ADAR2 and the ADAR2-Q mutant enzyme was observed where the fluorescence intensity with the wild-type enzyme increased with decreasing pH, whereas fluorescence intensity with the ADAR2-Q mutant was maximal at pH 7.0, but dropped off significantly with increasing or decreasing pH (Figure 4.11C). These data indicate that ADAR base-flipping is intrinsically pH-dependent and that RNA editing by the ADAR-Q mutant enzyme is less affected by acidification than the wild-type ADAR2 protein. To further compare the relative pH sensitivity of wild-type and mutant (ADAR-Q) proteins, we

quantified the site-specific editing of $5HT_{2C}$ transcripts by wild-type and ADAR-Q mutant enzymes in transfected HEK293T cells incubated under control (pH 7.4) or acidic (pH 6.7) conditions. Results from this analysis showed that while the extent of editing was increased for both ADAR1-Q and ADAR2-Q mutants under acidic conditions, acidification-induced increases in editing by ADAR1-Q and ADAR2-Q were attenuated relative to those exhibited by their wild-type ADAR counterparts (Figure 4.11D). These results suggest that protonation of ADAR1 at E1008 or ADAR2 at E488 partially accounts for the increases in RNA editing observed at acidic pH.

RNA editing increases during hypoxia

Various physiologic and pathophysiologic conditions have been shown to induce changes in intracellular or extracellular pH such as hypoxia, inflammatory signaling, tumorigenesis, and metabolic acidosis (236,237). Previous studies have shown that acid-base disturbances that occur during hypoxia induce both intra- and extracellular acidification (238). To determine whether physiologic manipulation of the cell culture environment could modulate the extent of RNA editing by ADAR1 and ADAR2, we used a cell culture model of hypoxia (229). Transfected HEK293T cells were incubated for 24 hours under hypoxic (1% O_2) or normoxic (20% O_2) conditions, followed by quantification of $5HT_{2C}$ editing profiles and determinations of the pH of the cell culture media. Results from these studies showed that hypoxia significantly decreased the pH of the cell culture medium by 0.6 ± 0.01 pH units, relative to normoxic conditions (Figure 4.13A) and that this decrease in pH was concomitant with an increase in site-selective editing of $5HT_{2C}$ transcripts (Figure 4.13B-C). ADAR1 and ADAR2-mediated editing of all five $5HT_{2C}$ sites significantly increased in a hypoxic environment compared to control cells incubated in under normoxic conditions. These results suggest that the extent of RNA editing is inversely correlated with pH changes produced by a physiologically relevant cell culture model of metabolic stress.

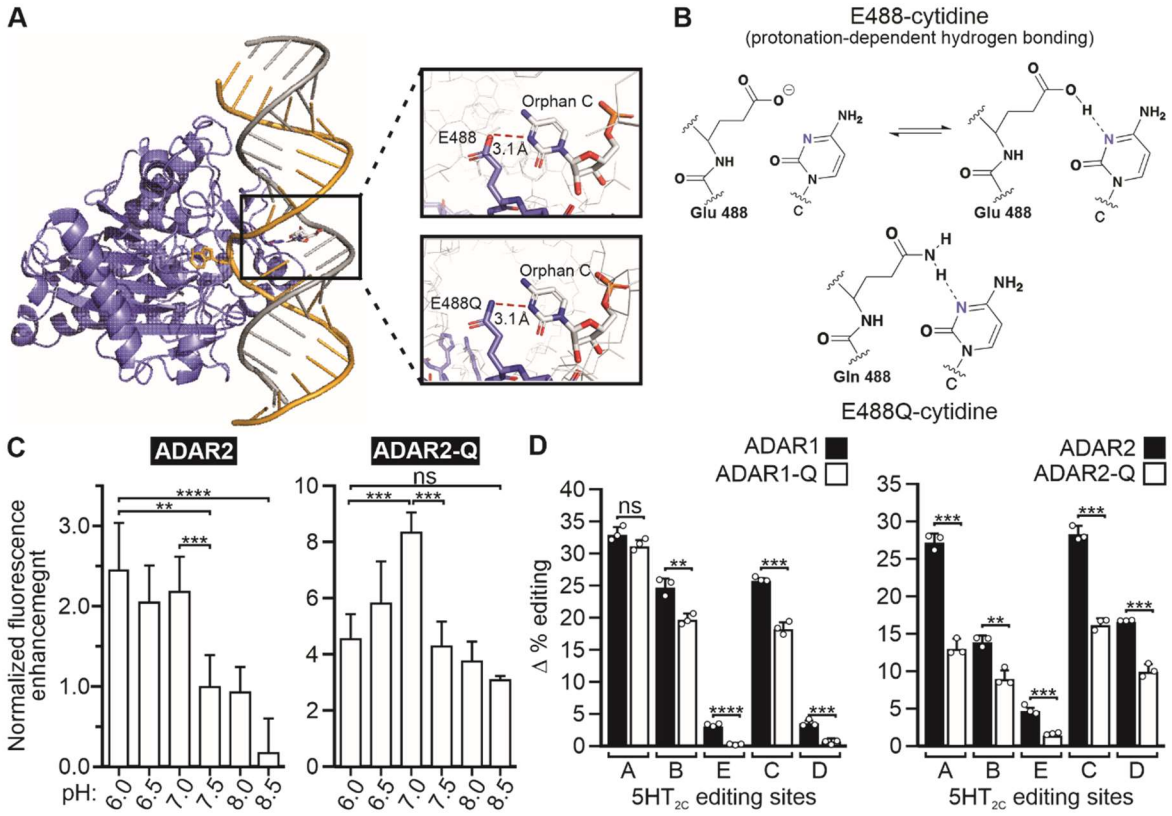

Figure 4.11. Effects of varying pH on the base-flipping ability of ADAR. (**A**) The crystal structure of ADAR2d bound to dsRNA (PDB ID: 5HP3 & 5ED1) shows the base-flipped conformation stabilized by contacts between residue 488 and the orphan base. (**B**) An illustration of the hydrogen bonding contact between ADAR2 and the orphan base showing protonation-dependent hydrogen bonding for wild-type ADAR2. (**C**) Normalized fluorescence enhancement from a dsRNA substrate containing 2-aminopurine in the edited position, corresponding to base-flipping by the ADAR2 enzyme. Plotted values are the means of three technical replicates ± standard deviation. Statistical significance between groups was determined using one-way ANOVA with Tukey's multiple comparisons test; **p ≤ 0.01; ***p ≤ 0.001; ****p ≤ 0.0001; ns, not significant. (**D**) Quantification of the extent of acidification-induced increases in $5HT_{2C}$ editing mediated by wild-type ADARs or ADAR-Q mutants (Δ % editing = % site-selective editing at pH 6.7 - % site-selective editing at pH 7.4). Plotted values are the means of three biological replicates (○) ± standard deviation. Statistical significance between groups for each $5HT_{2C}$ site was determined using the Holm-Sidak t-test for multiple comparisons; **p ≤ 0.01; ***p ≤ 0.001; ****p ≤ 0.0001.

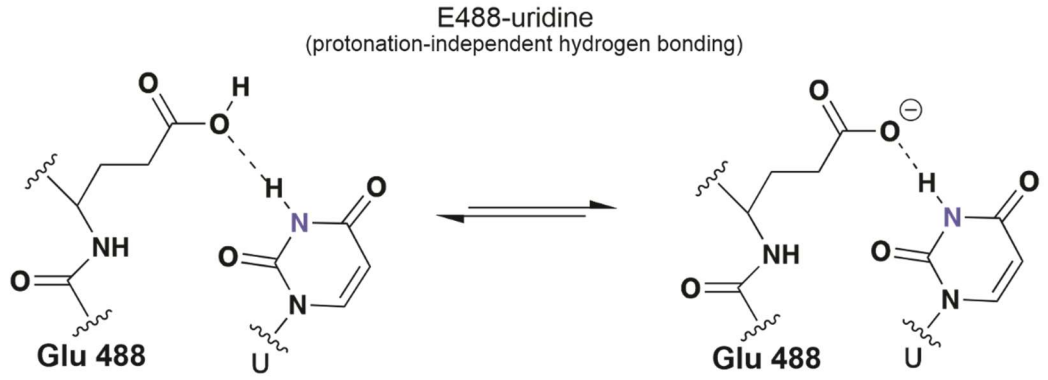

Figure 4.12. Protonation-independent hydrogen bonding. A schematic diagram of the hydrogen bonding contact between ADAR2 and the orphan base (uridine) showing protonation-independent hydrogen bonding for wild-type ADAR2.

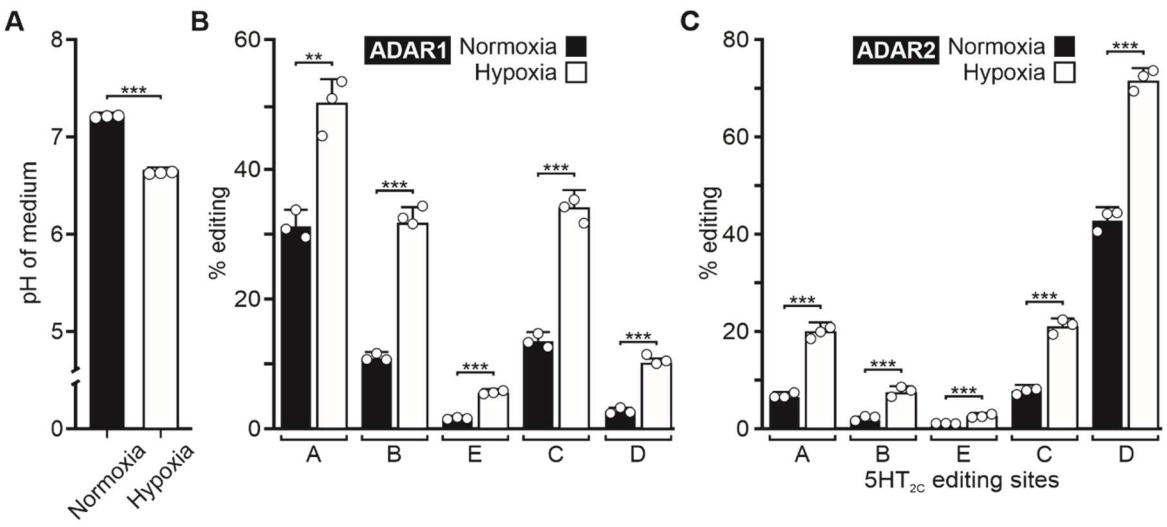

Figure 4.13. A-to-I editing in response to hypoxia. (**A**) pH of the cell culture medium following 24-hour incubation of HEK293T cells under normoxic (20% O_2) or hypoxic (1% O_2) conditions. Means ± standard deviation from three independent experiments (○) were compared using the unpaired t-test with Welch's correction; ***p ≤ 0.001. (**B**) Quantification of the extent of ADAR1 or (**C**) ADAR2-mediated $5HT_{2C}$ editing from HEK293T cells incubated under normoxic (20% O_2) or hypoxic (1% O_2) conditions. Plotted values are the means of three biological replicates (○) ± standard deviation. Statistical significance between groups for each $5HT_{2C}$ site was determined using the Holm-Sidak t-test for multiple comparisons; **p ≤ 0.01; ***p ≤ 0.001.

Discussion

The mechanisms underlying changes in RNA editing profiles in response to physiologic signals are not well-defined. Most of the known *trans*-acting regulators of editing modulate ADAR protein levels, yet steady-state ADAR protein expression cannot fully account for the observed spatiotemporal variations in A-to-I conversion (141,161-164,224,225). Though dynamic regulation of ADAR activity—rather than ADAR expression—may account for significant changes in RNA editing, the mechanisms regulating such activity remain elusive. Previous structural and biochemical characterization of ADARs and ADAR mutants has suggested pH-sensitive deamination of these enzymes (82,84,86). Therefore, our studies have focused on how changes in pH regulate RNA editing. Analysis of editing using both HEK293T cells and *in vitro* systems revealed significant increases in ADAR1 and ADAR2-mediated editing under acidic conditions relative to editing at a physiologic pH of ~7.4 (Figures 4.1-4.8 and Figure 4.10). Notably, several sites, including the A-, B-, and E-sites of $5HT_{2C}$ RNAs, as well as various adenosines within Gli1 transcripts, are virtually unrecognized or edited at very low levels by one or both ADARs at pH 7.4, but undergo robust editing as a result of acidification (Figure 4.1 and Figure 4.5). Although these increases in editing were accompanied by increases in intracellular ADAR protein levels, *in vitro* studies indicated that increased ADAR expression is not required to observe acidification-mediated increases in editing (Figure 4.10). Indeed, these *in vitro* data demonstrate an intrinsic and robust pH-sensitivity of ADAR catalysis (Figure 4.10). While acidification could alter the rate of editing by affecting ADAR binding and/or catalytic efficiency, pH-sensitive editing of Gli1 by ADAR2d (lacking the dsRBDs) showed that increased ADAR activity did not result solely from increased binding under acidic conditions (Figure 4.10D). Rather, our data show that the ADAR deaminase domain—and specifically the base-flipping loop—is fundamental to the intrinsic pH-sensitivity of ADAR catalysis (Figure 4.10D and Figure 4.11).

During base-flipping, a highly conserved glutamate residue within the ADAR base-flipping loop invades the vacated space and hydrogen bonds with the base opposite the flipped-out

adenosine to stabilize the strained nucleic acid conformation (Figure 4.11A-B) (82). Consistent with the hypothesis that this interaction may be sensitive to changes in proton concentration, mutation of this critical glutamate to a glutamine, which is fully protonated at pH 7.4, results in increased catalytic efficiency via enhanced base-flipping of the ADAR-Q mutant (84,86). Our analysis suggests that the ADAR2 reaction is accelerated by low pH regardless of the identity of the orphan base. Protonation of E488 enables this residue to donate a hydrogen-bond to contact an orphan cytidine (Figure 4.11A-B). In addition, protonation of this residue neutralizes the negative charge on the side chain, decreasing charge repulsion with RNA during the flipping step for either adenosine-uridine base pairs (Figure 4.12) or adenosine-cytidine mismatches (Figure 4.11B). Our studies further show that base-flipping and editing activity for wild-type ADARs increases with decreasing pH, yet the pH-dependency of these properties is diminished for ADAR-Q mutants (Figure 4.11C-D). While the pKa of ADAR1 E1008 and ADAR2 E488 have not been determined, our data suggest that protonation of these single amino acid residues within the ADARs enhances base-flipping, thereby partially accounting for the observed increases in RNA editing at acidic pH. The protonation of other amino acid residues within ADAR proteins as well as pH-dependent increases in the thermodynamic stability of targeted RNA duplexes also may contribute to increased editing under acidic conditions.

The pH optima for most enzymes coincide with the pH of the subcellular compartments in which they reside (239,240). For example, the pH optimum of many proteases involved in prohormone processing coincides with the intragranular pH of ~5.5, whereas the pH optimum of many cytoplasmic enzymes is ~7.4 (241,242). Surprisingly, ADARs function optimally between pH 6.5-7.0, well below the normal pH of the nucleus or cytoplasm (236). For many $5HT_{2C}$ sites, large stepwise changes in editing were observed between pH 7.4 and 7.3 (for ADAR1 editing) or between pH 6.9 and 6.8 (for ADAR2 editing) in HEK293T cells (Figure 4.7A-B), and between pH 7.5 and 7.0 *in vitro* (Figure 4.10), suggesting that ADARs could serve as pH sensors to modulate RNA editing patterns in response to physiologically-driven pH shifts, especially acidification.

Cytoplasmic acidification often results from the accumulation of acid equivalents produced as metabolic byproducts (236). Although cells engage various regulatory mechanisms to maintain pH homeostasis, these systems can be overwhelmed during periods of unusually high metabolic activity, leading to intracellular acidification (236). Cells grown in a hypoxic environment demonstrated both acidification of their culture medium as well as a significant increase in site-selective A-to-I conversion (Figure 4.13). While previous studies have reported increases in editing under hypoxic conditions, they lacked evidence to suggest that the observed increases in RNA editing are driven by concomitant increases in ADAR protein levels or through modulation of other cellular pathways (145-147). The present studies support the hypothesis that metabolic stress during hypoxia triggers intracellular acidification, which in turn enhances base-flipping activity to increase the overall ADAR catalytic rate and editing. Similar pH-dependent regulatory mechanisms may exist in conditions such as inflammation and epilepsy, which also are associated with both intracellular acidification as well as increased RNA editing (152-154,243-247).

During hypoxia/ischemia, epilepsy, and other pathophysiologic conditions in which pH homeostasis is disrupted, electrically-active cells such as neurons and cardiomyocytes experience broad disturbances in ion dynamics, often resulting in increased intracellular Ca^{2+} concentration to induce cytotoxicity and membrane hyperexcitability (236). Though the present studies of pH-dependent increases in RNA editing were limited to several model transcripts, it is likely that editing of many sites in the transcriptome increases upon intracellular acidification since editing is favored under such conditions. While it is unknown how such global increases in editing might influence overall physiology, studies using *Drosophila* model systems have shown that ADAR overexpression or knockdown results in decreased or increased neuronal excitability, respectively (157). Since many editing-dependent recoding events affect the function of proteins involved in membrane excitability, it is intriguing to speculate that increased editing of various

RNA targets may serve as a pH-dependent homeostatic mechanism to limit membrane hyperexcitability and protect against excitotoxic damage (157,248).

The observation that acidic pH enhances base-flipping and increases the rate of deamination by ADARs has implications beyond our understanding of mechanisms of natural regulation of A-to-I editing. Several recent reports have described efforts to direct ADAR reactions for therapeutic benefit (249,250). One approach uses a guide RNA to form a duplex at a target site that can recruit endogenous ADAR enzymes for deamination of a specific adenosine (251,252). Thus, this directed RNA editing approach can “repair” G-to-A mutations associated with genetic disease. Optimization of ADAR guide RNAs requires a comprehensive understanding of factors that control RNA editing efficiency. The results described here are likely to stimulate efforts to develop modifications to guide RNAs that mimic the effects of low pH.

Chapter V

Summary and Discussion

Summary

Adenosine deaminases acting on RNA (ADARs) catalyze adenosine-to-inosine (A-to-I) RNA editing to expand the diversity of genomically-encoded transcripts and proteins by introducing the non-canonical nucleoside inosine into metazoan double-stranded RNAs (dsRNAs). This RNA processing event is widespread, especially in the human transcriptome, and enables post-transcriptional regulation of many cellular processes. Despite the prevalence and profound biological impact of RNA editing, the mechanisms modulating ADARs and RNA editing are poorly understood. In this work, we have described two different approaches to investigate the modulation of RNA editing.

Currently, there is considerable interest in understanding how various editing sites are regulated in specific tissues. Many studies have shown that ADAR expression as well as overall RNA editing levels are particularly high in the brain (141,218). Within the brain, different regions display distinct levels of editing for the many transcripts undergoing this A-to-I modification . For example, one study examining serotonin 2C ($5HT_{2C}$) receptor RNA editing profiles in the murine brain showed that site-specific $5HT_{2C}$ RNA editing varies across different brain regions and that each of these profiles are distinct from the $5HT_{2C}$ RNA editing profile obtained from whole brain analyses (168). These results indicate that measurements of RNA editing from bulk tissue samples capture population-averaged data from different cell types and can obscure the unique transcriptional signatures of individual subpopulations within complex networks. Furthermore, tissue-specific expression of differentially edited isoforms suggests that unique $5HT_{2C}$ isoform distributions in different regions may support the functional specialization of those tissues. Whether particular $5HT_{2C}$-mediated behaviors regulate—or are regulated by—the specific $5HT_{2C}$

RNA editing profiles expressed in the cells responsible for generating those behaviors is unclear. To investigate this possibility, it is necessary to examine $5HT_{2C}$ RNA editing in a defined circuit. Therefore, in Chapter III, we employed a cell type-specific approach to study $5HT_{2C}$ RNA editing. Because $5HT_{2C}$ receptor expression on POMC neurons is essential in mediating anorexigenic responses, we sought to determine the role that $5HT_{2C}$ RNA editing in POMC neurons plays in the maintenance of energy homeostasis. To examine $5HT_{2C}$ RNA editing selectively in POMC neurons, we used a previously described mouse model (2C/POMC) in which $5HT_{2C}$ expression is suppressed in all cells except POMC neurons. The hypothalami of 2C/POMC mice displayed a different $5HT_{2C}$ RNA editing profile relative to those of control mice, indicating that POMC neurons have a unique $5HT_{2C}$ RNA editing profile—distinct from the population-averaged $5HT_{2C}$ editing in whole hypothalamus. To determine the extent to which $5HT_{2C}$ RNA editing in POMC neurons is sensitive to perturbations of the melanocortin pathway, we challenged 2C/POMC mice with diet manipulations or exercise and then assessed $5HT_{2C}$ RNA editing. We found that while calorie restriction and exercise respectively increase and decrease $5HT_{2C}$ editing in POMC neurons, high-fat diet does not have an impact. Finally, to begin to understand what effect distinct, edited $5HT_{2C}$ isoforms have on the maintenance of energy balance, we engineered mice that can be crossed to a POMC:Cre line to generate animals expressing only the fully-edited (VGV) or non-edited (INI) $5HT_{2C}$ isoforms in POMC neurons.

Another approach we took to explore the mechanisms regulating RNA editing was to investigate the modulation of ADAR proteins. Until recently, ADARs were the only known *trans*-acting regulators of RNA editing. Studies conducted within the last decade have described a number of additional *trans*-regulators of editing that primarily modulate ADAR protein levels, yet most current data indicates that steady-state ADAR protein expression cannot fully account for the variation in A-to-I editing observed for numerous transcripts expressed in discrete cell types, during development, or in response to changing physiologic conditions (141,161-164,224,225). Therefore, in Chapter IV we sought to determine whether other factors could modulate editing by

affecting ADAR enzymatic activity directly. To this end, we followed up on earlier observations suggesting a potential role for decreased pH in increasing ADAR activity. Our studies used a cell culture model system to show that intracellular acidification significantly increases the extent of ADAR1 and ADAR2-mediated RNA editing for several model RNAs at a pH significantly below that normally found in the cytoplasm or nucleus. We found that the modulation of RNA editing by intracellular acidification is dependent on both time and the magnitude of the change in pH. To examine the mechanism underlying pH-dependent increases in RNA editing, we performed *in vitro* editing assays to quantify deamination rate constants across a pH range. Our results showed that an acidic pH increases the rate of deamination by ADARs, and that the ADAR deaminase domain is fundamental to the intrinsic pH-sensitivity of ADAR catalysis. Furthermore, assessment of the base-flipping abilities of ADARs and mutant ADAR proteins indicates that base-flipping of wild-type ADARs is enhanced under acidic conditions and that protonation of a single, conserved glutamate within the deaminase domain partially accounts for this pH-dependent enhancement in base-flipping. Finally, we investigated how changes in pH that occur in a cell culture model of hypoxia might affect the extent of site-selective A-to-I conversion. Our results showed that the extent of RNA editing is inversely correlated with the reduction in pH produced by such a physiologically relevant cell culture model of metabolic stress.

Discussion

In Chapter III, we began studies to examine how $5HT_{2C}$ RNA editing contributes to the maintenance of energy homeostasis. To this end, we engineered mice that can be crossed to a POMC:Cre line to generate animals expressing only the fully-edited or non-edited $5HT_{2C}$ isoforms selectively in POMC neurons. Future studies will include generating the double mutant mice that carry both the POMC:Cre transgene and the conditionally expressed $5HT_{2C\text{-}VGV}$ or $5HT_{2C\text{-}INI}$ alleles. Similar to the experiments performed by the Elmquist lab to examine the phenotype of the

original 2C/POMC mice, which conditionally express multiple $5HT_{2C}$ isoforms in POMC neurons, our double mutant animals will be assessed for body composition, feeding behavior, energy expenditure, serum glucose and insulin levels, and locomotor activity. We anticipate that mice expressing the $5HT_{2C\text{-}INI}$ isoform selectively in POMC neurons will rescue the hyperphagia, hyperleptinemia, maturity-onset obesity and type II diabetes observed in $5HT_{2C}$-null mice (185,190). By contrast, it is unlikely that expression of the $5HT_{2C\text{-}VGV}$ isoform will rescue the $5HT_{2C}$-null phenotype since mice solely expressing the fully-edited $5HT_{2C}$ isoform display characteristics of Prader-Willi syndrome, some of which overlap with the $5HT_{2C}$-null phenotype. It also is possible that no single, edited $5HT_{2C}$ isoform expressed selectively in POMC neurons can rescue the $5HT_{2C}$-null phenotype, as it takes a combination of receptors with different functional properties to achieve the appropriate level of anorectic tone. Alternatively, it is also possible that both the $5HT_{2C\text{-}VGV}$ and $5HT_{2C\text{-}INI}$ expressing mice may appear phenotypically normal as restoration of any degree of $5HT_{2C}$ signaling on POMC neurons may be sufficient to maintain energy balance.

Another aim of the work described in Chapter III was to assess the sensitivity of $5HT_{2C}$ RNA editing in POMC neurons to fluctuations in energy status. Minimal changes in the extent of $5HT_{2C}$ RNA editing in 2C/POMC mice were observed in response to calorie restriction or exercise. Though these animals exhibited changes in editing at the B- and/or D-sites of $5HT_{2C}$ compared to control animals, the magnitude of these site-specific changes were ≤ 5%. Moreover, the distribution of $5HT_{2C}$ RNA isoforms remained essentially unchanged as a result of these manipulations. It remains to be seen whether other perturbations of feeding pathways such as administration of d-fenfluramine or Lorcaserin, two anti-obesity drugs targeting the serotonergic system, may have a larger impact on altering $5HT_{2C}$ editing profiles in POMC neurons. To probe how such cell-type specific changes in $5HT_{2C}$ RNA editing may contribute to alterations in POMC neuron activity, an important future direction is to use *ex vivo* electrophysiological techniques to assess the sensitivity of POMC neurons to $5HT_{2C}$ agonism. However, as there are currently no facile methods by which to purify $5HT_{2C}$ proteins, the distribution of $5HT_{2C}$ protein isoforms

generated by changes in RNA editing cannot be determined. For these reasons, it would be difficult to ascribe functional relevance to such minor changes in RNA editing.

Another future direction of the studies described in Chapter III is to determine the mechanism by which the observed changes in RNA editing occur. Though it is intriguing to speculate that $5HT_{2C}$ RNA editing profiles in POMC neurons may change dynamically in response to feeding signals as a part of a cellular strategy to modulate serotonergic signaling and maintain energy homeostasis , there is currently little evidence to suggest that ADARs or other *trans*-acting regulators of editing respond to feeding signals to mediate such a change. Furthermore, it is unclear why ADARs would be recruited only to $5HT_{2C}$ transcripts when many ADAR substrates exist in any given cell type. Indeed, beyond the requirement for an extended region of double-stranded RNA (dsRNA), no other *cis*-active elements are known to recruit ADARs to specific transcripts. Therefore, it would be interesting to use a whole transcriptome RNA-seq-based approach to determine how exercise, diet manipulation, or pharmacological treatment affect global levels of editing in POMC neurons.

Because there were only minor changes in $5HT_{2C}$ RNA editing in response to perturbations in the melanocortin feeding pathway, and because it is unclear how such changes in editing were produced, we designed an alternative research strategy (detailed in Chapter IV) to investigate other means by which RNA editing may be dynamically regulated. In essence, our approach to understanding the dynamic regulation of RNA editing in Chapter IV was opposite to that in Chapter III. Whereas in Chapter III we explored the possibility that specific behaviors may change RNA editing profiles of a single transcript without considering how those changes in editing may be mediated, in Chapter IV we investigated general mechanisms regulating ADAR activity and subsequent RNA editing, which can ultimately be studied *in vivo* to determine if such strategies are employed by physiologic systems to modulate levels of RNA editing. The studies presented in Chapter IV revealed large changes in RNA editing for multiple transcripts as a result of the robust and intrinsic pH-sensitivity of ADARs. While these results are interesting and expand our

understanding of the regulation of RNA editing, additional studies may provide further insight into the pH-dependency of ADAR activity and editing.

Though the studies in Chapter IV showed that protonation of a conserved glutamate within the ADAR base-flipping loop partially accounts for increased editing of transcripts at acidic pH, additional factors also likely contribute to this phenomenon. For example, increased thermodynamic stability of dsRNAs as well as protonation of other ionizable groups within the enzyme at acidic pH may facilitate aspects of ADAR-substrate binding, base-flipping, or deamination. While *in vitro* editing assays demonstrated that increased ADAR expression is not required to observe increased RNA editing, our cellular studies revealed elevated ADAR protein expression in transfected HEK293T cells subjected to acidic pH. To determine the extent to which increased ADAR expression regulates intracellular RNA editing at acidic pH, it would be interesting to perform similar cellular editing assays in a model system where despite cellular acidification, ADAR protein levels remain unchanged. To this end, an experiment could be performed in which the transfected amounts of plasmid encoding ADAR1 or ADAR2 are adjusted such that the expression of ADAR proteins under acidic conditions is equivalent to ADAR levels at pH 7.4. Alternatively, additional studies could be performed in a cell line with endogenous editing activity, such as HeLa cells, to determine if similar effects on pH-dependent RNA editing and ADAR expression are observed.

Another future direction of the work described in Chapter IV is the identification of an *in vivo* model system that demonstrates pH-dependent RNA editing. Because we showed that increases in RNA editing are concurrent with decreases in pH exhibited in a cell culture model of hypoxia, future studies may consider examining how hypoxia affects both intracellular pH as well as transcriptome-wide RNA editing profiles in murine neurons as these cells are particularly sensitive to low oxygen tension. If pH-dependent increases in RNA editing are observed in such a model (consistent with the results described in Chapter IV), it would be interesting to examine how these changes influence neuronal physiology in *ex vivo* brain slice preparations. As

discussed in Chapter IV, while it is unknown how such global increases in editing might influence physiology, studies using *Drosophila* model systems have shown that ADAR overexpression or knockdown results in decreased or increased neuronal excitability, respectively (157). Since many editing-dependent recoding events affect the function of proteins involved in membrane excitability, it is intriguing to speculate that increased editing of various RNA targets may serve as a pH-dependent homeostatic mechanism to limit membrane hyperexcitability and protect against excitotoxic damage (157,248). Therefore, based on these data, we would hypothesize that neuronal hypoxia results in pH-dependent increases in global RNA editing to decrease neuronal excitability.

The results described in Chapter IV have implications beyond our understanding of mechanisms of natural regulation of A-to-I editing. Several recent reports have described efforts to direct ADAR reactions for therapeutic benefit (249,250). One approach uses a guide RNA to form a duplex at a target site that can recruit endogenous ADAR enzymes for deamination of a specific adenosine (251,252). Thus, it would also be an interesting future direction to develop modifications to guide RNAs that mimic the effects of low pH and examine if such modified guide RNAs can more efficiently recruit ADARs to “repair” G-to-A mutations associated with genetic disease.

Overall, our studies indicate that the regulation of A-to-I RNA editing is one strategy by which cells may dynamically modulate gene expression under altered physiologic conditions. Changes in RNA editing levels can influence RNA-RNA or RNA-protein interactions, which can ultimately impact various aspects of cellular physiology. Though further investigation will be required to determine the biological significance of such changes in editing, the current studies provide critical insight into mechanisms that modulate A-to-I editing and contribute to transcriptional diversification.

References

1. Alberts, B. (2002) *Molecular biology of the cell*. 4th ed. Garland Science, New York.
2. Voet, D. and Voet, J.G. (2011) *Biochemistry*. 4th ed. John Wiley & Sons, Hoboken, NJ.
3. Venter, J.C., Adams, M.D., Myers, E.W., Li, P.W., Mural, R.J., Sutton, G.G., Smith, H.O., Yandell, M., Evans, C.A., Holt, R.A. *et al.* (2001) The sequence of the human genome. *Science*, **291**, 1304-1351.
4. Lander, E.S., Linton, L.M., Birren, B., Nusbaum, C., Zody, M.C., Baldwin, J., Devon, K., Dewar, K., Doyle, M., FitzHugh, W. *et al.* (2001) Initial sequencing and analysis of the human genome. *Nature*, **409**, 860-921.
5. International Human Genome Sequencing, C. (2004) Finishing the euchromatic sequence of the human genome. *Nature*, **431**, 931-945.
6. Grosjean, H. (2005) *Fine-tuning of RNA functions by modification and editing*. Springer, Berlin ; New York.
7. Licatalosi, D.D. and Darnell, R.B. (2010) RNA processing and its regulation: global insights into biological networks. *Nat Rev Genet*, **11**, 75-87.
8. Wang, E.T., Sandberg, R., Luo, S., Khrebtukova, I., Zhang, L., Mayr, C., Kingsmore, S.F., Schroth, G.P. and Burge, C.B. (2008) Alternative isoform regulation in human tissue transcriptomes. *Nature*, **456**, 470-476.
9. Roundtree, I.A., Evans, M.E., Pan, T. and He, C. (2017) Dynamic RNA Modifications in Gene Expression Regulation. *Cell*, **169**, 1187-1200.
10. Davis, F.F. and Allen, F.W. (1957) Ribonucleic acids from yeast which contain a fifth nucleotide. *J Biol Chem*, **227**, 907-915.
11. Cohn, W.E. (1960) Pseudouridine, a carbon-carbon linked ribonucleoside in ribonucleic acids: isolation, structure, and chemical characteristics. *J Biol Chem*, **235**, 1488-1498.
12. Ayadi, L., Galvanin, A., Pichot, F., Marchand, V. and Motorin, Y. (2019) RNA ribose methylation (2'-O-methylation): Occurrence, biosynthesis and biological functions. *Biochim Biophys Acta Gene Regul Mech*, **1862**, 253-269.
13. Yang, Y., Hsu, P.J., Chen, Y.S. and Yang, Y.G. (2018) Dynamic transcriptomic m(6)A decoration: writers, erasers, readers and functions in RNA metabolism. *Cell Res*, **28**, 616-624.
14. McCown, P.J., Ruszkowska, A., Kunkler, C.N., Breger, K., Hulewicz, J.P., Wang, M.C., Springer, N.A. and Brown, J.A. (2020) Naturally occurring modified ribonucleosides. *Wiley Interdiscip Rev RNA*, **11**, e1595.
15. Gott, J.M. and Emeson, R.B. (2000) Functions and mechanisms of RNA editing. *Annu Rev Genet*, **34**, 499-531.
16. Benne, R., Van den Burg, J., Brakenhoff, J.P., Sloof, P., Van Boom, J.H. and Tromp, M.C. (1986) Major transcript of the frameshifted coxII gene from trypanosome mitochondria contains four nucleotides that are not encoded in the DNA. *Cell*, **46**, 819-826.
17. Benne, R. (1994) RNA editing in trypanosomes. *Eur J Biochem*, **221**, 9-23.
18. Kohn, A.B., Sanford, R.S., Yoshida, M.A. and Moroz, L.L. (2015) Parallel Evolution and Lineage-Specific Expansion of RNA Editing in Ctenophores. *Integr Comp Biol*, **55**, 1111-1120.
19. Chen, S.H., Habib, G., Yang, C.Y., Gu, Z.W., Lee, B.R., Weng, S.A., Silberman, S.R., Cai, S.J., Deslypere, J.P., Rosseneu, M. *et al.* (1987) Apolipoprotein B-48 is the product of a messenger RNA with an organ-specific in-frame stop codon. *Science*, **238**, 363-366.
20. Powell, L.M., Wallis, S.C., Pease, R.J., Edwards, Y.H., Knott, T.J. and Scott, J. (1987) A novel form of tissue-specific RNA processing produces apolipoprotein-B48 in intestine. *Cell*, **50**, 831-840.

21. Higuchi, K., Hospattankar, A.V., Law, S.W., Meglin, N., Cortright, J. and Brewer, H.B., Jr. (1988) Human apolipoprotein B (apoB) mRNA: identification of two distinct apoB mRNAs, an mRNA with the apoB-100 sequence and an apoB mRNA containing a premature in-frame translational stop codon, in both liver and intestine. *Proc Natl Acad Sci U S A*, **85**, 1772-1776.
22. Rebagliati, M.R. and Melton, D.A. (1987) Antisense RNA injections in fertilized frog eggs reveal an RNA duplex unwinding activity. *Cell*, **48**, 599-605.
23. Bass, B.L. and Weintraub, H. (1987) A developmentally regulated activity that unwinds RNA duplexes. *Cell*, **48**, 607-613.
24. Bass, B.L. and Weintraub, H. (1988) An unwinding activity that covalently modifies its double-stranded RNA substrate. *Cell*, **55**, 1089-1098.
25. Wagner, R.W., Smith, J.E., Cooperman, B.S. and Nishikura, K. (1989) A double-stranded RNA unwinding activity introduces structural alterations by means of adenosine to inosine conversions in mammalian cells and Xenopus eggs. *Proc Natl Acad Sci U S A*, **86**, 2647-2651.
26. Wagner, R.W. and Nishikura, K. (1988) Cell cycle expression of RNA duplex unwindase activity in mammalian cells. *Mol Cell Biol*, **8**, 770-777.
27. Sommer, B., Kohler, M., Sprengel, R. and Seeburg, P.H. (1991) RNA editing in brain controls a determinant of ion flow in glutamate-gated channels. *Cell*, **67**, 11-19.
28. Burns, C.M., Chu, H., Rueter, S.M., Hutchinson, L.K., Canton, H., Sanders-Bush, E. and Emeson, R.B. (1997) Regulation of serotonin-2C receptor G-protein coupling by RNA editing. *Nature*, **387**, 303-308.
29. Ramaswami, G. and Li, J.B. (2016) Identification of human RNA editing sites: A historical perspective. *Methods*, **107**, 42-47.
30. O'Connell, M.A. and Keller, W. (1994) Purification and properties of double-stranded RNA-specific adenosine deaminase from calf thymus. *Proc Natl Acad Sci U S A*, **91**, 10596-10600.
31. O'Connell, M.A., Krause, S., Higuchi, M., Hsuan, J.J., Totty, N.F., Jenny, A. and Keller, W. (1995) Cloning of cDNAs encoding mammalian double-stranded RNA-specific adenosine deaminase. *Mol Cell Biol*, **15**, 1389-1397.
32. Melcher, T., Maas, S., Herb, A., Sprengel, R., Seeburg, P.H. and Higuchi, M. (1996) A mammalian RNA editing enzyme. *Nature*, **379**, 460-464.
33. Melcher, T., Maas, S., Herb, A., Sprengel, R., Higuchi, M. and Seeburg, P.H. (1996) RED2, a brain-specific member of the RNA-specific adenosine deaminase family. *J Biol Chem*, **271**, 31795-31798.
34. Polson, A.G., Crain, P.F., Pomerantz, S.C., McCloskey, J.A. and Bass, B.L. (1991) The mechanism of adenosine to inosine conversion by the double-stranded RNA unwinding/modifying activity: a high-performance liquid chromatography-mass spectrometry analysis. *Biochemistry*, **30**, 11507-11514.
35. Slavov, D., Clark, M. and Gardiner, K. (2000) Comparative analysis of the RED1 and RED2 A-to-I RNA editing genes from mammals, pufferfish and zebrafish. *Gene*, **250**, 41-51.
36. Slavov, D., Crnogorac-Jurcevic, T., Clark, M. and Gardiner, K. (2000) Comparative analysis of the DRADA A-to-I RNA editing gene from mammals, pufferfish and zebrafish. *Gene*, **250**, 53-60.
37. Lehmann, K.A. and Bass, B.L. (2000) Double-stranded RNA adenosine deaminases ADAR1 and ADAR2 have overlapping specificities. *Biochemistry*, **39**, 12875-12884.
38. Jin, Y., Zhang, W. and Li, Q. (2009) Origins and evolution of ADAR-mediated RNA editing. *IUBMB Life*, **61**, 572-578.

39. Tonkin, L.A., Saccomanno, L., Morse, D.P., Brodigan, T., Krause, M. and Bass, B.L. (2002) RNA editing by ADARs is important for normal behavior in Caenorhabditis elegans. *EMBO J*, **21**, 6025-6035.
40. Albertin, C.B., Simakov, O., Mitros, T., Wang, Z.Y., Pungor, J.R., Edsinger-Gonzales, E., Brenner, S., Ragsdale, C.W. and Rokhsar, D.S. (2015) The octopus genome and the evolution of cephalopod neural and morphological novelties. *Nature*, **524**, 220-224.
41. Belcaid, M., Casaburi, G., McAnulty, S.J., Schmidbaur, H., Suria, A.M., Moriano-Gutierrez, S., Pankey, M.S., Oakley, T.H., Kremer, N., Koch, E.J. *et al.* (2019) Symbiotic organs shaped by distinct modes of genome evolution in cephalopods. *Proc Natl Acad Sci U S A*, **116**, 3030-3035.
42. Palladino, M.J., Keegan, L.P., O'Connell, M.A. and Reenan, R.A. (2000) A-to-I pre-mRNA editing in Drosophila is primarily involved in adult nervous system function and integrity. *Cell*, **102**, 437-449.
43. Patterson, J.B. and Samuel, C.E. (1995) Expression and regulation by interferon of a double-stranded-RNA-specific adenosine deaminase from human cells: evidence for two forms of the deaminase. *Mol Cell Biol*, **15**, 5376-5388.
44. George, C.X. and Samuel, C.E. (1999) Human RNA-specific adenosine deaminase ADAR1 transcripts possess alternative exon 1 structures that initiate from different promoters, one constitutively active and the other interferon inducible. *Proc Natl Acad Sci U S A*, **96**, 4621-4626.
45. Eckmann, C.R., Neunteufl, A., Pfaffstetter, L. and Jantsch, M.F. (2001) The human but not the Xenopus RNA-editing enzyme ADAR1 has an atypical nuclear localization signal and displays the characteristics of a shuttling protein. *Mol Biol Cell*, **12**, 1911-1924.
46. Rueter, S.M., Dawson, T.R. and Emeson, R.B. (1999) Regulation of alternative splicing by RNA editing. *Nature*, **399**, 75-80.
47. Feng, Y., Sansam, C.L., Singh, M. and Emeson, R.B. (2006) Altered RNA editing in mice lacking ADAR2 autoregulation. *Mol Cell Biol*, **26**, 480-488.
48. Kim, U., Wang, Y., Sanford, T., Zeng, Y. and Nishikura, K. (1994) Molecular cloning of cDNA for double-stranded RNA adenosine deaminase, a candidate enzyme for nuclear RNA editing. *Proc Natl Acad Sci U S A*, **91**, 11457-11461.
49. Grosjean, H. (2009) *DNA and RNA modification enzymes : structure, mechanism, function and evolution*. Landes Bioscience, Austin, Tex.
50. Herbert, A., Alfken, J., Kim, Y.G., Mian, I.S., Nishikura, K. and Rich, A. (1997) A Z-DNA binding domain present in the human editing enzyme, double-stranded RNA adenosine deaminase. *Proc Natl Acad Sci U S A*, **94**, 8421-8426.
51. Chen, C.X., Cho, D.S., Wang, Q., Lai, F., Carter, K.C. and Nishikura, K. (2000) A third member of the RNA-specific adenosine deaminase gene family, ADAR3, contains both single- and double-stranded RNA binding domains. *RNA*, **6**, 755-767.
52. Mian, I.S., Moser, M.J., Holley, W.R. and Chatterjee, A. (1998) Statistical modelling and phylogenetic analysis of a deaminase domain. *J Comput Biol*, **5**, 57-72.
53. Lai, F., Drakas, R. and Nishikura, K. (1995) Mutagenic analysis of double-stranded RNA adenosine deaminase, a candidate enzyme for RNA editing of glutamate-gated ion channel transcripts. *J Biol Chem*, **270**, 17098-17105.
54. Chang, Z.Y., Nygaard, P., Chinault, A.C. and Kellems, R.E. (1991) Deduced amino acid sequence of Escherichia coli adenosine deaminase reveals evolutionarily conserved amino acid residues: implications for catalytic function. *Biochemistry*, **30**, 2273-2280.
55. Goodman, R.A., Macbeth, M.R. and Beal, P.A. (2012) ADAR proteins: structure and catalytic mechanism. *Curr Top Microbiol Immunol*, **353**, 1-33.
56. Betts, L., Xiang, S., Short, S.A., Wolfenden, R. and Carter, C.W., Jr. (1994) Cytidine deaminase. The 2.3 A crystal structure of an enzyme: transition-state analog complex. *J Mol Biol*, **235**, 635-656.

57. Kuratani, M., Ishii, R., Bessho, Y., Fukunaga, R., Sengoku, T., Shirouzu, M., Sekine, S. and Yokoyama, S. (2005) Crystal structure of tRNA adenosine deaminase (TadA) from Aquifex aeolicus. *J Biol Chem*, **280**, 16002-16008.
58. Macbeth, M.R., Schubert, H.L., Vandemark, A.P., Lingam, A.T., Hill, C.P. and Bass, B.L. (2005) Inositol hexakisphosphate is bound in the ADAR2 core and required for RNA editing. *Science*, **309**, 1534-1539.
59. Prochnow, C., Bransteitter, R., Klein, M.G., Goodman, M.F. and Chen, X.S. (2007) The APOBEC-2 crystal structure and functional implications for the deaminase AID. *Nature*, **445**, 447-451.
60. Holden, L.G., Prochnow, C., Chang, Y.P., Bransteitter, R., Chelico, L., Sen, U., Stevens, R.C., Goodman, M.F. and Chen, X.S. (2008) Crystal structure of the anti-viral APOBEC3G catalytic domain and functional implications. *Nature*, **456**, 121-124.
61. Wang, Y., Zheng, Y. and Beal, P.A. (2017) Adenosine Deaminases That Act on RNA (ADARs). *Enzymes*, **41**, 215-268.
62. St Johnston, D., Brown, N.H., Gall, J.G. and Jantsch, M. (1992) A conserved double-stranded RNA-binding domain. *Proc Natl Acad Sci U S A*, **89**, 10979-10983.
63. Gibson, T.J. and Thompson, J.D. (1994) Detection of dsRNA-binding domains in RNA helicase A and Drosophila maleless: implications for monomeric RNA helicases. *Nucleic Acids Res*, **22**, 2552-2556.
64. Chang, K.Y. and Ramos, A. (2005) The double-stranded RNA-binding motif, a versatile macromolecular docking platform. *FEBS J*, **272**, 2109-2117.
65. Barraud, P., Heale, B.S., O'Connell, M.A. and Allain, F.H. (2012) Solution structure of the N-terminal dsRBD of Drosophila ADAR and interaction studies with RNA. *Biochimie*, **94**, 1499-1509.
66. Bycroft, M., Grunert, S., Murzin, A.G., Proctor, M. and St Johnston, D. (1995) NMR solution structure of a dsRNA binding domain from Drosophila staufen protein reveals homology to the N-terminal domain of ribosomal protein S5. *EMBO J*, **14**, 3563-3571.
67. Stefl, R., Xu, M., Skrisovska, L., Emeson, R.B. and Allain, F.H. (2006) Structure and specific RNA binding of ADAR2 double-stranded RNA binding motifs. *Structure*, **14**, 345-355.
68. Ramos, A., Grunert, S., Adams, J., Micklem, D.R., Proctor, M.R., Freund, S., Bycroft, M., St Johnston, D. and Varani, G. (2000) RNA recognition by a Staufen double-stranded RNA-binding domain. *EMBO J*, **19**, 997-1009.
69. Wu, H., Henras, A., Chanfreau, G. and Feigon, J. (2004) Structural basis for recognition of the AGNN tetraloop RNA fold by the double-stranded RNA-binding domain of Rnt1p RNase III. *Proc Natl Acad Sci U S A*, **101**, 8307-8312.
70. Stefl, R., Oberstrass, F.C., Hood, J.L., Jourdan, M., Zimmermann, M., Skrisovska, L., Maris, C., Peng, L., Hofr, C., Emeson, R.B. *et al.* (2010) The solution structure of the ADAR2 dsRBM-RNA complex reveals a sequence-specific readout of the minor groove. *Cell*, **143**, 225-237.
71. Liu, Y., Lei, M. and Samuel, C.E. (2000) Chimeric double-stranded RNA-specific adenosine deaminase ADAR1 proteins reveal functional selectivity of double-stranded RNA-binding domains from ADAR1 and protein kinase PKR. *Proc Natl Acad Sci U S A*, **97**, 12541-12546.
72. Cho, D.S., Yang, W., Lee, J.T., Shiekhattar, R., Murray, J.M. and Nishikura, K. (2003) Requirement of dimerization for RNA editing activity of adenosine deaminases acting on RNA. *J Biol Chem*, **278**, 17093-17102.
73. Chilibeck, K.A., Wu, T., Liang, C., Schellenberg, M.J., Gesner, E.M., Lynch, J.M. and MacMillan, A.M. (2006) FRET analysis of in vivo dimerization by RNA-editing enzymes. *J Biol Chem*, **281**, 16530-16535.

74. Macbeth, M.R. and Bass, B.L. (2007) Large-scale overexpression and purification of ADARs from Saccharomyces cerevisiae for biophysical and biochemical studies. *Methods Enzymol*, **424**, 319-331.
75. Poulsen, H., Jorgensen, R., Heding, A., Nielsen, F.C., Bonven, B. and Egebjerg, J. (2006) Dimerization of ADAR2 is mediated by the double-stranded RNA binding domain. *RNA*, **12**, 1350-1360.
76. Gallo, A., Keegan, L.P., Ring, G.M. and O'Connell, M.A. (2003) An ADAR that edits transcripts encoding ion channel subunits functions as a dimer. *EMBO J*, **22**, 3421-3430.
77. Valente, L. and Nishikura, K. (2007) RNA binding-independent dimerization of adenosine deaminases acting on RNA and dominant negative effects of nonfunctional subunits on dimer functions. *J Biol Chem*, **282**, 16054-16061.
78. Stephens, O.M., Yi-Brunozzi, H.Y. and Beal, P.A. (2000) Analysis of the RNA-editing reaction of ADAR2 with structural and fluorescent analogues of the GluR-B R/G editing site. *Biochemistry*, **39**, 12243-12251.
79. Carter, C.W., Jr. (1995) The nucleoside deaminases for cytidine and adenosine: structure, transition state stabilization, mechanism, and evolution. *Biochimie*, **77**, 92-98.
80. Luo, M. and Schramm, V.L. (2008) Transition state structure of E. coli tRNA-specific adenosine deaminase. *J Am Chem Soc*, **130**, 2649-2655.
81. Maydanovych, O., Easterwood, L.M., Cui, T., Veliz, E.A., Pokharel, S. and Beal, P.A. (2007) Probing adenosine-to-inosine editing reactions using RNA-containing nucleoside analogs. *Methods Enzymol*, **424**, 369-386.
82. Matthews, M.M., Thomas, J.M., Zheng, Y., Tran, K., Phelps, K.J., Scott, A.I., Havel, J., Fisher, A.J. and Beal, P.A. (2016) Structures of human ADAR2 bound to dsRNA reveal base-flipping mechanism and basis for site selectivity. *Nat Struct Mol Biol*, **23**, 426-433.
83. Klimasauskas, S., Kumar, S., Roberts, R.J. and Cheng, X. (1994) HhaI methyltransferase flips its target base out of the DNA helix. *Cell*, **76**, 357-369.
84. Wang, Y., Havel, J. and Beal, P.A. (2015) A Phenotypic Screen for Functional Mutants of Human Adenosine Deaminase Acting on RNA 1. *ACS Chem Biol*, **10**, 2512-2519.
85. Rice, G.I., Kasher, P.R., Forte, G.M., Mannion, N.M., Greenwood, S.M., Szynkiewicz, M., Dickerson, J.E., Bhaskar, S.S., Zampini, M., Briggs, T.A. *et al.* (2012) Mutations in ADAR1 cause Aicardi-Goutieres syndrome associated with a type I interferon signature. *Nat Genet*, **44**, 1243-1248.
86. Kuttan, A. and Bass, B.L. (2012) Mechanistic insights into editing-site specificity of ADARs. *Proc Natl Acad Sci U S A*, **109**, E3295-3304.
87. Holz, B., Klimasauskas, S., Serva, S. and Weinhold, E. (1998) 2-Aminopurine as a fluorescent probe for DNA base flipping by methyltransferases. *Nucleic Acids Res*, **26**, 1076-1083.
88. Ward, D.C., Reich, E. and Stryer, L. (1969) Fluorescence studies of nucleotides and polynucleotides. I. Formycin, 2-aminopurine riboside, 2,6-diaminopurine riboside, and their derivatives. *J Biol Chem*, **244**, 1228-1237.
89. Wilson, D.K., Rudolph, F.B. and Quiocho, F.A. (1991) Atomic structure of adenosine deaminase complexed with a transition-state analog: understanding catalysis and immunodeficiency mutations. *Science*, **252**, 1278-1284.
90. Veliz, E.A., Easterwood, L.M. and Beal, P.A. (2003) Substrate analogues for an RNA-editing adenosine deaminase: mechanistic investigation and inhibitor design. *J Am Chem Soc*, **125**, 10867-10876.
91. Haudenschild, B.L., Maydanovych, O., Veliz, E.A., Macbeth, M.R., Bass, B.L. and Beal, P.A. (2004) A transition state analogue for an RNA-editing reaction. *J Am Chem Soc*, **126**, 11213-11219.

92. Phelps, K.J., Tran, K., Eifler, T., Erickson, A.I., Fisher, A.J. and Beal, P.A. (2015) Recognition of duplex RNA by the deaminase domain of the RNA editing enzyme ADAR2. *Nucleic Acids Res*, **43**, 1123-1132.
93. Nishikura, K., Yoo, C., Kim, U., Murray, J.M., Estes, P.A., Cash, F.E. and Liebhaber, S.A. (1991) Substrate specificity of the dsRNA unwinding/modifying activity. *EMBO J*, **10**, 3523-3532.
94. Polson, A.G. and Bass, B.L. (1994) Preferential selection of adenosines for modification by double-stranded RNA adenosine deaminase. *EMBO J*, **13**, 5701-5711.
95. Lehmann, K.A. and Bass, B.L. (1999) The importance of internal loops within RNA substrates of ADAR1. *J Mol Biol*, **291**, 1-13.
96. Dawson, T.R., Sansam, C.L. and Emeson, R.B. (2004) Structure and sequence determinants required for the RNA editing of ADAR2 substrates. *J Biol Chem*, **279**, 4941-4951.
97. Reenan, R.A. (2005) Molecular determinants and guided evolution of species-specific RNA editing. *Nature*, **434**, 409-413.
98. Barraud, P. and Allain, F.H. (2012) ADAR proteins: double-stranded RNA and Z-DNA binding domains. *Curr Top Microbiol Immunol*, **353**, 35-60.
99. Enstero, M., Daniel, C., Wahlstedt, H., Major, F. and Ohman, M. (2009) Recognition and coupling of A-to-I edited sites are determined by the tertiary structure of the RNA. *Nucleic Acids Res*, **37**, 6916-6926.
100. Wong, S.K., Sato, S. and Lazinski, D.W. (2001) Substrate recognition by ADAR1 and ADAR2. *RNA*, **7**, 846-858.
101. Kallman, A.M., Sahlin, M. and Ohman, M. (2003) ADAR2 A-->I editing: site selectivity and editing efficiency are separate events. *Nucleic Acids Res*, **31**, 4874-4881.
102. Eggington, J.M., Greene, T. and Bass, B.L. (2011) Predicting sites of ADAR editing in double-stranded RNA. *Nat Commun*, **2**, 319.
103. Walkley, C.R. and Li, J.B. (2017) Rewriting the transcriptome: adenosine-to-inosine RNA editing by ADARs. *Genome Biol*, **18**, 205.
104. Bazak, L., Haviv, A., Barak, M., Jacob-Hirsch, J., Deng, P., Zhang, R., Isaacs, F.J., Rechavi, G., Li, J.B., Eisenberg, E. *et al.* (2014) A-to-I RNA editing occurs at over a hundred million genomic sites, located in a majority of human genes. *Genome Res*, **24**, 365-376.
105. Levanon, E.Y., Eisenberg, E., Yelin, R., Nemzer, S., Hallegger, M., Shemesh, R., Fligelman, Z.Y., Shoshan, A., Pollock, S.R., Sztybel, D. *et al.* (2004) Systematic identification of abundant A-to-I editing sites in the human transcriptome. *Nat Biotechnol*, **22**, 1001-1005.
106. Ramaswami, G., Lin, W., Piskol, R., Tan, M.H., Davis, C. and Li, J.B. (2012) Accurate identification of human Alu and non-Alu RNA editing sites. *Nat Methods*, **9**, 579-581.
107. Ramaswami, G., Zhang, R., Piskol, R., Keegan, L.P., Deng, P., O'Connell, M.A. and Li, J.B. (2013) Identifying RNA editing sites using RNA sequencing data alone. *Nat Methods*, **10**, 128-132.
108. Porath, H.T., Carmi, S. and Levanon, E.Y. (2014) A genome-wide map of hyper-edited RNA reveals numerous new sites. *Nat Commun*, **5**, 4726.
109. Carmi, S., Borukhov, I. and Levanon, E.Y. (2011) Identification of widespread ultra-edited human RNAs. *PLoS Genet*, **7**, e1002317.
110. Li, J.B., Levanon, E.Y., Yoon, J.K., Aach, J., Xie, B., Leproust, E., Zhang, K., Gao, Y. and Church, G.M. (2009) Genome-wide identification of human RNA editing sites by parallel DNA capturing and sequencing. *Science*, **324**, 1210-1213.
111. Nishikura, K. (2010) Functions and regulation of RNA editing by ADAR deaminases. *Annu Rev Biochem*, **79**, 321-349.

112. Mannion, N., Arieti, F., Gallo, A., Keegan, L.P. and O'Connell, M.A. (2015) New Insights into the Biological Role of Mammalian ADARs; the RNA Editing Proteins. *Biomolecules*, **5**, 2338-2362.
113. Kim, D.D., Kim, T.T., Walsh, T., Kobayashi, Y., Matise, T.C., Buyske, S. and Gabriel, A. (2004) Widespread RNA editing of embedded alu elements in the human transcriptome. *Genome Res*, **14**, 1719-1725.
114. Athanasiadis, A., Rich, A. and Maas, S. (2004) Widespread A-to-I RNA editing of Alu-containing mRNAs in the human transcriptome. *PLoS Biol*, **2**, e391.
115. Lev-Maor, G., Sorek, R., Levanon, E.Y., Paz, N., Eisenberg, E. and Ast, G. (2007) RNA-editing-mediated exon evolution. *Genome Biol*, **8**, R29.
116. Prasanth, K.V., Prasanth, S.G., Xuan, Z., Hearn, S., Freier, S.M., Bennett, C.F., Zhang, M.Q. and Spector, D.L. (2005) Regulating gene expression through RNA nuclear retention. *Cell*, **123**, 249-263.
117. Zhang, Z. and Carmichael, G.G. (2001) The fate of dsRNA in the nucleus: a p54(nrb)-containing complex mediates the nuclear retention of promiscuously A-to-I edited RNAs. *Cell*, **106**, 465-475.
118. Kawamura, Y., Saito, K., Kin, T., Ono, Y., Asai, K., Sunohara, T., Okada, T.N., Siomi, M.C. and Siomi, H. (2008) Drosophila endogenous small RNAs bind to Argonaute 2 in somatic cells. *Nature*, **453**, 793-797.
119. Reikine, S., Nguyen, J.B. and Modis, Y. (2014) Pattern Recognition and Signaling Mechanisms of RIG-I and MDA5. *Front Immunol*, **5**, 342.
120. Bass, B.L., Weintraub, H., Cattaneo, R. and Billeter, M.A. (1989) Biased hypermutation of viral RNA genomes could be due to unwinding/modification of double-stranded RNA. *Cell*, **56**, 331.
121. Taylor, D.R., Puig, M., Darnell, M.E., Mihalik, K. and Feinstone, S.M. (2005) New antiviral pathway that mediates hepatitis C virus replicon interferon sensitivity through ADAR1. *J Virol*, **79**, 6291-6298.
122. Samuel, C.E. (2011) Adenosine deaminases acting on RNA (ADARs) are both antiviral and proviral. *Virology*, **411**, 180-193.
123. Hartner, J.C., Walkley, C.R., Lu, J. and Orkin, S.H. (2009) ADAR1 is essential for the maintenance of hematopoiesis and suppression of interferon signaling. *Nat Immunol*, **10**, 109-115.
124. Mannion, N.M., Greenwood, S.M., Young, R., Cox, S., Brindle, J., Read, D., Nellaker, C., Vesely, C., Ponting, C.P., McLaughlin, P.J. *et al.* (2014) The RNA-editing enzyme ADAR1 controls innate immune responses to RNA. *Cell Rep*, **9**, 1482-1494.
125. Liddicoat, B.J., Piskol, R., Chalk, A.M., Ramaswami, G., Higuchi, M., Hartner, J.C., Li, J.B., Seeburg, P.H. and Walkley, C.R. (2015) RNA editing by ADAR1 prevents MDA5 sensing of endogenous dsRNA as nonself. *Science*, **349**, 1115-1120.
126. Bartel, D.P. (2004) MicroRNAs: genomics, biogenesis, mechanism, and function. *Cell*, **116**, 281-297.
127. Yang, W., Chendrimada, T.P., Wang, Q., Higuchi, M., Seeburg, P.H., Shiekhattar, R. and Nishikura, K. (2006) Modulation of microRNA processing and expression through RNA editing by ADAR deaminases. *Nat Struct Mol Biol*, **13**, 13-21.
128. Kawahara, Y., Zinshteyn, B., Chendrimada, T.P., Shiekhattar, R. and Nishikura, K. (2007) RNA editing of the microRNA-151 precursor blocks cleavage by the Dicer-TRBP complex. *EMBO Rep*, **8**, 763-769.
129. Kawahara, Y., Zinshteyn, B., Sethupathy, P., Iizasa, H., Hatzigeorgiou, A.G. and Nishikura, K. (2007) Redirection of silencing targets by adenosine-to-inosine editing of miRNAs. *Science*, **315**, 1137-1140.

130. Hoernes, T.P., Faserl, K., Juen, M.A., Kremser, J., Gasser, C., Fuchs, E., Shi, X., Siewert, A., Lindner, H., Kreutz, C. *et al.* (2018) Translation of non-standard codon nucleotides reveals minimal requirements for codon-anticodon interactions. *Nat Commun*, **9**, 4865.
131. Licht, K., Hartl, M., Amman, F., Anrather, D., Janisiw, M.P. and Jantsch, M.F. (2019) Inosine induces context-dependent recoding and translational stalling. *Nucleic Acids Res*, **47**, 3-14.
132. Verdoorn, T.A., Burnashev, N., Monyer, H., Seeburg, P.H. and Sakmann, B. (1991) Structural determinants of ion flow through recombinant glutamate receptor channels. *Science*, **252**, 1715-1718.
133. Brusa, R., Zimmermann, F., Koh, D.S., Feldmeyer, D., Gass, P., Seeburg, P.H. and Sprengel, R. (1995) Early-onset epilepsy and postnatal lethality associated with an editing-deficient GluR-B allele in mice. *Science*, **270**, 1677-1680.
134. Higuchi, M., Maas, S., Single, F.N., Hartner, J., Rozov, A., Burnashev, N., Feldmeyer, D., Sprengel, R. and Seeburg, P.H. (2000) Point mutation in an AMPA receptor gene rescues lethality in mice deficient in the RNA-editing enzyme ADAR2. *Nature*, **406**, 78-81.
135. Bhalla, T., Rosenthal, J.J., Holmgren, M. and Reenan, R. (2004) Control of human potassium channel inactivation by editing of a small mRNA hairpin. *Nat Struct Mol Biol*, **11**, 950-956.
136. Miyake, K., Ohta, T., Nakayama, H., Doe, N., Terao, Y., Oiki, E., Nagatomo, I., Yamashita, Y., Abe, T., Nishikura, K. *et al.* (2016) CAPS1 RNA Editing Promotes Dense Core Vesicle Exocytosis. *Cell Rep*, **17**, 2004-2014.
137. Shimokawa, T., Rahman, M.F., Tostar, U., Sonkoly, E., Stahle, M., Pivarcsi, A., Palaniswamy, R. and Zaphiropoulos, P.G. (2013) RNA editing of the GLI1 transcription factor modulates the output of Hedgehog signaling. *RNA Biol*, **10**, 321-333.
138. Ramaswami, G. and Li, J.B. (2014) RADAR: a rigorously annotated database of A-to-I RNA editing. *Nucleic Acids Res*, **42**, D109-113.
139. Liscovitch-Brauer, N., Alon, S., Porath, H.T., Elstein, B., Unger, R., Ziv, T., Admon, A., Levanon, E.Y., Rosenthal, J.J.C. and Eisenberg, E. (2017) Trade-off between Transcriptome Plasticity and Genome Evolution in Cephalopods. *Cell*, **169**, 191-202 e111.
140. Xu, G. and Zhang, J. (2014) Human coding RNA editing is generally nonadaptive. *Proc Natl Acad Sci U S A*, **111**, 3769-3774.
141. Tan, M.H., Li, Q., Shanmugam, R., Piskol, R., Kohler, J., Young, A.N., Liu, K.I., Zhang, R., Ramaswami, G., Ariyoshi, K. *et al.* (2017) Dynamic landscape and regulation of RNA editing in mammals. *Nature*, **550**, 249-254.
142. Paz-Yaacov, N., Bazak, L., Buchumenski, I., Porath, H.T., Danan-Gotthold, M., Knisbacher, B.A., Eisenberg, E. and Levanon, E.Y. (2015) Elevated RNA Editing Activity Is a Major Contributor to Transcriptomic Diversity in Tumors. *Cell Rep*, **13**, 267-276.
143. Han, L., Diao, L., Yu, S., Xu, X., Li, J., Zhang, R., Yang, Y., Werner, H.M.J., Eterovic, A.K., Yuan, Y. *et al.* (2015) The Genomic Landscape and Clinical Relevance of A-to-I RNA Editing in Human Cancers. *Cancer Cell*, **28**, 515-528.
144. Fumagalli, D., Gacquer, D., Rothe, F., Lefort, A., Libert, F., Brown, D., Kheddoumi, N., Shlien, A., Konopka, T., Salgado, R. *et al.* (2015) Principles Governing A-to-I RNA Editing in the Breast Cancer Transcriptome. *Cell Rep*, **13**, 277-289.
145. Nevo-Caspi, Y., Amariglio, N., Rechavi, G. and Paret, G. (2011) A-to-I RNA editing is induced upon hypoxia. *Shock*, **35**, 585-589.
146. Ben-Zvi, M., Amariglio, N., Paret, G. and Nevo-Caspi, Y. (2013) F11R expression upon hypoxia is regulated by RNA editing. *PLoS One*, **8**, e77702.
147. Nigita, G., Acunzo, M., Romano, G., Veneziano, D., Lagana, A., Vitiello, M., Wernicke, D., Ferro, A. and Croce, C.M. (2016) microRNA editing in seed region aligns with cellular changes in hypoxic conditions. *Nucleic Acids Res*, **44**, 6298-6308.

148. Ma, C.P., Liu, H., Yi-Feng Chang, I., Wang, W.C., Chen, Y.T., Wu, S.M., Chen, H.W., Kuo, Y.P., Shih, C.T., Li, C.Y. *et al.* (2019) ADAR1 promotes robust hypoxia signaling via distinct regulation of multiple HIF-1alpha-inhibiting factors. *EMBO Rep*, **20**.
149. Ma, E., Gu, X.Q., Wu, X., Xu, T. and Haddad, G.G. (2001) Mutation in pre-mRNA adenosine deaminase markedly attenuates neuronal tolerance to O2 deprivation in Drosophila melanogaster. *J Clin Invest*, **107**, 685-693.
150. Hideyama, T., Yamashita, T., Aizawa, H., Tsuji, S., Kakita, A., Takahashi, H. and Kwak, S. (2012) Profound downregulation of the RNA editing enzyme ADAR2 in ALS spinal motor neurons. *Neurobiol Dis*, **45**, 1121-1128.
151. Hideyama, T., Yamashita, T., Suzuki, T., Tsuji, S., Higuchi, M., Seeburg, P.H., Takahashi, R., Misawa, H. and Kwak, S. (2010) Induced loss of ADAR2 engenders slow death of motor neurons from Q/R site-unedited GluR2. *J Neurosci*, **30**, 11917-11925.
152. Vollmar, W., Gloger, J., Berger, E., Kortenbruck, G., Kohling, R., Speckmann, E.J. and Musshoff, U. (2004) RNA editing (R/G site) and flip-flop splicing of the AMPA receptor subunit GluR2 in nervous tissue of epilepsy patients. *Neurobiol Dis*, **15**, 371-379.
153. Streit, A.K., Derst, C., Wegner, S., Heinemann, U., Zahn, R.K. and Decher, N. (2011) RNA editing of Kv1.1 channels may account for reduced ictogenic potential of 4-aminopyridine in chronic epileptic rats. *Epilepsia*, **52**, 645-648.
154. Srivastava, P.K., Bagnati, M., Delahaye-Duriez, A., Ko, J.H., Rotival, M., Langley, S.R., Shkura, K., Mazzuferi, M., Danis, B., van Eyll, J. *et al.* (2017) Genome-wide analysis of differential RNA editing in epilepsy. *Genome Res*, **27**, 440-450.
155. Sanjana, N.E., Levanon, E.Y., Hueske, E.A., Ambrose, J.M. and Li, J.B. (2012) Activity-dependent A-to-I RNA editing in rat cortical neurons. *Genetics*, **192**, 281-287.
156. Balik, A., Penn, A.C., Nemoda, Z. and Greger, I.H. (2013) Activity-regulated RNA editing in select neuronal subfields in hippocampus. *Nucleic Acids Res*, **41**, 1124-1134.
157. Li, X., Overton, I.M., Baines, R.A., Keegan, L.P. and O'Connell, M.A. (2014) The ADAR RNA editing enzyme controls neuronal excitability in Drosophila melanogaster. *Nucleic Acids Res*, **42**, 1139-1151.
158. Garrett, S. and Rosenthal, J.J. (2012) RNA editing underlies temperature adaptation in K+ channels from polar octopuses. *Science*, **335**, 848-851.
159. Rieder, L.E., Savva, Y.A., Reyna, M.A., Chang, Y.J., Dorsky, J.S., Rezaei, A. and Reenan, R.A. (2015) Dynamic response of RNA editing to temperature in Drosophila. *BMC Biol*, **13**, 1.
160. Rosenthal, J.J. (2015) The emerging role of RNA editing in plasticity. *J Exp Biol*, **218**, 1812-1821.
161. Hood, J.L., Morabito, M.V., Martinez, C.R., 3rd, Gilbert, J.A., Ferrick, E.A., Ayers, G.D., Chappell, J.D., Dermody, T.S. and Emeson, R.B. (2014) Reovirus-mediated induction of ADAR1 (p150) minimally alters RNA editing patterns in discrete brain regions. *Mol Cell Neurosci*, **61**, 97-109.
162. Wahlstedt, H., Daniel, C., Enstero, M. and Ohman, M. (2009) Large-scale mRNA sequencing determines global regulation of RNA editing during brain development. *Genome Res*, **19**, 978-986.
163. Sapiro, A.L., Freund, E.C., Restrepo, L., Qiao, H.H., Bhate, A., Li, Q., Ni, J.Q., Mosca, T.J. and Li, J.B. (2020) Zinc Finger RNA-Binding Protein Zn72D Regulates ADAR-Mediated RNA Editing in Neurons. *Cell Rep*, **31**, 107654.
164. Porath, H.T., Hazan, E., Shpigler, H., Cohen, M., Band, M., Ben-Shahar, Y., Levanon, E.Y., Eisenberg, E. and Bloch, G. (2019) RNA editing is abundant and correlates with task performance in a social bumblebee. *Nat Commun*, **10**, 1605.
165. Marcucci, R., Brindle, J., Paro, S., Casadio, A., Hempel, S., Morrice, N., Bisso, A., Keegan, L.P., Del Sal, G. and O'Connell, M.A. (2011) Pin1 and WWP2 regulate GluR2 Q/R site RNA editing by ADAR2 with opposing effects. *EMBO J*, **30**, 4211-4222.

166. Freund, E.C., Sapiro, A.L., Li, Q., Linder, S., Moresco, J.J., Yates, J.R., 3rd and Li, J.B. (2020) Unbiased Identification of trans Regulators of ADAR and A-to-I RNA Editing. *Cell Rep*, **31**, 107656.
167. Goodwin, S., McPherson, J.D. and McCombie, W.R. (2016) Coming of age: ten years of next-generation sequencing technologies. *Nat Rev Genet*, **17**, 333-351.
168. Morabito, M.V., Ulbricht, R.J., O'Neil, R.T., Airey, D.C., Lu, P., Zhang, B., Wang, L. and Emeson, R.B. (2010) High-throughput multiplexed transcript analysis yields enhanced resolution of 5-hydroxytryptamine 2C receptor mRNA editing profiles. *Mol Pharmacol*, **77**, 895-902.
169. Zhang, R., Li, X., Ramaswami, G., Smith, K.S., Turecki, G., Montgomery, S.B. and Li, J.B. (2014) Quantifying RNA allelic ratios by microfluidic multiplex PCR and sequencing. *Nat Methods*, **11**, 51-54.
170. Jinnah, H. and Ulbricht, R.J. (2019) Using mouse models to unlock the secrets of non-synonymous RNA editing. *Methods*, **156**, 40-45.
171. Diroma, M.A., Ciaccia, L., Pesole, G. and Picardi, E. (2019) Elucidating the editome: bioinformatics approaches for RNA editing detection. *Brief Bioinform*, **20**, 436-447.
172. Jepson, J.E. and Reenan, R.A. (2007) Genetic approaches to studying adenosine-to-inosine RNA editing. *Methods Enzymol*, **424**, 265-287.
173. Carr, I.M., Robinson, J.I., Dimitriou, R., Markham, A.F., Morgan, A.W. and Bonthron, D.T. (2009) Inferring relative proportions of DNA variants from sequencing electropherograms. *Bioinformatics*, **25**, 3244-3250.
174. Shen, W., Le, S., Li, Y. and Hu, F. (2016) SeqKit: A Cross-Platform and Ultrafast Toolkit for FASTA/Q File Manipulation. *PLoS One*, **11**, e0163962.
175. Droop, A.P. (2016) fqtools: an efficient software suite for modern FASTQ file manipulation. *Bioinformatics*, **32**, 1883-1884.
176. Li, L., Song, Y., Shi, X., Liu, J., Xiong, S., Chen, W., Fu, Q., Huang, Z., Gu, N. and Zhang, R. (2018) The landscape of miRNA editing in animals and its impact on miRNA biogenesis and targeting. *Genome Res*, **28**, 132-143.
177. Hoyer, D., Clarke, D.E., Fozard, J.R., Hartig, P.R., Martin, G.R., Mylecharane, E.J., Saxena, P.R. and Humphrey, P.P. (1994) International Union of Pharmacology classification of receptors for 5-hydroxytryptamine (Serotonin). *Pharmacol Rev*, **46**, 157-203.
178. Hoyer, D., Hannon, J.P. and Martin, G.R. (2002) Molecular, pharmacological and functional diversity of 5-HT receptors. *Pharmacol Biochem Behav*, **71**, 533-554.
179. Barnes, N.M. and Sharp, T. (1999) A review of central 5-HT receptors and their function. *Neuropharmacology*, **38**, 1083-1152.
180. Bockaert, J., Claeysen, S., Becamel, C., Dumuis, A. and Marin, P. (2006) Neuronal 5-HT metabotropic receptors: fine-tuning of their structure, signaling, and roles in synaptic modulation. *Cell Tissue Res*, **326**, 553-572.
181. Heisler, L.K., Cowley, M.A., Kishi, T., Tecott, L.H., Fan, W., Low, M.J., Smart, J.L., Rubinstein, M., Tatro, J., Zigman, J.M. *et al.* (2003) Central serotonin and melanocortin pathways regulating energy homeostasis. *Ann N Y Acad Sci*, **994**, 169-174.
182. Heisler, L.K., Cowley, M.A., Tecott, L.H., Fan, W., Low, M.J., Smart, J.L., Rubinstein, M., Tatro, J.B., Marcus, J.N., Holstege, H. *et al.* (2002) Activation of central melanocortin pathways by fenfluramine. *Science*, **297**, 609-611.
183. Heisler, L.K., Jobst, E.E., Sutton, G.M., Zhou, L., Borok, E., Thornton-Jones, Z., Liu, H.Y., Zigman, J.M., Balthasar, N., Kishi, T. *et al.* (2006) Serotonin reciprocally regulates melanocortin neurons to modulate food intake. *Neuron*, **51**, 239-249.
184. Lam, D.D., Przydzial, M.J., Ridley, S.H., Yeo, G.S., Rochford, J.J., O'Rahilly, S. and Heisler, L.K. (2008) Serotonin 5-HT2C receptor agonist promotes hypophagia via downstream activation of melanocortin 4 receptors. *Endocrinology*, **149**, 1323-1328.

185. Xu, Y., Jones, J.E., Kohno, D., Williams, K.W., Lee, C.E., Choi, M.J., Anderson, J.G., Heisler, L.K., Zigman, J.M., Lowell, B.B. *et al.* (2008) 5-HT2CRs expressed by pro-opiomelanocortin neurons regulate energy homeostasis. *Neuron*, **60**, 582-589.
186. Xu, Y., Jones, J.E., Lauzon, D.A., Anderson, J.G., Balthasar, N., Heisler, L.K., Zinn, A.R., Lowell, B.B. and Elmquist, J.K. (2010) A serotonin and melanocortin circuit mediates D-fenfluramine anorexia. *J Neurosci*, **30**, 14630-14634.
187. Vickers, S.P., Clifton, P.G., Dourish, C.T. and Tecott, L.H. (1999) Reduced satiating effect of d-fenfluramine in serotonin 5-HT(2C) receptor mutant mice. *Psychopharmacology (Berl)*, **143**, 309-314.
188. Berglund, E.D., Liu, C., Sohn, J.W., Liu, T., Kim, M.H., Lee, C.E., Vianna, C.R., Williams, K.W., Xu, Y. and Elmquist, J.K. (2013) Serotonin 2C receptors in pro-opiomelanocortin neurons regulate energy and glucose homeostasis. *J Clin Invest*, **123**, 5061-5070.
189. Zhou, L., Sutton, G.M., Rochford, J.J., Semple, R.K., Lam, D.D., Oksanen, L.J., Thornton-Jones, Z.D., Clifton, P.G., Yueh, C.Y., Evans, M.L. *et al.* (2007) Serotonin 2C receptor agonists improve type 2 diabetes via melanocortin-4 receptor signaling pathways. *Cell Metab*, **6**, 398-405.
190. Tecott, L.H., Sun, L.M., Akana, S.F., Strack, A.M., Lowenstein, D.H., Dallman, M.F. and Julius, D. (1995) Eating disorder and epilepsy in mice lacking 5-HT2c serotonin receptors. *Nature*, **374**, 542-546.
191. Nonogaki, K., Strack, A.M., Dallman, M.F. and Tecott, L.H. (1998) Leptin-independent hyperphagia and type 2 diabetes in mice with a mutated serotonin 5-HT2C receptor gene. *Nat Med*, **4**, 1152-1156.
192. Tecott, L.H. (2007) Serotonin and the orchestration of energy balance. *Cell Metab*, **6**, 352-361.
193. Adan, R.A., Cone, R.D., Burbach, J.P. and Gispen, W.H. (1994) Differential effects of melanocortin peptides on neural melanocortin receptors. *Mol Pharmacol*, **46**, 1182-1190.
194. Fan, W., Boston, B.A., Kesterson, R.A., Hruby, V.J. and Cone, R.D. (1997) Role of melanocortinergic neurons in feeding and the agouti obesity syndrome. *Nature*, **385**, 165-168.
195. Marsh, D.J., Hollopeter, G., Huszar, D., Laufer, R., Yagaloff, K.A., Fisher, S.L., Burn, P. and Palmiter, R.D. (1999) Response of melanocortin-4 receptor-deficient mice to anorectic and orexigenic peptides. *Nat Genet*, **21**, 119-122.
196. Sohn, J.W., Xu, Y., Jones, J.E., Wickman, K., Williams, K.W. and Elmquist, J.K. (2011) Serotonin 2C receptor activates a distinct population of arcuate pro-opiomelanocortin neurons via TRPC channels. *Neuron*, **71**, 488-497.
197. Ollmann, M.M., Wilson, B.D., Yang, Y.K., Kerns, J.A., Chen, Y., Gantz, I. and Barsh, G.S. (1997) Antagonism of central melanocortin receptors in vitro and in vivo by agouti-related protein. *Science*, **278**, 135-138.
198. Hutcheson, J.D., Ryzhova, L.M., Setola, V. and Merryman, W.D. (2012) 5-HT(2B) antagonism arrests non-canonical TGF-beta1-induced valvular myofibroblast differentiation. *J Mol Cell Cardiol*, **53**, 707-714.
199. Hutcheson, J.D., Setola, V., Roth, B.L. and Merryman, W.D. (2011) Serotonin receptors and heart valve disease--it was meant 2B. *Pharmacol Ther*, **132**, 146-157.
200. West, J.D., Carrier, E.J., Bloodworth, N.C., Schroer, A.K., Chen, P., Ryzhova, L.M., Gladson, S., Shay, S., Hutcheson, J.D. and Merryman, W.D. (2016) Serotonin 2B Receptor Antagonism Prevents Heritable Pulmonary Arterial Hypertension. *PLoS One*, **11**, e0148657.
201. Niswender, C.M., Copeland, S.C., Herrick-Davis, K., Emeson, R.B. and Sanders-Bush, E. (1999) RNA editing of the human serotonin 5-hydroxytryptamine 2C receptor silences constitutive activity. *J Biol Chem*, **274**, 9472-9478.

202. Morabito, M.V., Abbas, A.I., Hood, J.L., Kesterson, R.A., Jacobs, M.M., Kump, D.S., Hachey, D.L., Roth, B.L. and Emeson, R.B. (2010) Mice with altered serotonin 2C receptor RNA editing display characteristics of Prader-Willi syndrome. *Neurobiol Dis*, **39**, 169-180.
203. Lutter, M., Sakata, I., Osborne-Lawrence, S., Rovinsky, S.A., Anderson, J.G., Jung, S., Birnbaum, S., Yanagisawa, M., Elmquist, J.K., Nestler, E.J. *et al.* (2008) The orexigenic hormone ghrelin defends against depressive symptoms of chronic stress. *Nat Neurosci*, **11**, 752-753.
204. Kishore, S. and Stamm, S. (2006) The snoRNA HBII-52 regulates alternative splicing of the serotonin receptor 2C. *Science*, **311**, 230-232.
205. Kishore, S. and Stamm, S. (2006) Regulation of alternative splicing by snoRNAs. *Cold Spring Harb Symp Quant Biol*, **71**, 329-334.
206. O'Neil, R.T., Wang, X., Morabito, M.V. and Emeson, R.B. (2017) Comparative analysis of A-to-I editing in human and non-human primate brains reveals conserved patterns and context-dependent regulation of RNA editing. *Mol Brain*, **10**, 11.
207. Gan, Z., Zhao, L., Yang, L., Huang, P., Zhao, F., Li, W. and Liu, Y. (2006) RNA editing by ADAR2 is metabolically regulated in pancreatic islets and beta-cells. *J Biol Chem*, **281**, 33386-33394.
208. Malakar, P., Chartarifsky, L., Hija, A., Leibowitz, G., Glaser, B., Dor, Y. and Karni, R. (2016) Insulin receptor alternative splicing is regulated by insulin signaling and modulates beta cell survival. *Sci Rep*, **6**, 31222.
209. Roh, E., Song, D.K. and Kim, M.S. (2016) Emerging role of the brain in the homeostatic regulation of energy and glucose metabolism. *Exp Mol Med*, **48**, e216.
210. Jensen, T.E. and Richter, E.A. (2012) Regulation of glucose and glycogen metabolism during and after exercise. *J Physiol*, **590**, 1069-1076.
211. Jacobs, B.L. and Fornal, C.A. (1999) Activity of serotonergic neurons in behaving animals. *Neuropsychopharmacology*, **21**, 9S-15S.
212. Cong, L., Ran, F.A., Cox, D., Lin, S., Barretto, R., Habib, N., Hsu, P.D., Wu, X., Jiang, W., Marraffini, L.A. *et al.* (2013) Multiplex genome engineering using CRISPR/Cas systems. *Science*, **339**, 819-823.
213. Cong, L. and Zhang, F. (2015) Genome engineering using CRISPR-Cas9 system. *Methods Mol Biol*, **1239**, 197-217.
214. Keller, W., Wolf, J. and Gerber, A. (1999) Editing of messenger RNA precursors and of tRNAs by adenosine to inosine conversion. *FEBS Lett*, **452**, 71-76.
215. Fitzgerald, L.W., Iyer, G., Conklin, D.S., Krause, C.M., Marshall, A., Patterson, J.P., Tran, D.P., Jonak, G.J. and Hartig, P.R. (1999) Messenger RNA editing of the human serotonin 5-HT2C receptor. *Neuropsychopharmacology*, **21**, 82S-90S.
216. Niswender, C.M., Sanders-Bush, E. and Emeson, R.B. (1998) Identification and characterization of RNA editing events within the 5-HT2C receptor. *Ann N Y Acad Sci*, **861**, 38-48.
217. Bass, B.L. (2002) RNA editing by adenosine deaminases that act on RNA. *Annu Rev Biochem*, **71**, 817-846.
218. Paul, M.S. and Bass, B.L. (1998) Inosine exists in mRNA at tissue-specific levels and is most abundant in brain mRNA. *EMBO J*, **17**, 1120-1127.
219. Jacobs, M.M., Fogg, R.L., Emeson, R.B. and Stanwood, G.D. (2009) ADAR1 and ADAR2 expression and editing activity during forebrain development. *Dev Neurosci*, **31**, 223-237.
220. Hartner, J.C., Schmittwolf, C., Kispert, A., Muller, A.M., Higuchi, M. and Seeburg, P.H. (2004) Liver disintegration in the mouse embryo caused by deficiency in the RNA-editing enzyme ADAR1. *J Biol Chem*, **279**, 4894-4902.
221. Wang, Q., Miyakoda, M., Yang, W., Khillan, J., Stachura, D.L., Weiss, M.J. and Nishikura, K. (2004) Stress-induced apoptosis associated with null mutation of ADAR1 RNA editing deaminase gene. *J Biol Chem*, **279**, 4952-4961.

222. Niswender, C.M., Herrick-Davis, K., Dilley, G.E., Meltzer, H.Y., Overholser, J.C., Stockmeier, C.A., Emeson, R.B. and Sanders-Bush, E. (2001) RNA editing of the human serotonin 5-HT2C receptor. alterations in suicide and implications for serotonergic pharmacotherapy. *Neuropsychopharmacology*, **24**, 478-491.
223. Breen, M.S., Dobbyn, A., Li, Q., Roussos, P., Hoffman, G.E., Stahl, E., Chess, A., Sklar, P., Li, J.B., Devlin, B. *et al.* (2019) Global landscape and genetic regulation of RNA editing in cortical samples from individuals with schizophrenia. *Nat Neurosci*, **22**, 1402-1412.
224. Li, J.B. and Church, G.M. (2013) Deciphering the functions and regulation of brain-enriched A-to-I RNA editing. *Nat Neurosci*, **16**, 1518-1522.
225. Schaffer, A.A., Kopel, E., Hendel, A., Picardi, E., Levanon, E.Y. and Eisenberg, E. (2020) The cell line A-to-I RNA editing catalogue. *Nucleic Acids Res*, **48**, 5849-5858.
226. Eifler, T., Pokharel, S. and Beal, P.A. (2013) RNA-Seq analysis identifies a novel set of editing substrates for human ADAR2 present in Saccharomyces cerevisiae. *Biochemistry*, **52**, 7857-7869.
227. Kondo, A. and Osawa, T. (2017) Establishment of an Extracellular Acidic pH Culture System. *J Vis Exp*.
228. Kondo, A., Yamamoto, S., Nakaki, R., Shimamura, T., Hamakubo, T., Sakai, J., Kodama, T., Yoshida, T., Aburatani, H. and Osawa, T. (2017) Extracellular Acidic pH Activates the Sterol Regulatory Element-Binding Protein 2 to Promote Tumor Progression. *Cell Rep*, **18**, 2228-2242.
229. Wu, D. and Yotnda, P. (2011) Induction and testing of hypoxia in cell culture. *J Vis Exp*.
230. Mizrahi, R.A., Phelps, K.J., Ching, A.Y. and Beal, P.A. (2012) Nucleoside analog studies indicate mechanistic differences between RNA-editing adenosine deaminases. *Nucleic Acids Res*, **40**, 9825-9835.
231. Desterro, J.M., Keegan, L.P., Lafarga, M., Berciano, M.T., O'Connell, M. and Carmo-Fonseca, M. (2003) Dynamic association of RNA-editing enzymes with the nucleolus. *J Cell Sci*, **116**, 1805-1818.
232. Maas, S. and Gommans, W.M. (2009) Identification of a selective nuclear import signal in adenosine deaminases acting on RNA. *Nucleic Acids Res*, **37**, 5822-5829.
233. Thi Tran, U. and Kitami, T. (2019) Niclosamide activates the NLRP3 inflammasome by intracellular acidification and mitochondrial inhibition. *Commun Biol*, **2**, 2.
234. Fritzell, K., Xu, L.D., Otrocka, M., Andreasson, C. and Ohman, M. (2019) Sensitive ADAR editing reporter in cancer cells enables high-throughput screening of small molecule libraries. *Nucleic Acids Res*, **47**, e22.
235. Huynh, K. and Partch, C.L. (2015) Analysis of protein stability and ligand interactions by thermal shift assay. *Curr Protoc Protein Sci*, **79**, 28 29 21-28 29 14.
236. Casey, J.R., Grinstein, S. and Orlowski, J. (2010) Sensors and regulators of intracellular pH. *Nat Rev Mol Cell Biol*, **11**, 50-61.
237. Kamel, K.S., Oh, M.S. and Halperin, M.L. (2020) L-lactic acidosis: pathophysiology, classification, and causes; emphasis on biochemical and metabolic basis. *Kidney Int*, **97**, 75-88.
238. Yao, H. and Haddad, G.G. (2004) Calcium and pH homeostasis in neurons during hypoxia and ischemia. *Cell Calcium*, **36**, 247-255.
239. Garcia-Moreno, B. (2009) Adaptations of proteins to cellular and subcellular pH. *J Biol*, **8**, 98.
240. Talley, K. and Alexov, E. (2010) On the pH-optimum of activity and stability of proteins. *Proteins*, **78**, 2699-2706.
241. Brett, C.L., Donowitz, M. and Rao, R. (2006) Does the proteome encode organellar pH? *FEBS Lett*, **580**, 717-719.

242. Davidson, H.W., Peshavaria, M. and Hutton, J.C. (1987) Proteolytic conversion of proinsulin into insulin. Identification of a Ca2+-dependent acidic endopeptidase in isolated insulin-secretory granules. *Biochem J*, **246**, 279-286.
243. Tyrtyshnaia, A.A., Lysenko, L.V., Madamba, F., Manzhulo, I.V., Khotimchenko, M.Y. and Kleschevnikov, A.M. (2016) Acute neuroinflammation provokes intracellular acidification in mouse hippocampus. *J Neuroinflammation*, **13**, 283.
244. Yang, J.H., Luo, X., Nie, Y., Su, Y., Zhao, Q., Kabir, K., Zhang, D. and Rabinovici, R. (2003) Widespread inosine-containing mRNA in lymphocytes regulated by ADAR1 in response to inflammation. *Immunology*, **109**, 15-23.
245. Wang, G., Wang, H., Singh, S., Zhou, P., Yang, S., Wang, Y., Zhu, Z., Zhang, J., Chen, A., Billiar, T. *et al.* (2015) ADAR1 Prevents Liver Injury from Inflammation and Suppresses Interferon Production in Hepatocytes. *Am J Pathol*, **185**, 3224-3237.
246. Raimondo, J.V., Burman, R.J., Katz, A.A. and Akerman, C.J. (2015) Ion dynamics during seizures. *Front Cell Neurosci*, **9**, 419.
247. Raimondo, J.V., Irkle, A., Wefelmeyer, W., Newey, S.E. and Akerman, C.J. (2012) Genetically encoded proton sensors reveal activity-dependent pH changes in neurons. *Front Mol Neurosci*, **5**, 68.
248. Rosenthal, J.J. and Seeburg, P.H. (2012) A-to-I RNA editing: effects on proteins key to neural excitability. *Neuron*, **74**, 432-439.
249. Cox, D.B.T., Gootenberg, J.S., Abudayyeh, O.O., Franklin, B., Kellner, M.J., Joung, J. and Zhang, F. (2017) RNA editing with CRISPR-Cas13. *Science*, **358**, 1019-1027.
250. Montiel-Gonzalez, M.F., Vallecillo-Viejo, I.C. and Rosenthal, J.J. (2016) An efficient system for selectively altering genetic information within mRNAs. *Nucleic Acids Res*, **44**, e157.
251. Qu, L., Yi, Z., Zhu, S., Wang, C., Cao, Z., Zhou, Z., Yuan, P., Yu, Y., Tian, F., Liu, Z. *et al.* (2019) Programmable RNA editing by recruiting endogenous ADAR using engineered RNAs. *Nat Biotechnol*, **37**, 1059-1069.
252. Merkle, T., Merz, S., Reautschnig, P., Blaha, A., Li, Q., Vogel, P., Wettengel, J., Li, J.B. and Stafforst, T. (2019) Precise RNA editing by recruiting endogenous ADARs with antisense oligonucleotides. *Nat Biotechnol*, **37**, 133-138.